Energy efficiency through variable speed drive control on a cascading mine cooling system

D van Greunen

24887129

Dissertation submitted in fulfilment of the requirements for the degree *Magister in Mechanical Engineering* at the Potchefstroom Campus of the North-West University

Supervisor: Prof M Kleingeld

May 2014

Abstract

Title: Energy efficiency through variable speed drive control on a cascading mine cooling system

Author: Declan van Greunen

Promoter: Prof. M. Kleingeld

School: Mechanical Engineering

Faculty: Engineering

Degree: Master of Engineering (Mechanical)

An ever-expanding global industry focuses attention on energy supply and use. Cost-effective electrical energy production and reduced consumption pave the way for this expansion. Eskom's demand-side management (DSM) initiative provides the opportunity for reduced electricity consumption with cost-effective implementation for their respective clients.

South African gold mines have to extend their operations to up to 4000 m below the surface to maintain profitable operations. Deep-level mining therefore requires large and energy-intensive cooling installations to provide safe working conditions. These installations generally consist of industrial chillers, cooling towers, bulk air coolers and water transport systems. All of these components operate in unison to provide chilled service water and cooled ventilation air underground.

In this study the improved energy efficiency and control of a South African gold mine's cooling plant is investigated. The plant is separated into a primary and secondary cooling load, resulting in a cascading cooling system. Necessary research was conducted to determine the optimal solution to improve the plant's performance and electrical energy usage.

Variable speed drives (VSD) were installed on the chiller evaporator and condenser water pumps to provide variable flow control of the water through the chillers, resulting in reduced motor electricity usage. Potential electricity savings were simulated. Proposed savings were estimated at 600 kW (13.6%) daily, with an expected saving of R 2 275 000 yearly, resulting

in a payback period of less than 9 months. Results indicated are based on total savings, as VSD savings and control savings were combined.

The VSDs that were installed, were controlled according to an optimum simulation model's philosophy. A real-time energy management program was used to control the VSDs and monitor the respective systems. The program's remote capabilities allow for off-site monitoring and control adjustments. A control strategy, which was implemented using the management program, is discussed. Energy efficiency was achieved through the respective installations and control improvements.

The results were analysed over an assessment period of three months to determine the viability of the intervention. A newly installed Bulk Air Cooler (BAC) added to the service delivery of the cooling plant post installation of the VSDs. Focusing on service delivery to underground showed a savings of 1.7 MW (33.6%) daily and a payback period of 3.6 months (0.3 years). The overall implementation showed an average energy saving of 2.3 MW (47.1%) daily, with the result that a daily saving of R 23 988.20 was experienced, reducing the payback period to 2.3 months (0.2 years).

Through the installation of energy-efficiency technology and a suitable control philosophy, a cost-effective, energy-efficiency improvement was created on the case-study cooling plant.

Keywords: Energy efficiency, chiller, gold mine, Demand Side Management, Variable Speed Drive, variable water flow.

Acknowledgements

Prof. Eddie Mathews, Dr. Marius Kleingeld, Temm International (Pty) Ltd. and HVAC International (Pty) Ltd. for providing me with the opportunity and funding to complete this study.

Prof. Leon Liebenberg, Dr. Johann van Rensburg and Walter Booysen for providing guidance in the study.

Dr. Deon Arndt for providing technical advice and assistance.

Abrie Schutte for mentoring and assisting with the project implementation.

Colleagues Alistair Holman and Dr. Gideon du Plessis for guidance and assistance in case study project implementation.

Christo Korb, Danie Olwagen and Pieter du Plessis at South Deep mine for assisting in case study project implementation.

Prime Instrumentation for case study project installation and commissioning assistance.

Johann Basson, Dr. Gideon du Plessis and Elsie Fourie for proofreading and critically reviewing the thesis.

My family and friends for their continued support and encouragement throughout the study.

Table of Contents

List of figures

List of tables

Nomenclature

Δ	change	(-)
Approach	temperature approach of direct contact heat exchanger	(˚C)
AEU	annual energy used	(kWh)
CI	confidence interval	(-)
c_p	specific heat at constant pressure	(J/kg.˚C)
CS_{VSD}	cost savings from installing VSDs	(R)
C_{VSD}	cost of installing VSDs	(R)
D	impeller diameter	(m)
ES_{VSD}	energy savings through VSD	(kWh)
ET	electricity tariff	(c/kWh)
η	efficiency	(%)
h	specific enthalpy	(J/kg)
H	system head/pressure	(kPa)
hr	operating hours	(hrs)
kW_a	actual capacity of an electric motor	(kW)
kW_r	rated capacity of an electric motor	(kW)
L	load factor	(-)
LCC	Life Cycle Cost	(R)
$\dot{m}$	mass flow rate	(kg/s)
N	rotational speed	(min^{-1})
P	power	(kW)
PBP	payback period	(years)
P_q	reactive power	(kVA_r)

P_r	real/active power	(kW)
P_s	apparent power	(kVA)
$\dot{Q}$	heat transfer rate	(W)
Q	flow rate	(ℓ/s)
R	ideal gas constant	(J/mol.K)
Range	temperature range of direct contact heat exchanger	(˚C)
s	entropy	(kJ/kg.K)
S_{SR}	motor speed reduction energy savings	(%)
T	temperature	(˚C)
T_{wb}	wetbulb temperature	(˚C)
v	specific volume	(m^3/kg)
W	input electrical power	(W)

Abbreviations

AC	alternating current
BAC	bulk air cooler
COP	coefficient of performance
CV	root-mean-square error
DC	direct current
DSM	demand side management
EMS	energy management system
ESCO	energy services company
GA	genetic algorithm
HEM	high efficiency motor
HVAC	heating ventilation and air conditioning
IGBT	insulated gate bipolar transistor
MIMO	multi-input multi-output
PF	power factor
PFC	power factor correction
PID	proportional integral derivative
RBF	radial basis function
SCOP	system coefficient of performance
VSD	Variable Speed Drive

Chapter 1 – Introduction

1.1 Background

Electrical energy producers need to constantly expand their generation capacity to supply the growth of private and industrial consumers. Consumers are dependent on the supply availability, along with increasing costs. This paves the way for reduced electricity consumption and energy efficiency improvements, benefiting all parties concerned.

In South Africa the state of electricity supply and demand has been critical since 2007. Eskom, the country's electricity utility, is presently expanding its generation capacity [1]. The availability of this new capacity is, however, being hindered due to construction delays. Additionally, an average tariff increase of 25% over the last five years for the funding of this new generation capacity is placing severe financial strain on consumers [2].

A subsidy project implemented by Eskom to assist in reducing the strain experienced on the electricity system is the Demand Side Management (DSM) programme. One of the strategic implementation industries of this programme is South African mines. Here the plant, financed by many of the past capital investments, are less efficient due to their installation when the mines were developed, resulting in the use of older equipment and control methodologies. Additionally, safety factors built into many systems consume additional unnecessary energy.

One of the systems that has a large potential for energy efficiency improvement is industrial cooling [3]. These systems include a combination of industrial chillers, pumps and fans. The cooling plant operates to provide chilled water and cooled air to underground production areas to assist in the removal of heat components such as machinery and virgin rock [4]. This provides a safe mining environment for a labour-dependent workforce, which is regulated by South African law [5], [6]. Lower ambient temperatures furthermore reduce worker fatigue [7].

A common component in the cooling system is the electric motor. Electric motors' running costs can increase to above 100 times its original purchase cost [3]. This creates a need to improve the energy-efficiency of these components, resulting in reduced running costs.

The power output of pumps and chillers are often throttled. This occurs because of system limitations, or mechanical reduction of the driven fluid by valves. The potential thus exists to

reduce the power input to these motors, as opposed to restricting the power available in the system.

Many means of mechanical speed reduction, such as gearboxes, have been utilised in motor systems [8]. These, however, still utilise the full power rating of the motor. A more modern approach to motor speed reduction is the limitation of supply frequency applied to an electric motor. This is achieved by passing the electricity delivered to the motor through a variable speed drive (VSD) [9].

A VSD is a component which has the capability to alter the voltage-frequency output. Reducing the voltage frequency delivered to an electric motor results in reduced motor-speed output. The motor therefore consumes less power, thereby drawing less current from the electricity supply. As a VSD can change the speed at which a motor operates, additional benefits such as variable speed control will be possible.

VSDs are implemented internationally in various industries, ranging from building HVAC systems to municipal pumping stations to mines [8], [10], [11], [12], [13]. The capacity for energy-efficiency improvement with these drives is expected where a physical restriction is placed on an electric motor (such as system pressure in a pumping network). Table 1, below, shows the potential for energy savings when a VSD is applied to an electric motor. It can be seen that the relationship is not linear, but a power function.

Table 1: Potential electricity savings from a reduction in motor speed [14]

Average speed reduction (%)	Potential electricity savings (%)
10	22
20	44
30	61
40	73
50	83
60	89

VSDs in addition serve as soft starters, allowing for smoother start-ups and similarly shutdowns [15]106. This is done by ramping the motor speed up and down in the same way that operational control of the pump would be implemented. By implementing a VSD on a motor electrical strain can be reduced on the system and feeding network. This is more noticeable with the prevention of current spikes during motor start-up which can typically be more than 500% of a motors running current [16].

1.2 Motivation for this study

The initiation of this study is intended to highlight the energy inefficiency often found on mine cooling systems. Alternative chiller evaporator- and condenser water flow-rate control methodologies are to be analysed. Payback periods on the investment of VSD installations will be shown to be well within industry standards. As such the scope is indicated for similar energy-efficiency initiatives on other mine cooling plants.

1.3 Goals of the study

This study aims to improve the energy efficiency of a mine surface cooling plant. Improved energy efficiency will be achieved through the installation and control of VSDs on the chiller evaporator and condenser water pump motors. This control will suit the plant requirements and strive to achieve optimal power savings. The respective system components are to be controlled and monitored using a real-time energy management system (EMS).

The energy efficiency achieved will show the potential of such an installation and control combination. This will be represented by the payback period of the installation.

1.4 Scope of study

The scope of this study focuses on the surface cooling plant of a deep-level gold mine located in South Africa's Gauteng province. The mine's cooling plant and all the auxiliaries are analysed with the available data. This includes chillers, cooling towers, bulk air coolers and the respective water pumps and fans. Chillers in the cooling plant are separated into a primary and secondary cooling load, resulting in a cascading system.

The only control variable to be adjusted throughout the study is the water flow through the chillers' evaporator and condenser systems. This flow will be controlled by adjusting the respective pump motor speeds through the VSDs installed.

1.5 Layout of dissertation

Chapter 1 provides a brief introduction into the study and its background. This is followed by the aims, goals and scope of the study, and the layout of the dissertation is presented.

Chapter 2 presents a detailed and comprehensive background and literature study. This information details the need for the study, other strategies implemented in industry and

information pertaining to achieving and analysing the energy-efficiency improvement of the cooling plant.

In chapter 3 the surface cooling system of the case-study gold mine is analysed. An energy audit will be completed with the relevant electricity loads. This audit will be used to compile a power baseline, or reference data set. Additional variables will be collected and analysed to integrate into the baseline. This will allow for the scaling of the baseline and actual power profiles, as these variables alter after the necessary installations and commissioning have been completed. The present energy efficiency and control philosophy of the system will be determined. Expected system and service delivery changes are discussed.

Chapter 4 investigates the expected outcome of the installation with regards to improved energy efficiency. The investigation includes a simulation designed in Process Toolbox, along with verification calculations. A proposed control philosophy is presented to achieve the energy-efficiency improvement. Installations are detailed along with the resultant control implemented.

Chapter 5 focuses on a performance-based assessment that was implemented for three months in a pilot mine after successful commissioning. This assessment will compare power data according to the scaled baseline previously mentioned. This baseline will differ from day to day as the relevant variables alter. The power data will additionally be compared on a year-on-year basis for a direct analysis. Time-of-use is analysed by electricity operating costs. The effect of the additional service delivery required by a new Bulk Air Cooler (BAC) will be analysed. All relevant system results will be presented and discussed.

Chapter 6 presents a conclusion to the overall outcome of the project. The effectiveness and accuracy of the implemented system will be indicated. The energy-efficiency improvement and related results will be detailed. Recommendations will be provided as to other possible improvement strategies on the mine.

Chapter 2 – Review of state-of-the-art in cooling of deep mines in South Africa

2.1 Background of the South African electricity sector

With industrial growth, electricity utilities have to keep on increasing their power generation capacity. This, along with population growth, is forcing energy utilities to not only develop new generation capacity, but to also subsidise energy-efficiency projects, ranging from general households to large industrial power consumers.

In 2010 South Africa produced 33% of Africa's electricity. In addition it consumed 38.4% of the total generated capacity on the continent [17]. In 2011 South Africa was the sixth cheapest source of electricity in the world, selling power at an average cost of 0.91 (US¢)/kWh to the consuming public [18]. The main growth in South African industry leading to an increase in electricity consumption occurred in the period 1993-97. This was due to changes in the structure of the economy after the democratisation of the country [19].

In South Africa alone the population has increased on average by 1.2% per annum from 2001 to 2011 [20]. With the population exceeding 51.1 million people in 2012, an additional 600 000 people will be drawing power from the national grid each year [21]. The industrial production growth rate increased on average by 3.2% annually from 2001 to 2011 [22]. In addition, distribution and transmission losses of 6.3% and 3.1% respectively resulted, due to illegal connections and related activities in 2012 [2]. All this threatens the availability of South Africa's electricity supply.

Eskom, South Africa's electricity utility, is state-owned and has the monopoly for affordable electricity in the country. In the 1980s Eskom had representatives promoting sales of electricity at extremely cheap tariffs due to a surplus production capacity. Prior to 2006/2007 the last generation capacity Eskom added to the grid predates 2005 and only accounts for one GW from 2001 to 2005 [23]. This, in addition to power stations being mothballed, resulted in severe strain being placed on the grid.

The electricity sector in South Africa reached a critical state in 2007 when rolling blackouts (an Eskom forced load-shedding scheme) were implemented. This was a direct result of Eskom's failure to meet the demand on the national grid. Eskom further failed to substantially increase its power generation capacity over the years [24].

By January 2008 the situation reached a critical state, with Eskom requesting its larger industrial consumers to shut down their operations. This prevented a national grid failure due to electricity demand exceeding supply, similar to that experienced in India in 2012 [25], [26]. The vast majority of these consumers were gold and platinum mines [24]. The mining sector consumes 14.5% of South Africa's electricity supply. Temporary shutdowns of mining operations thus provided vital relief [2]. However, with South Africa being one of the world's largest platinum and gold producers, the shutdown of operations would lead to severe economic strain [27], [28], [29].

Eskom is presently building two power stations and a pumped storage scheme [1]. The first unit of these two stations is only expected to be completed in 2014, while the second's construction is expected to be fully operational by 2018. This infrastructure promises an additional 9588 MW standard supply and 1332 MW peak demand supply to be added to the national grid [30], [31].

The private sector has since 2011 been allowed the opportunity to sell electricity to Eskom [32], [33]. This allowed private investors the opportunity to provide funding for large green electricity projects, such as wind farms, photo voltaic solar plants and solar collection plants. Green energy refers to energy that is renewed naturally and releases little pollution to the environment, such as the sun and wind. It is a source of power generation with a lower carbon footprint than present mass generation methods.

The cost of developing green electricity plants is still expensive relative to coal-fired power stations. This is due to the present high cost of the technology used to collect the renewable energy. However, statistics show that certain renewable electricity sources will become more affordable over time as they mature technically and where large capital investments are made. At present 85% of Eskom's supply is dependent on coal-fired power stations [2]. As coal is an abundant resource in South Africa, electricity produced by burning coal is the cheapest form of primary energy for electricity production. This is, however, one of the worst carbon footprint production methods. The distribution of Eskom's generation capacity is illustrated in Figure 1.

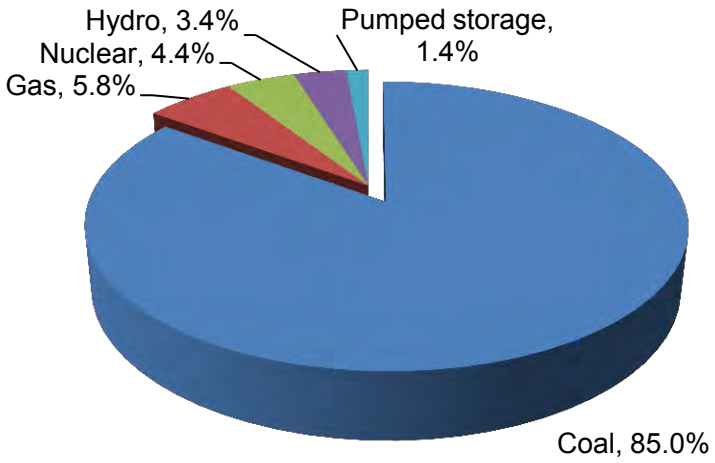

Figure 1: South Africa's national electricity utility's (Eskom) power generation capacity for 2012 (42 GW) [2]

Eskom's present production expansion has resulted in it recently requesting a yearly tariff increase of 16% over the next five years. The National Energy Regulator of South Africa (NERSA) granted an 8% increase over a period of five years after an outcry by both the public and industry. A 16% increase would have financially crippled many private consumers and businesses. The constant tariff increases over the last five years have already placed a large financial strain on consumers. As indicated in Figure 2, an average increase of 25% per annum in tariffs has already been implemented over the last five years [2].

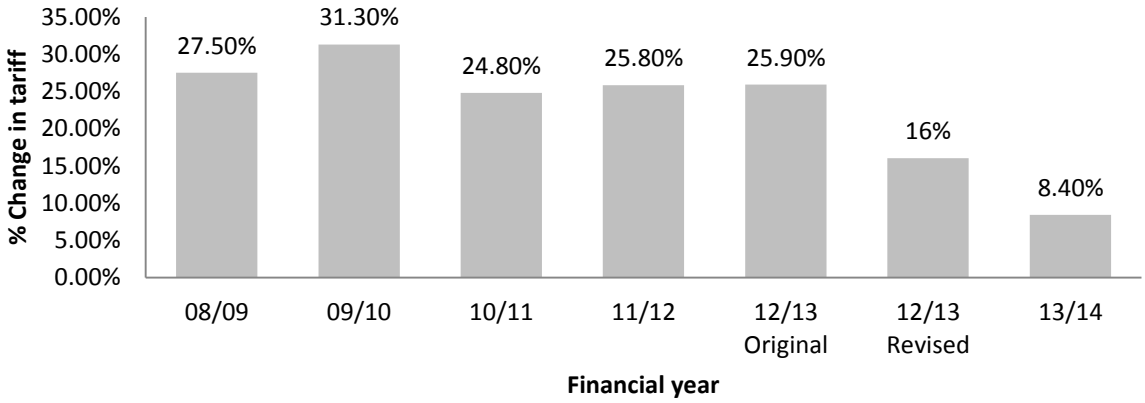

Figure 2: Average electricity tariff increases for South Africa from 2008 to 2012 [2], [35]

One of the subsidy projects being implemented by Eskom is a Demand Side Management (DSM) programme. This aims to reduce the power demand while new generation capacity is being added to the grid, as previously discussed.

2.2 Demand Side Management potential on South African mines

With South Africa having an electricity-intensive economy, the market for efficiency improvement throughout industry is large. This is particularly true for the mining industry. As large capital investments originate from the development of new mines, the technology of the mechanical/electrical systems is outdated and inefficient. Most new technology is only implemented after equipment failure, or by external parties with specific incentives.

With Eskom experiencing strain on its grid and high probable inefficiencies in mining industry, it is reasonable to expect to find projects to reduce loading from the mines. As Eskom's DSM initiative provides funding for their projects, it is vital to find projects where the payback period for the equivalent electricity saved is as short as possible. This limits the number and size of viable projects. Fortunately the existence of a project on one site implies that it can be similarly implemented on other sites as well.

The first step is to separate the different electricity consumers on the mines. As seen in Figure 3 below, the four main consumers with savings potential are pumping, compressed air, processing and materials handling [3].

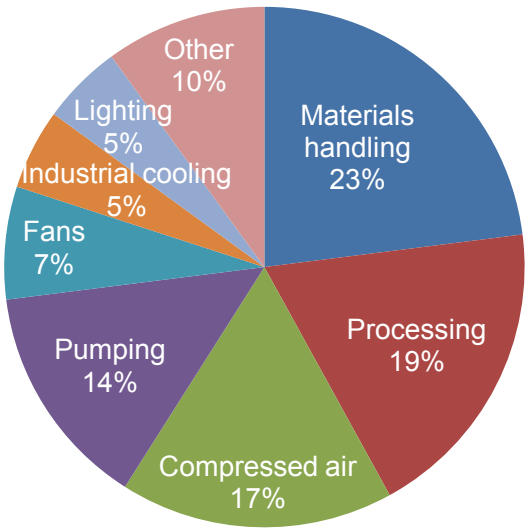

Figure 3: Typical electricity savings potential for South African mines [3]

With the implementation of new projects on mines, any strategy that includes underground work tends to take longer due to restricted access. This is also true for processing plants on precious mineral mines such as gold and platinum. Surface projects are thus the first to be

more viable. This leaves surface pumping, chillers, fans and compressed air generation as solutions.

One of the operations that combine three of these systems is industrial cooling. Here the pumps and fans are crucial in the cooling and transportation processes. A core element of each of these systems is the electric motor. With the running cost of a motor being 100 times higher over its lifetime than its purchase cost, it is crucial to make motors and their supply system as efficient as possible [3].

Barriers that need to be overcome with energy-efficiency projects include budgets (capital and operational costs), risk of failure, a lack of knowledge, internal incentives and the present market structure [34]. The majority of these barriers are already overcome with the DSM implementation scheme. As capital costs are provided for, the risk of failure is reduced (proven track record of similar projects). Present market structures provide easy access to energy-efficient improvements, thus one must simply overcome large future operational costs and provide for internal incentives.

An additional Eskom DSM programme exists in load-shifting schemes. The aim of projects here is to reduce the use of electricity by large power consumers during national peak consumption hours. The large consumers already have the incentive to reduce operational costs through the Megaflex tariff structure. Figure 4 illustrates the distribution of this structure. The green, yellow and red sections indicate off-peak, standard and peak consumption periods respectively. The cost of electricity for these consumers is similarly distributed from least to most expensive consumption periods, based on these consumption periods. The tariffs for these periods, applicable to this case study, are indicated in Table 2 and Table 3.

The difference in summer to winter costs, especially from standard to peak periods, is largely due to household heating in the winter months. This results in a large additional load being placed on the electricity grid. As such the electricity price is increased exponentially to force consumers (both industrial and private) to reduce electricity consumption during these hours, thus reducing the total load on the electricity grid.

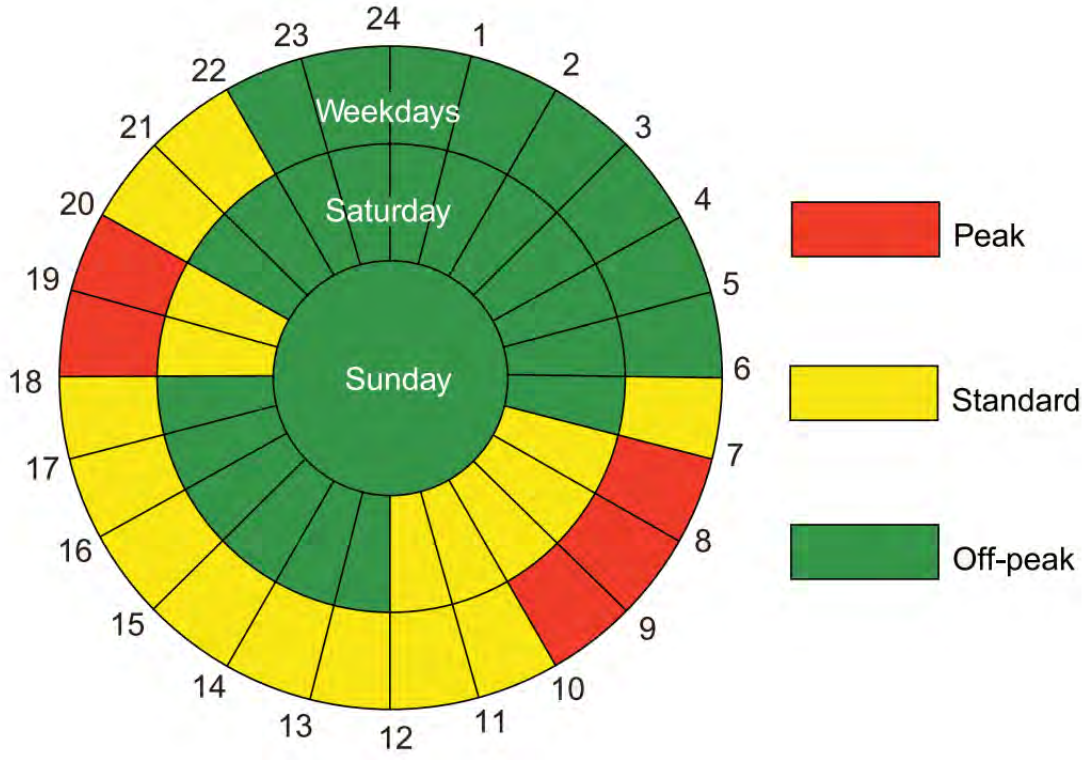

Figure 4: Eskom Megaflex electricity tariff structure [36]

Table 2: Eskom 2011/2012 Megaflex tariff structure [36]

Demand time	Summer September – May tariffs (c/kWh)	Winter June – August tariffs (c/kWh)
Off-peak	24.93	28.94
Standard	35.65	54.17
Peak	58.19	208.43

Table 3: Eskom 2012/2013 Megaflex tariff structure [36]

Demand time	Summer September – May tariffs (c/kWh)	Winter June – August tariffs (c/kWh)
Off-peak	28.69	33.03
Standard	41.04	61.78
Peak	66.98	237.72

2.3 Effective cooling in deep mines

Mining in South Africa is labour intensive, despite the availability of technical machinery. This is done to support job creation in a country with high unemployment levels [37]. A result is strict regulation of working conditions enforced by the Mine Health and Safety Act of 1996 (MHSA) and its amendment, the Mine Health and Safety Bill of 2008 [5], [6]. A platform is additionally created to create skilled labour with good industry experience.

From a mining perspective, one needs to consider the many sources of heat below ground. It is these sources that need to be controlled or cooled to provide a safe mining environment. Underground temperatures need to be kept below 27 ˚C (wet bulb) to maintain 100% worker efficiency [7]. This creates the need for effective cooling. Major controllable heat sources include the rock face, broken-out rock (virgin rock), fissure water and machinery [4]. These heat sources can be separated into two groups: temperature-dependent heat sources (TDHs) and temperature-independent heat sources (TIHs) [7]. Figure 5 illustrates the distribution of heat sources underground.

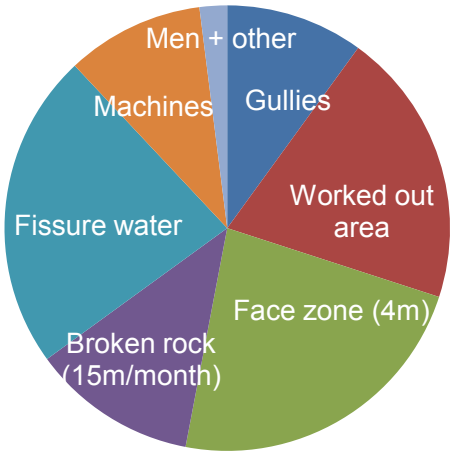

Figure 5: Typical stope heat components (adapted from [4])

Another source of heat entering the mine ventilation air that needs to be considered is adiabatic compression (commonly known as autocompression). This is where air entering the shaft will increase in temperature and pressure (without any heat transfer from the shaft or evaporation of moisture). Adiabatic compression occurs due to the mass of atmospheric

air applying pressure on the air mass in the mine shaft. The process is a conversion of potential energy to internal energy [7].

Temperature regulation not only provides a safe working environment, but it also reduces worker fatigue [38], [39]. Reducing the fatigue of workers increases the potential for productive time spent underground. Figure 6 illustrates the decrease in productivity experienced in relation to various ambient temperatures.

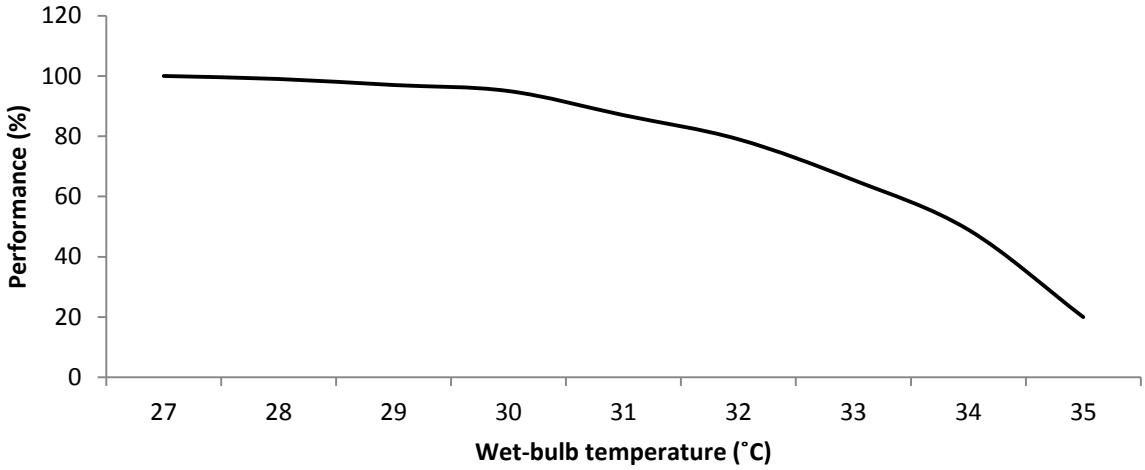

Figure 6: Changes in production rate of underground mining workers with a change in working temperature (adapted from [39])

An active solution to counter the heat underground is to send chilled water and cooled air from the surface to the affected areas. Figure 7 shows a typical deep-mine surface cooling network. The water is largely used to cool the rock face and ore which is being mined. Chilled water can capture the heat load from the rock before it enters the air [7]. It also controls the dust after blasting.

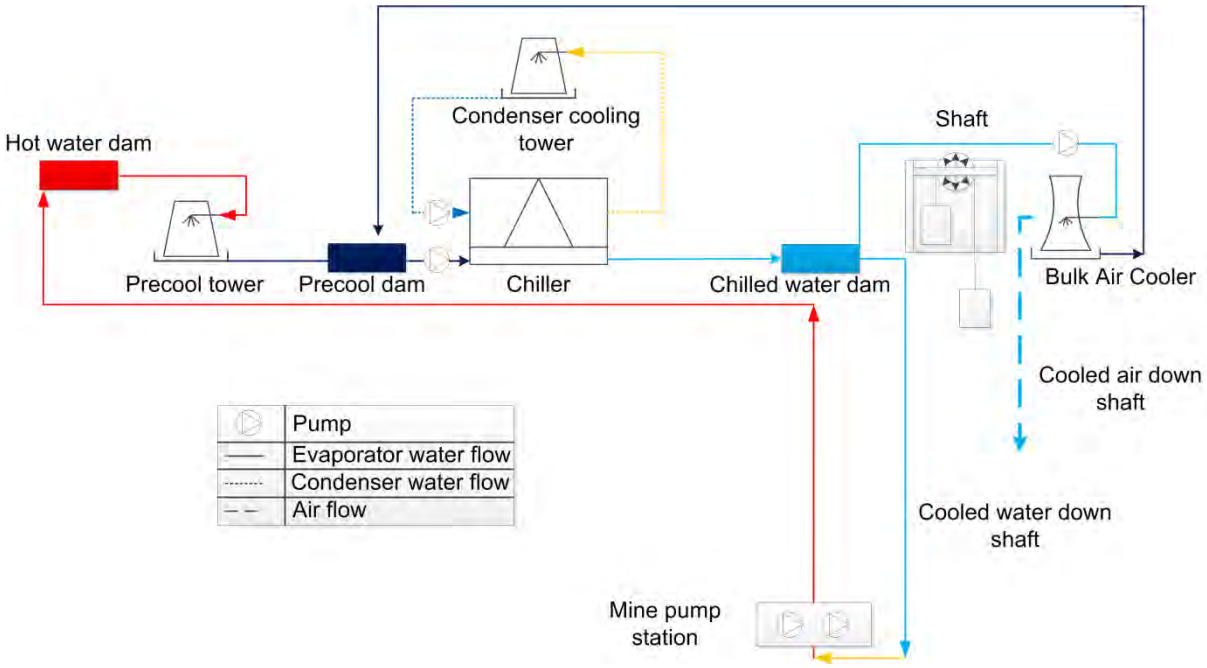

Figure 7: Schematic layout of a typical deep-mine surface cooling network (adapted from [7])

Some South African gold mines are 3000 to 4000 m deep to reach high concentration ore bodies. In these extreme cases ice is at times additionally made and sent down to maintain a low water temperature [40], [41]. Figure 8 illustrates the increase in virgin-rock temperature with increased mining depth of various gold-mining regions in South Africa [39].

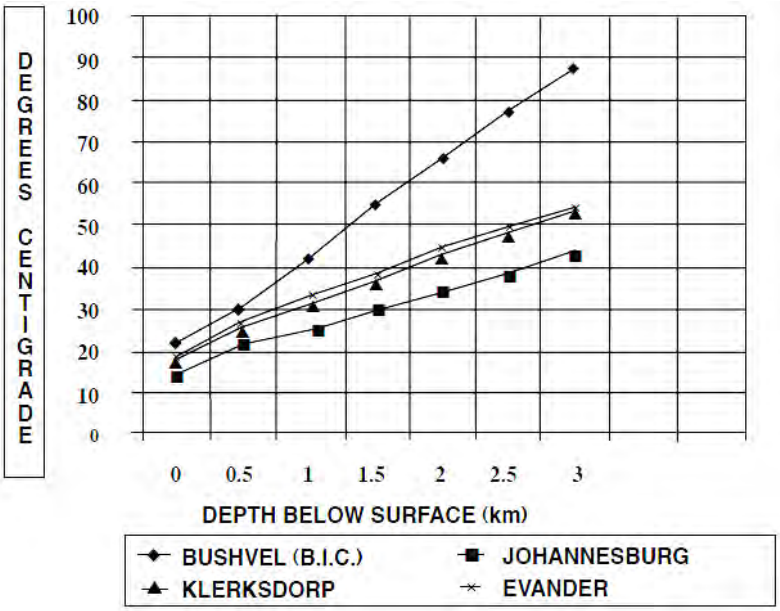

Figure 8: Virgin-rock temperatures plotted against mining depth for the project implementation region [39]

The chilled water is cooled to such low temperatures as the water temperature can increase up to 5 degrees per degree where sent underground (chilled water at 3 ˚C on the surface could end up at 15 ˚C when it is being used below ground [1]). In order to get the water to such low temperatures, chillers (often referred to as fridge plants on a mine) are used to cool the water. These plants operate by using a refrigerant to draw heat from the water through a refrigeration cycle and various forms of heat exchangers.

The cooled air is sent underground through BACs. These coolers draw ambient air through cooling towers by means of large fans. The cooling towers act as a heat exchanger, where the air is pulled through chilled water (from the cooling plant) which is sprayed in the tower. This cooled air assists in improving working conditions, as discussed.

The cooling load of the chillers and BACs is seasonally dependent. With ambient temperatures naturally decreasing in the winter months, natural thermal energy (lower ambient temperatures) allows the chillers to operate at lower loads. This is a crucial energy factor, as electricity use for household heating throughout the country increases over the winter months. A more in-depth discussion on these cooling methods is presented in Chapter 2.4.

[1] Danie Olwagen – Fridge plant foreman – Goldfields South Deep South shaft – August 2012

2.4 Surface fridge plants

2.4.1 Overview

As discussed, there is a constant requirement for cooling in deep mines. The heart of this cooling strategy is delivered in the form of industrial chillers. These large industrial plants are often technologically outdated due to them being installed during the establishment of the mines. It is not feasible to replace their chillers with more technologically-advanced plants due to additional capital costs. Modern control philosophy and efficiency installations are thus often implemented on these plants. The plants are coupled with cooling towers and bulk air coolers to respectively ease the cooling load and provide cooled ventilation air.

To apply an effective energy-efficiency project on such chillers, it is vital to understand their method of operation. This includes the mechanical functionality, the interaction of the working fluids in the system and the auxiliary components.

2.4.2 Chillers

A chiller generally consists of two component sections, namely heat exchangers and compression mediums. The heat exchangers shown in Chapter 2.4.5 are typical constructions of the evaporator and condenser. The evaporator and condenser operate with the refrigerant in a two-phase state at a constant pressure (liquid and vapour) [42]. The refrigerant exits the condenser as a saturated liquid and exits the evaporator as a saturated vapour. These two points are crucial in calculating other values in the system.

Very little work is experienced between the refrigerant leaving the condenser and entering the evaporator. By placing a throttling device between the two components, the fluid is throttled from the high- to the low-pressure side [42]. The throttling device is usually an expansion valve or capilliary tube. Use of the throttling device makes the process adiabatic and thus theoretically isentropic [42].

The main working (electricity intensive) component in this system is the compressor. It is here between its two constant pressure mediums that the fluid changes state. It is assumed that the fluid enters the compressor as a saturated vapour (similarly the state at which it leaves the evaporator). This assumption is vital, as less compression will take place if the fluid enters the compressor in a partial liquid state [42].

The coefficient of performance (COP) which is a means of determining a chiller's efficiency, is also largely dependent on the compressor's electricity usage. It is thus important that the compressor operates at as low a loading as possible. At the same time the highest potential thermal energy must be extracted from the fluid to be cooled in the evaporator [42].

Thermodynamic cycles in chillers

Two refrigeration cycles are used throughout industry, namely the vapour-compression and ammonia-absorption cycles. The main difference between the two cycles is the manner in which compression is achieved. Additionally, as its name states, the ammonia-absorption cycle is designed specifically for ammonia to act as the working fluid. Where the vapour-compression cycle utilises a compressor, the typical ammonia-absorption cycle comprises four components, as seen in Figure 9. This system uses very little work input, as the pressure pumping system involves a liquid [42].

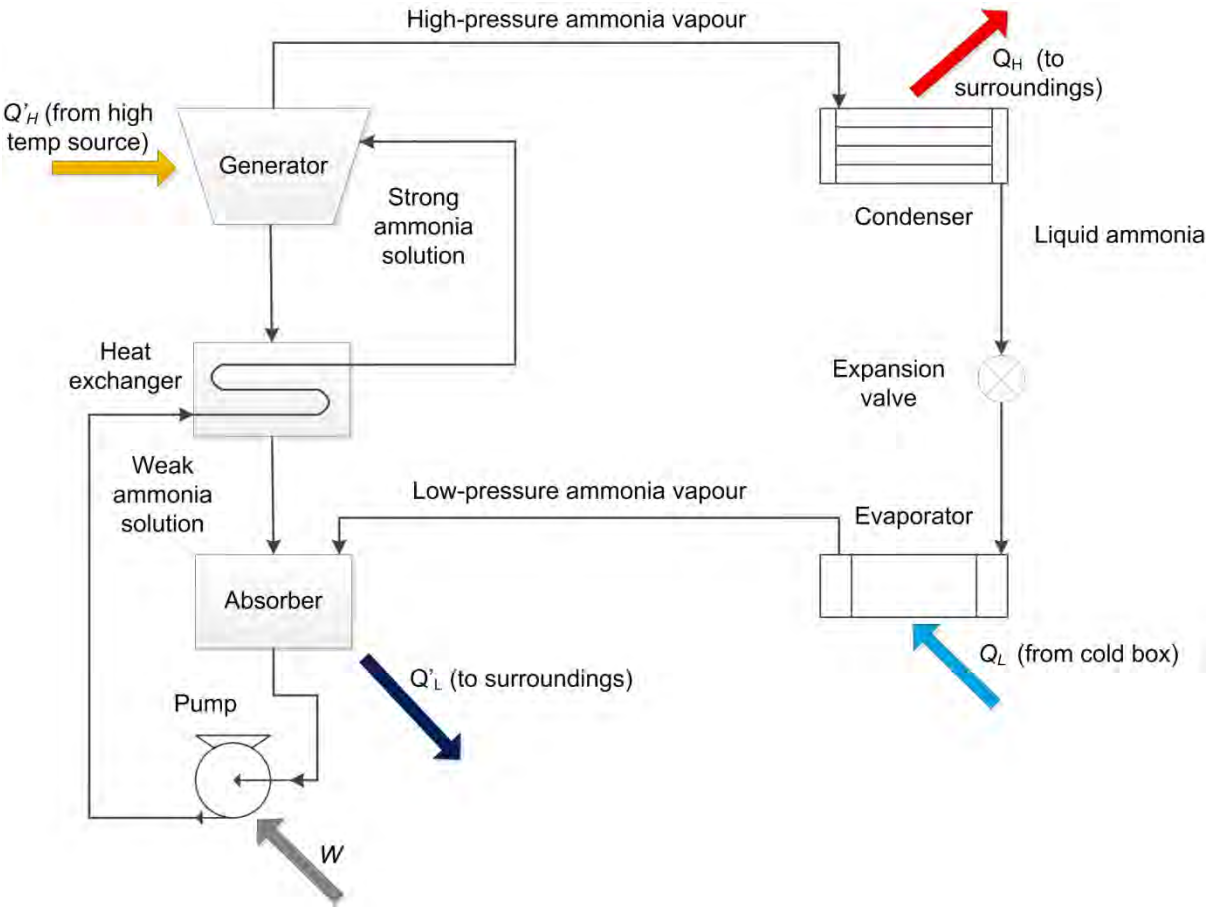

Figure 9: Typical ammonia chiller schematic (adapted from [42])

In this system a low-pressure ammonia vapour enters the absorber where it is absorbed into a weak ammonia solution. This fluid is then pumped through the heat exchanger to the generator, where a higher pressure and temperature are maintained.

The basic ideal vapour-compression refrigeration cycle is shown in Figure 10. The net work input for the cycle is represented by the area enclosed by the progress lines 1-2-3-4-1. As indicated in the figure, there are two constant pressure processes (2 to 3 and 4 to 1) and two constant isentropic processes (1 to 2 and 3 to 4') [42].

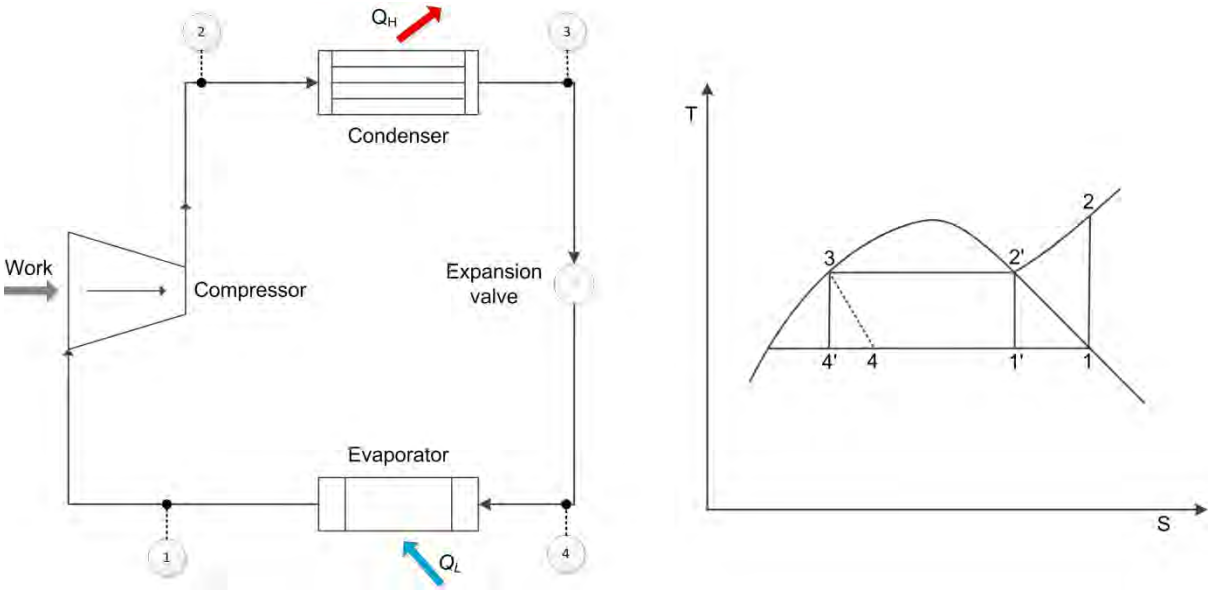

Figure 10: Ideal vapour-compression refrigeration cycle of a chiller. (adapted from [42])

An actual refrigeration cycle deviates from these assumptions mainly due to pressure drops and heat loss in a system [42]. The vapour entering the compressor will most likely be superheated as opposed to being saturated. When the fluid is passing through the compressor an entropy loss occurs due to heat loss. A natural pressure drop coupled with heat loss occurs across the condenser. The fluid leaving the condenser is usually below the saturation temperature. Similarly a drop in enthalpy occurs which allows for more heat to be transferred to the refrigerant in the evaporator. A similar pressure drop occurs across the evaporator. The fluid will increase in temperature in the piping between the evaporator and the compressor, entering the compressor as a superheated vapour. This however results in additional work in the compressor due to a higher initial specific volume [42]. This process is indicated in Figure 11.

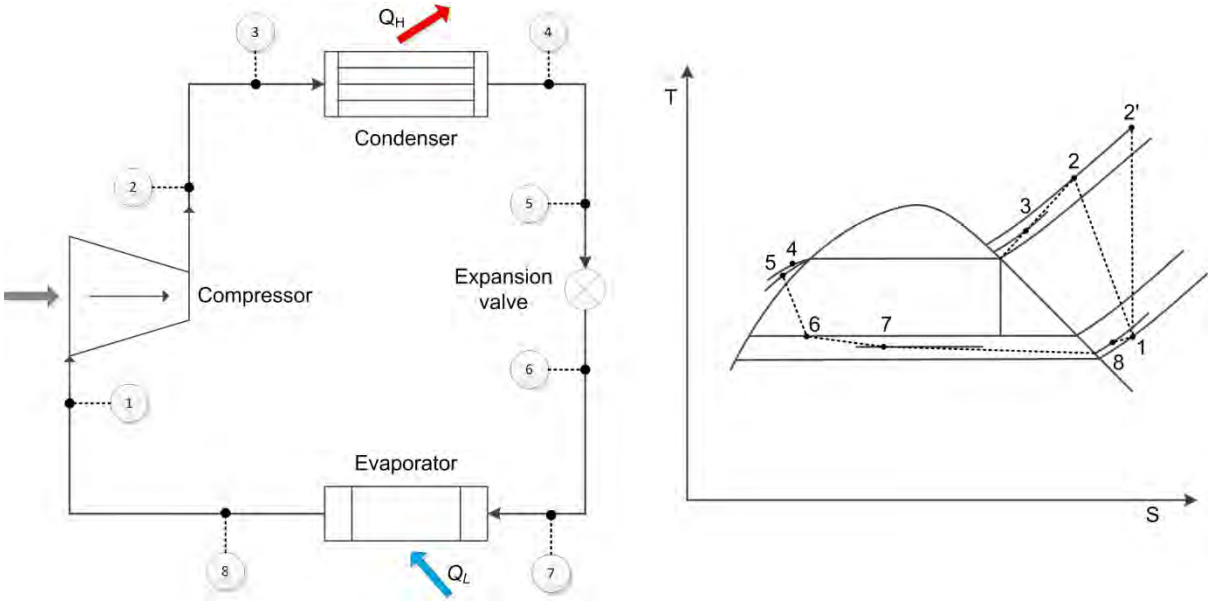

Figure 11: An actual vapour-compression refrigeration cycle. (adapted from [42])

General practice is to analyse the refrigeration cycle as an ideal cycle. This is done with a working substance (refrigerant) that changes phase during the cycle. The deviation from this ideal cycle is then determined by the level of insulation and pipe length in the system [42]. As natural pressure drops and thermal energy loss to the environment occur throughout any system, there will always be a deviation from the idealistic design [42]. Equation 1, below, shows the ideal gas law applicable to the ideal cycle.

$$Pv = RT \tag{1}$$

The ideal gas law needs to be understood to interpret the parts of the refrigeration process. An ideal gas is one that obeys the relation in equation 1 [43]. This ideal gas relation tends to approximate the P-*v*-T behaviour of real gases at low densities. One should be careful to identify the state of the refrigerant before applying the ideal gas law [43].

Refrigerants used in vapour-compression refrigeration systems

A large number of refrigerants are used in vapour-compression cycles. Ammonia and sulphur dioxide were largely used in the first vapour-compression refrigeration systems. The use of these substances was soon limited due to their high toxicity and flammability in high concentrations [44], [45]. This reduces its use in industry due to hazards caused by potential leaking of the gas, particularly in underground applications. The substance is in addition

corrosive to copper or copper alloys [44]. Chiller plants will have water sprayers above the plant for use in the event of a leakage of these gases. As the gases are soluble in water, the sprayers will prevent the gases from entering the atmosphere, or posing a further threat to operating staff. Table 4 below summarises the old and new refrigerants used in the cooling process.

Table 4: Alternative refrigerants used in industry [42]

Old Refrigerant	**R-11**	**R-12**	**R-13**	**R-22**	**R-502**	**R-503**
Alternative Refrigerant	R-123	R-134a	R-23 (low T)	NH_3	R-404a	R-23 (low T)
	R-245fa	R-152a	CO_2	R-410a	R407-a	CO_2
	-	R-401a	R-170 (ethane)	-	R507a	-

The old refrigerants have over time been replaced due to their negative effect on the stratosphere (ozone). In many countries the use of these refrigerants has been banned. These compounds are commonly known as chlorofluorocarbons (CFCs).

Two considerations are important when selecting a refrigerant: the temperature at which the refrigerant will operate, and the type of equipment to be used. While the refrigerant undergoes a change of phase, it is maintained at saturation pressure. The equipment needs to accommodate these pressures at which the refrigerant operates. A lower pressure will thus require large equipment to provide for larger volumes. Similarly, a high pressure will require smaller volumes. The equipment will, however, need to withstand the high pressures [43].

As different volume capabilities are required for different applications, a different compressor is similarly utilised. Centrifugal compressors are best suited for low pressures and high specific volumes, whereas reciprocating compressors are best adapted for high pressures and low specific volumes [43].

A chiller can often be designed to operate at maximum load for an optimal efficiency. It is thus vital to operate a chiller within its design constraints. Failure to operate within the design limits could result in damage such as burst pipes. Such system failures can however be prevented through the installation and monitoring of sensors across a machine. These sensors will measure data such as temperatures, pressures and vibration.

2.4.3 Cooling towers

Mine chiller systems generate heat, which needs to be removed from the system. Hot water pumped from underground also needs to be cooled in the most cost-effective manner. A cooling tower is a means of extracting this heat from the respective water sources and expelling it directly to the ambient air. This occurs through evaporative cooling from the hot water into the cooler ambient air and is a combination of mass- and both latent and sensible heat transfer [46]. As previously indicated in Figure 7, separate cooling towers operate along the hot-water source and the chiller condenser circuit. Figure 12 shows the typical schematic of a cooling tower.

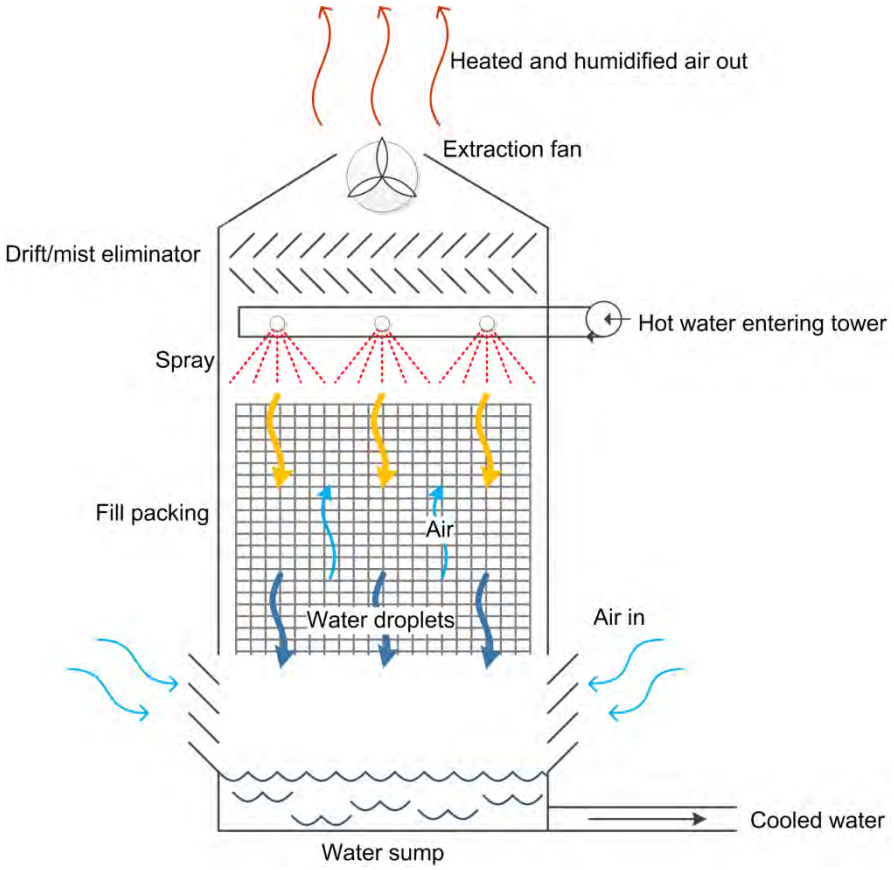

Figure 12: Direct-contact evaporative cooling tower (adapted from [46])

Cooling towers consume approximately only 5% of the water when compared to once-through systems (due to the humidified air), with the capability to cool the water to within 6 to 3 ˚C of the ambient wet-bulb temperatures [46]. Thus it is the cheapest and most efficient cooling method when compared to similar systems.

Heat and mass transfer is increased by pumping the water through sprayers in the tower, increasing the contact surface area. As seen in Figure 12, the air is counterflowed by means of a fan at the top of the tower. The water exchanges heat with the ambient air, while the water mass transferred is proportional to the dry-bulb temperature. Figure 13 shows the relationship between water and air in a counterflow cooling tower.

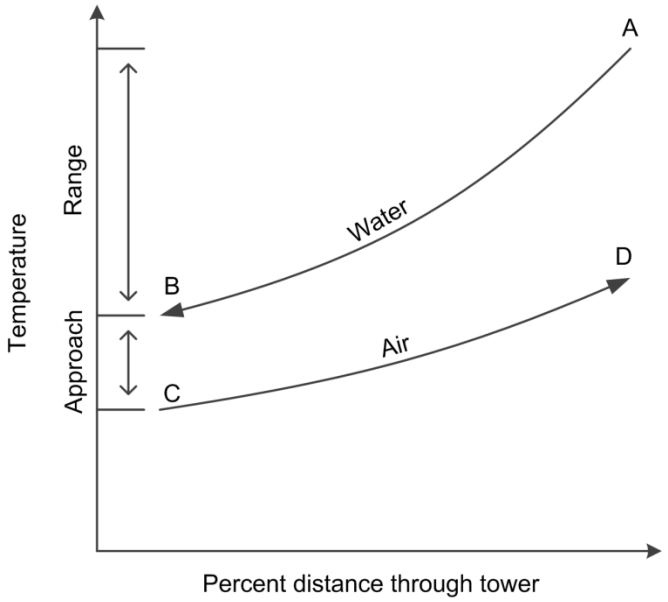

Figure 13: Temperature relationship between water and air in a counterflow cooling tower [46]

As indicated in Figure 13, the drop in water temperature (A to B) across the cooling tower is denoting the *range,* while the rise in ambient air wet-bulb temperature (C to D) is the *approach*. The range of a cooling tower is determined by the water heat load and flow rate, not by the size or thermal capability of the tower [46]. The relationships in Figure 13 can be represented by the equations listed below [46].

$$Range = T_A - T_B \tag{2}$$

$$Approach = T_D - T_{C(wb)} \tag{3}$$

$$\eta_w = \frac{\dot{Q}_{actual}}{\dot{Q}_{ideal}} = \frac{T_A - T_B}{T_A - T_{C(wb)}} \tag{4}$$

As discussed, the water flow rate affects the range of the cooling tower, thus, as indicated in equation 4, it also affects the tower's efficiency. It is thus vital to consider the implications of these parameters when evaluating the performance regarding energy usage.

2.4.4 Bulk Air Coolers

Bulk air cooling is the cooling of the entire mine (subsurface) through a centrally-located unit. These units are installed to provide better subsurface ambient conditions year round, as previously discussed. The coolers are located near the shaft and inject the cooled air below the main cage loading area in the shaft. This cooling, in addition, removes heat from the wall rock throughout the mine. The cooling load is often wasted on upper levels due to smaller heat loads.

The air in a BAC is generally cooled in a two-stage horizontal spray chamber. The water is sprayed throughout the chamber length, covering the entire cross section. A BAC operates on the opposite principle of a cooling tower. Here a heat load is transferred from the ambient air to the chilled water, while the air mass is additionally humidified through the process. Condensation occurs through the BAC due to the cold temperatures, resulting in additional water being added to the system, although in small amounts. Figure 14 shows the schematic of a typical two-stage BAC.

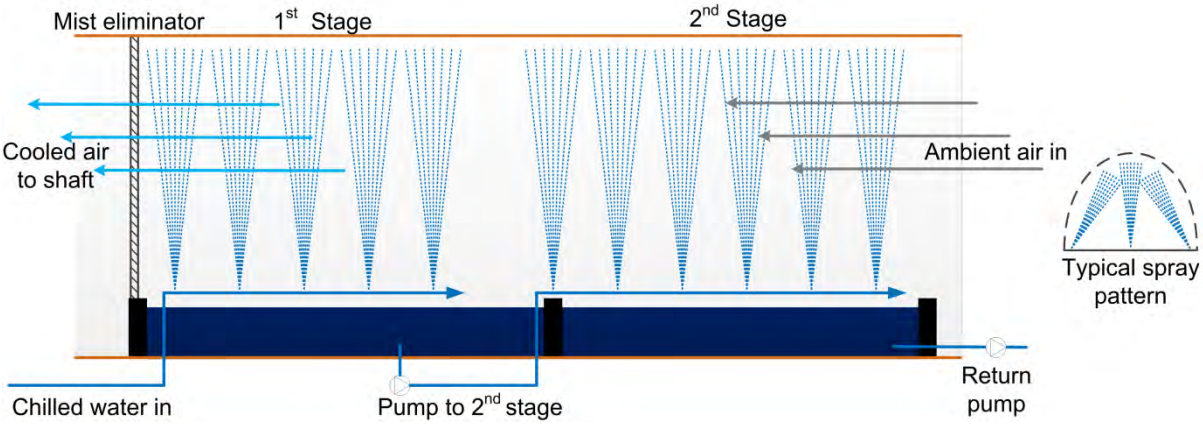

Figure 14: Typical schematic of a two-stage bulk air cooler (adapted from [7])

2.4.5 Heat exchangers

The two common heat exchangers used in the refrigeration process are shell-and-tube and plate heat exchangers [7]. Shell-and-tube heat exchangers are the most common used in mine refrigeration, where machines have a 700 to 1400 kW compressor power range. Shell-and-tube heat exchangers should not be expected to cool water below 3 ˚C. The larger chillers use plate heat exchangers, where the water can be cooled within 1˚ of freezing without the danger of rupturing [7]. Figure 15 and Figure 16 show images and typical schematics of a shell-and-tube and plate heat exchanger respectively.

Understanding the first law of thermodynamics is the first step in analysing a heat exchanger. This law is also known as the “conservation of energy” principle. The law states that energy can neither be created, nor destroyed during a process; it can only change form [43]. It is this change of form or transfer of energy that is applied in the heat exchangers.

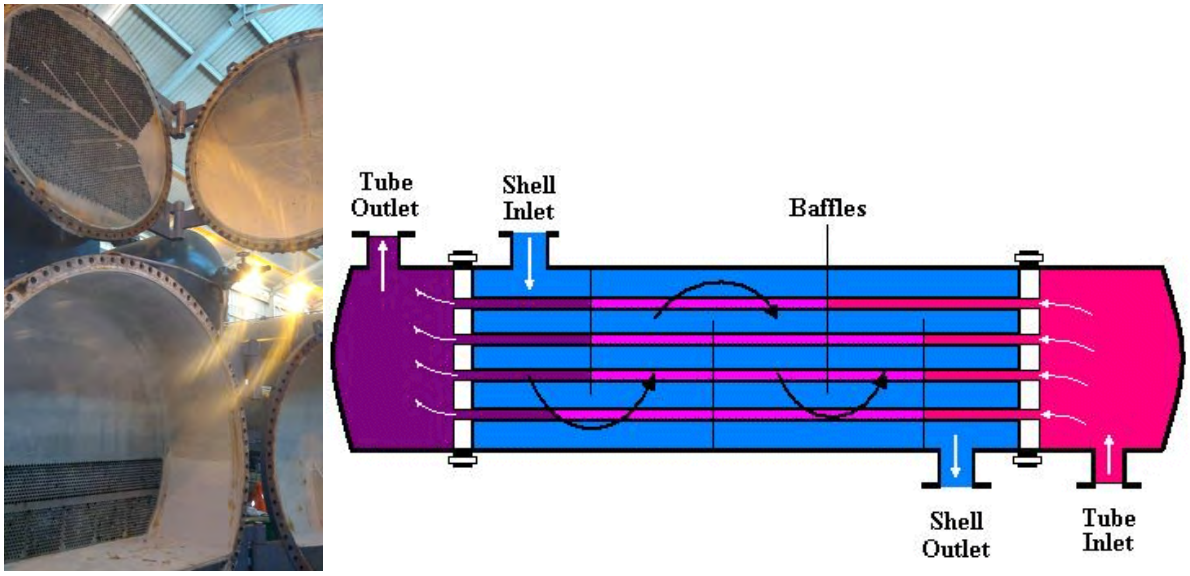

Figure 15: Image and flow diagram of a shell-and-tube heat exchanger [47]

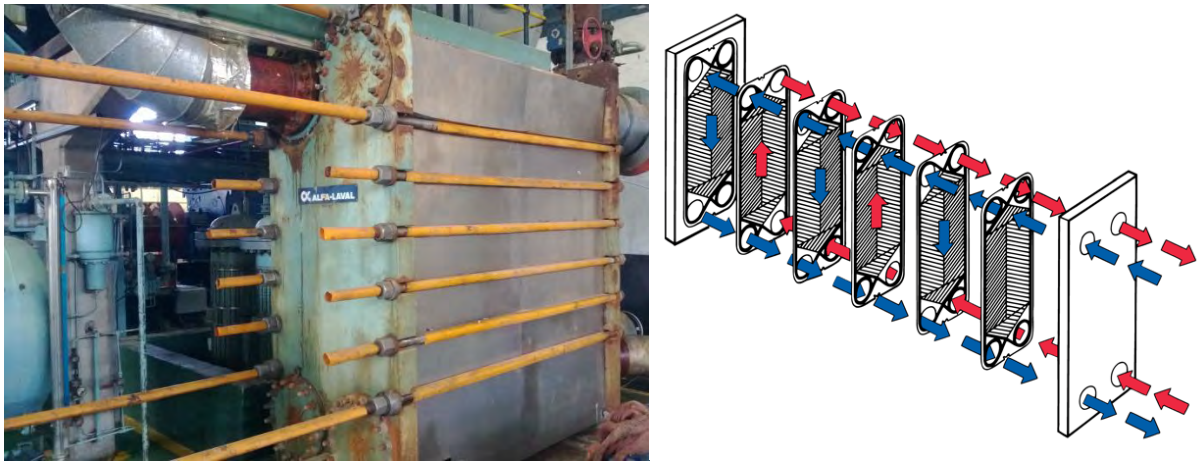

Figure 16: Image and flow diagram of a plate heat exchanger [48]

2.4.6 Pumps

The refrigerant in a chiller is moved through the system by the work output of the compressor, whereas water in the evaporator and condenser is moved by the work output of the pumps. These pumps are separate from the chiller, thus operating as auxiliary components. By not acting directly within the refrigeration cycle, they are components that can be separately controlled. A pump’s motor speed can be adjusted by changing the

number of poles, or by changing the applied frequency. Changing the poles is a physical change, requiring the rewiring of the motor. This results in a step change in the speed [9]. Changing the frequency applied to a motor results in less current being drawn by the motor, thus reducing its power and speed. The set-up of the pumping system on chillers affects the type of control strategy one would consider implementing.

Typically two types of pumping configurations exist when directly applied to chillers: parallel pumps, pumping into a common manifold piping system supplying a network of chillers, and direct inline pumps, which are dedicated individually per chiller. Each system has its advantages and disadvantages. With parallel pumping there is always an additional pump to allow for continuous operation of all chillers, even if a pump fails. This, however, results in additional capital investment. There is, in addition, a pressure drop over the chiller range once water exits the common manifold, thus requiring valves to control the inlet pressure and flow at each chiller. With inline pumping it is easier to control the pressure and flow across each individual chiller by controlling the pump speed. However, if a pump fails, the chiller will be inoperable until the pump is fixed. Figure 17 below shows the typical performance curves of a centrifugal pump.

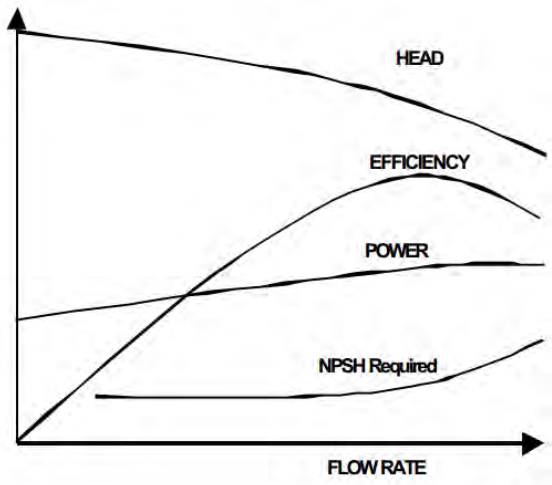

Figure 17: Typical pump performance curves of a centrifugal pump [49]

The mathematics which defines the curves indicated in Figure 17 is known as the Affinity Laws. The laws describe the physical change or resultant impact from changes in pump/motor speed, impeller diameter or system head. The respective laws state that the flow rate is directly proportional to the pump impeller speed; the pump head is proportional to the square of the flow rate and the pump power is proportional to the cube of the flow rate. These laws govern a simplistic method for determining the resultant electric power drawn by

a motor by changing specifications of the pump head, flow rate and/or impeller diameter. These laws are represented by the equations below [50], [51] and illustrated in Figure 18.

$$\frac{Q_1}{Q_2} = \frac{D_1}{D_2} \tag{5}$$

$$\frac{Q_1}{Q_2} = \frac{N_1}{N_2} \tag{6}$$

$$\frac{H_1}{H_2} = \left(\frac{Q_1}{Q_2}\right)^2 \tag{7}$$

$$\frac{P_1}{P_2} = \left(\frac{Q_1}{Q_2}\right)^3 \tag{8}$$

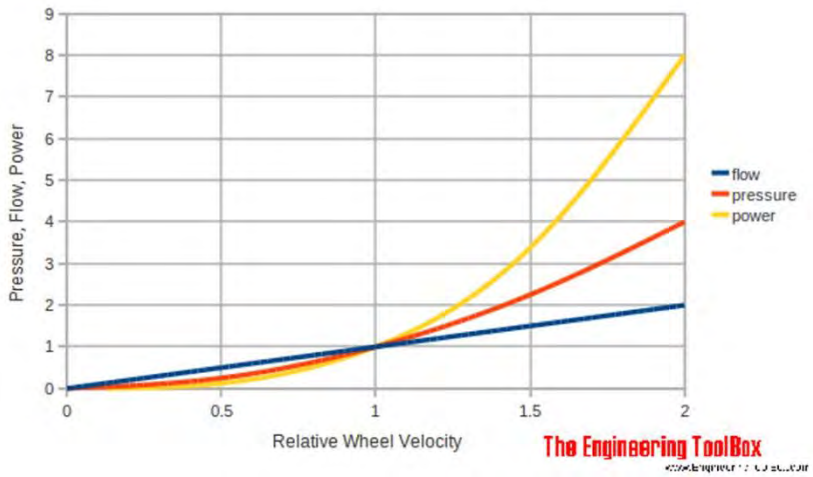

Figure 18: Graphic representation of pumping Affinity Laws for constant wheel diameter with the wheel velocity changing [51]

The life-cycle cost (LCC) of pumps should play a significant role when designing a system. Important elements used for determining LCCs are purchase costs, maintenance costs and electricity costs. An LCC analysis was conducted on a selection of five pump types [52]. As shown in Figure 19, hydracell, centrifugal and sidechannel pumps display the lowest LCCs. The key principle observed from Figure 19 is that the LCCs can vary significantly by the type of pump used.

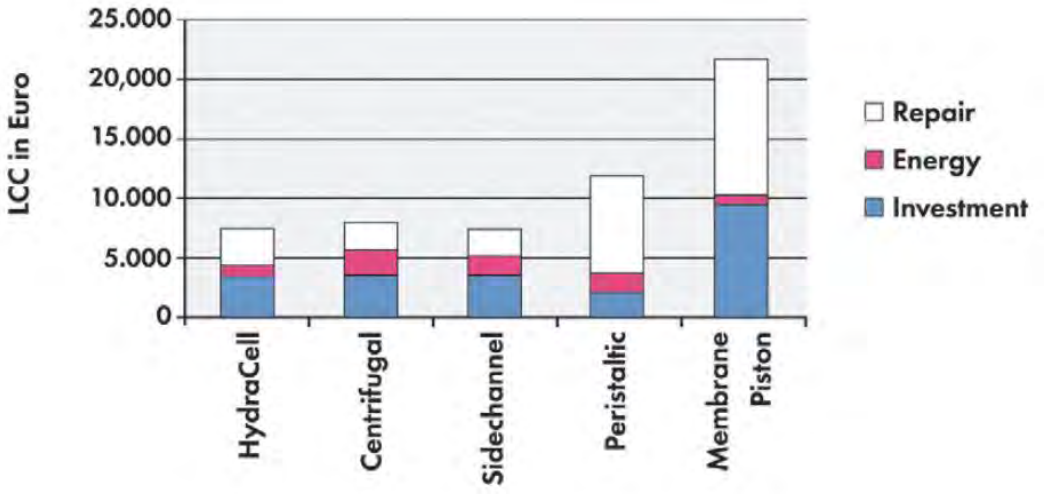

Figure 19: Life-cycle costs (LCCs) of pumps delivering 1.4m^3/hr at 5 bar [52].

As indicated in Figure 20, the control of centrifugal pumps largely affects the pumps' efficiency. This plays a limiting factor in controlling the pressure of a pumping system. In comparison, positive displacement pumps are able to achieve a much higher efficiency throughout the pressure/head range. Positive displacement pumps are, however, limited in size, thus centrifugal pumps are utilised more in mining applications. It is thus very important to select a pump with its peak efficiency operating close to the system resistance and flow requirements.

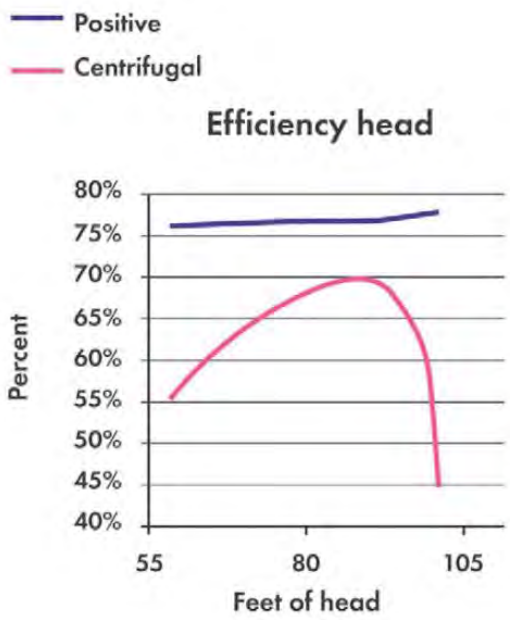

Figure 20: The effect of pressure variation on different pump types [52]

It is reasonable to deduce that sustainable pump operational efficiency is directly related to electricity savings [53]. These savings are also coupled with reduced maintenance time and costs and could be easily achieved by using pumps without seals. A result is less wear, especially where corrosive or abrasive fluids could have damaged seals. Seal damage could furthermore result in external damage to components where leakages occur. Reduced downtime from maintenance or breakdowns also provides less risk to the productivity of a plant.

Performance losses of pumps arise from lack of maintenance and partial load operations [54]. At approximately 40% of a maximum flow rate, vibration, radial load and excessive noise increases are experienced. An increase in electricity savings on a motor therefore results in possible inefficiencies on the operating pump. An increase in pump maintenance could also be seen. As can be seen in Figure 21, the maintenance of the pump impeller is vital in maintaining its efficiency. Planned maintenance will result in direct electricity savings where maximum potential flow is achieved.

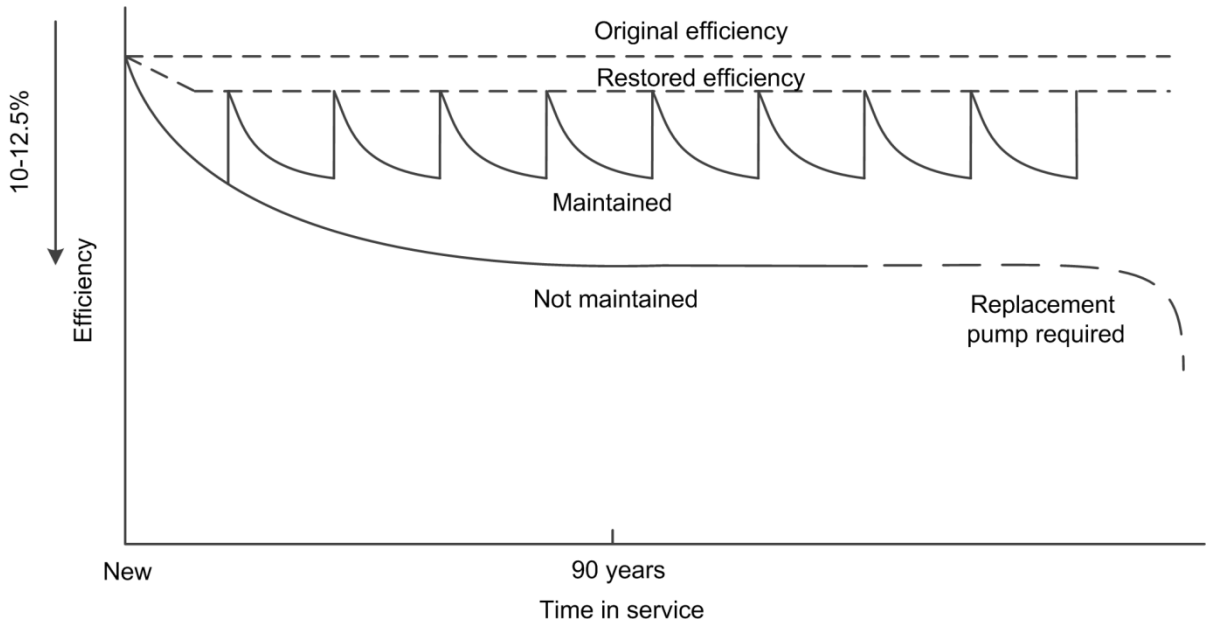

Figure 21: The effect of periodic maintenance on pump efficiency (adapted from [53])

Cavitation can result in extensive damage to pumping infrastructure. Cavitation occurs when a void/cavity is generated in a fluid [53]. This occurs when a fluid ruptures, as it is subjected to a pressure below a pressure threshold. This is due to a phase change in the fluid as the ambient pressure falls below the vapour pressure of the ambient temperature. These cavities expand to a large size and rapidly collapse, resulting in a sharp noise. Spots of high

temperature, coupled by shock waves, also result. All this contributes to a loss in pumping efficiency.

2.4.7 Chiller performance prediction

Empirical prediction models are developed to determine the energy performance of water chillers by using formulation and parameter estimation. These models are separated into two categories, namely gray-box and black-box models, where gray-box models are semi-empirical and black-box models are empirical. Lee et al [54] compared the accuracy of eleven empirical performance-predicting models on centrifugal chillers. The prediction accuracy of these models was evaluated using the coefficient of variation of root-mean-square error (CV) and the confidence interval (CI).

Performance prediction is ultimately practical when applied within a control scheme. Lu and Chen et al [55] developed a forecast scheme which proved to be cost-efficient when applied to a large HVAC system. This system was used as opposed to a lag scheme used in a general method. The scheme implements cooling load requirement forecasting, thus optimising the system ahead of the demand.

Navarro-Esbrí [56] presented a black-box model for a variable speed vapour compression refrigeration system. The model was based on a radial basis function (RBF) network. This model uses a feed-forward network. The inputs of the model include chilled water inlet temperature (T_{in}), condensing water inlet temperature (T_{in}), refrigerant evaporator outlet temperature (T_{out}) and the compressor motor speed (N). This results in a low-cost data requirement. It was suggested that such a model would be a useful tool for energy optimisation and fault detection and diagnosis. With a similar strategy, Romero et al [57] found the most accurate linear black-box model to operate with a Box-Jenkins structure.

Remote access and evaluation of systems allow for technical expertise to be applied to systems without the time delay of travelling to a site. An online supervisory control strategy was presented by Ma et al [58]. The system could predict environmental factors, energy efficiency of the system and the system's response to changes in control settings. The performance map and exhaustive search-based method (PEMS) was developed to source suitable solutions to optimisation problems. This model proved to have the same control accuracy as the genetic algorithm (GA) method. It additionally achieved a computational cost

reduction of 96%. The energy efficiency of the strategy, however, failed to impress with a most disappointing annual electricity saving increase of 0.9%.

These prediction models and methods are crucial in understanding the system capabilities of the EMS to be implemented. The potential for improvement of the program is shown by the prediction capabilities existing in practice. Although the EMS is a real-time system, knowledge of potential future operational conditions could open the gateway for full control capabilities of an entire chiller.

2.4.8 Chiller performance evaluation

The performance of a chiller can be determined by calculating its coefficient of performance. The COP of a centrifugal chiller is defined as the ratio of the evaporator cooling capacity to the compressor electrical power represented by equation 9, below [54].

$$COP = \frac{\dot{Q}}{W} = \frac{\dot{m}c_p\Delta T}{W} = \frac{\dot{m}\Delta h}{W} \tag{9}$$

The performance of an entire system is based on the total power requirement of the chillers and condenser and evaporator pumps and fans [59]. Chillers account for about 60%, while pumps and fans account for about 30% of the total power. An entire cooling system's performance is determined by calculating the system coefficient of performance (SCOP). This is defined as the ratio of the combined evaporator cooling capacity to the sum of the total electricity consumption of the chillers, pumps and fans (represented by equation 10, below) [59]. It can also be utilised to evaluate a single chiller and its pumps/fans.

$$SCOP = \frac{Total\ cooling\ capacity\ of\ the\ system}{Total\ energy\ consumption\ of\ chillers,\ pumps\ and\ fans} \tag{10}$$

A strategy for switching between an 'n' number of chillers is described by Yao et al [60]. Figure 22, below, shows the optimum point of switching from one- to two-chiller operation, as applied in a case study. This is determined by SCOP and COP with chiller operating status management. Significant savings were achieved when a switch point was applied at approximately 1896 kW. This indicates the importance of analysing the system SCOP and not just individual chiller COPs.

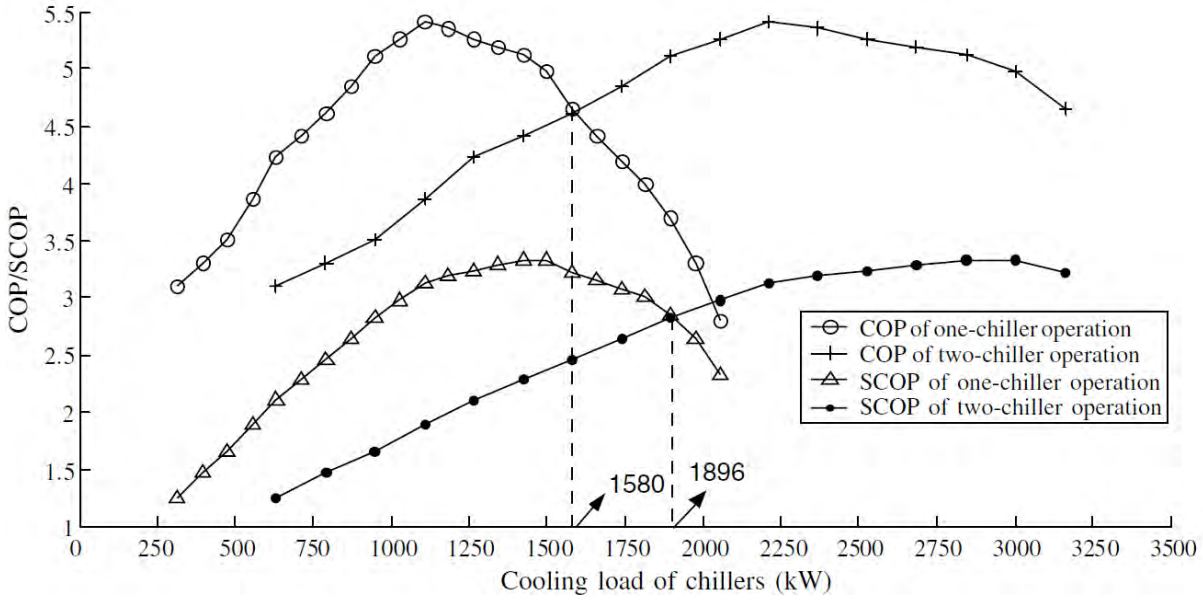

Figure 22: COP and SCOP of a cooling system under one- and two-chiller operation [60]

2.4.9 Chiller efficiency strategies

Various constructions of chillers and control methods are used throughout industry. It is vital to analyse these systems to be able to optimise the construction and control methodology of the plants. Control methodology can be applied across different chiller types. One can also change the construction, and thus operation, of a chiller to better suit the application.

Three pumping schemes were analysed by Tirmizi et al [61]. The systems were for a building's HVAC system. Variable speed pumping achieved the best electricity savings across a large temperature range. An important factor was the limited use of a backpass flow across the chiller. This avoided a low delta temperature across the evaporator due to a lack of circulated water. The other schemes included constant speed and a combination of constant and variable speed pumps. Both of these applications utilised the backpass flow available in the system. The electricity consumption of the worst and best system had an average variance of 45 MWh, or 14%.

Manske et al [62] developed a mathematical model of a large two-temperature level cold-storage distribution facility. Focusing on evaporative condenser sizing and head pressure control, it showed an annual electricity consumption reduction of 11%.

Yu et al [63] developed a thermodynamic model of an air-cooled screw chiller. By applying a variable speed condenser fan strategy, an increase in COP of 4 to 127.5% was achieved. Applying the model to an office building with a comparable-sized chiller achieved a 12.2 to 44 kWh/m^2 (5.6 to 20.2%) electricity saving. By applying a similar strategy to a water-cooled chiller in a hotel, Yu et al [64] achieved an electricity saving of 8.6%. Eight operating schemes were compared, including constant and varying speed control methodologies.

A novel cascaded refrigeration system was developed by Kairouani et al [65]. A vapour absorption system, supplied by geothermal energy, was cascaded with a conventional vapour-compression system. By changing the compression refrigerant between R717, R22 and R134a and using an ammonia-water mixture for the absorption system, a 37% to 54% increase in COP was achieved.

Inefficient use of existing infrastructure often occurs due to operation staff's lack of technical training and knowledge. Pelzer et al [66] developed a control and optimisation system to implement at such chiller sites. The system has the ability to simulate and optimise the existing installations. This system, when applied, results in significant electricity savings without the alteration of delivery temperatures.

Lian et al [60] developed an optimal operation model for a large cooling system with the aim of improving the SCOP. This model led to increased power usage by the individual chillers. However, when the entire system (pumps included) was analysed, electricity savings of up to 10% were reached with variable flow pumping.

A load-based speed control was developed by Yu et al [67]. The control was designed to focus on enhancing the electricity usage of a water-cooled chiller. The optimum design operation is where the speed of the cooling tower fans and the condenser pumps is controlled along a linear function of the chiller part load ratio. A COP increase of 1.4% to 16% was achieved with this control strategy. A 5.3% reduction in operating costs was seen when implemented at an office building, with a cost payback of within two years.

A variable-speed vapour compression model was developed by Navarro-Esbrí [68]. The aim of the model was to optimise the energy efficiency of a chiller. Using easily and cheaply-sourced data, an accurate prediction model within errors of less than 10% was achieved. It was determined that the compressor speed and secondary fluid inlet temperatures had the greatest influence on system efficiencies. Secondary fluid flow rates had, in addition, a very

small effect on the efficiency of the plant. However, fine-tuning these components will assist in the chiller's efficiency.

A fuzzy neural network controller was proposed by Tian et al [69], incorporating a backward feed system. The algorithm had capabilities of learning a system's functions and parameters. Controlled parameters used included the degree of evaporation superheat and temperature/pressure. Controlling parameters included the varied frequency supplied to the compressor and the position of the expansion valve. The multi-input multi-output (MIMO) system reduced its steady-state error from +-0.03MPa to +-0.01MPa by the sixth run, thus showing its capability to learn from the system and optimise it through continuous control.

2.4.10 Alternative cooling strategies

As discussed, sending chilled water and air underground does not supply sufficient cooling in extreme cases. Mines operating more than 3660 m below the surface fall into the category of ultradeep mines that require ice cooling [7]. Cooling capacity in the form of hard ice can remove 4.5 times the heat load as the same flow of chilled water. The COPs of these ice systems have become competitive with traditional cooling methods with improved technology.

Bellas et al [70] analysed applications of ice slurries throughout various industries. These applications include comfort cooling, food processing and preservation, as well as possible future applications. As the strategy is proving itself in many technical applications, suitability in the mining sector is easily realised.

Mine cooling is part of the comfort cooling application, as it assists in improving working conditions. Ice slurries sent underground provide a larger cooling capacity per volume when compared to chilled water, thus significant pumping savings can be achieved [70]. The heat loss is, in addition, considerably less when sending ice slurry underground. This occurs when the ice melts before substantial heat loss takes place during transportation. Recent installations have included the production of hard ice for transportation underground, resulting in a higher cooling load being supplied per volume of transported material.

Ice can be produced on a large scale by establishing the triple point of water. This is where a vapour-liquid-solid (triple point) phase is achieved, as indicated in Figure 23, where there are many solid phases for water, creating multiple triple points. There is, however, only one triple

point where all three phases are achieved. The change of one solid phase to another is called an allotropic transformation [42].

IDE technologies developed technology capable of achieving the triple point of water. This is done by creating a controlled vacuum [40], [41]. As shown in Figure 24, the ice is removed from the mixture and pumped into the bottom of a secondary vessel. The ice solidifies at the top of this vessel, where it is scraped off by rotating blades. This ice is then transported to the shaft by means of a conveyor. This technology is presently operational at Anglo Gold Ashanti's Mponeng mine, the world's deepest. Mponeng is located approximately 40 km from where the case study is being implemented. This indicates the depth that mining in the region has extended to in order to reach profitable gold reefs. It thus shows the probability of such systems being implemented on the case-study mine during future operations.

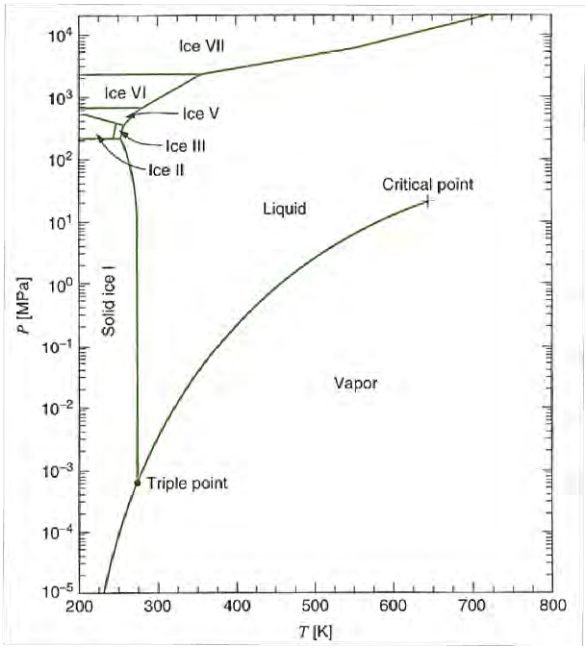

Figure 23: Water-phase diagram [42]

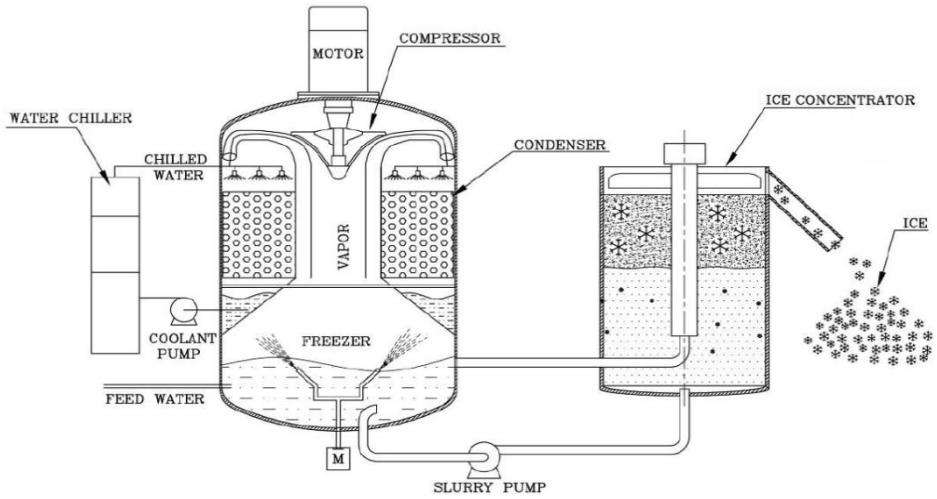

Figure 24: Flow diagram of a Vacuum Ice Maker for deep-mine cooling [41]

2.5 Electric motors

Electric motors are a vital component in any cooling system. They act as the driving components for all the mechanical working components (compressors, pumps and fans). It is thus crucial to optimise the motors and ensure that there are no unnecessary losses.

Motor design efficiency can only be reduced by intrinsic losses, which include fixed losses and variable losses [14]. Fixed losses, being independent of the motor load, consist of magnetic core, friction and windage losses. Variable losses, being dependent on the motor load, consists of resistance losses in the stator and rotor and miscellaneous stray losses. Figure 25 and Figure 26 show the typical breakdown of losses occurring in a motor.

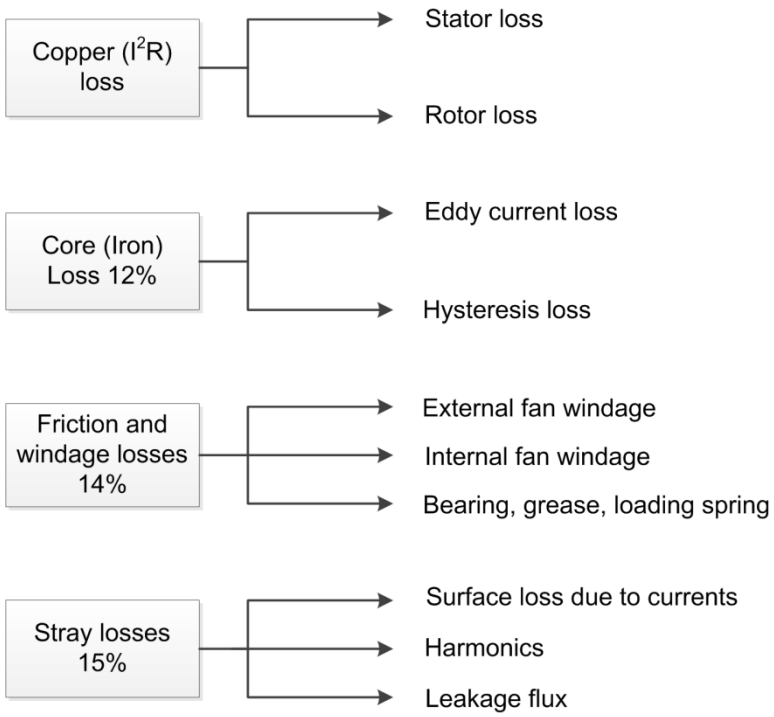

Figure 25: Typical motor losses [14], [71]

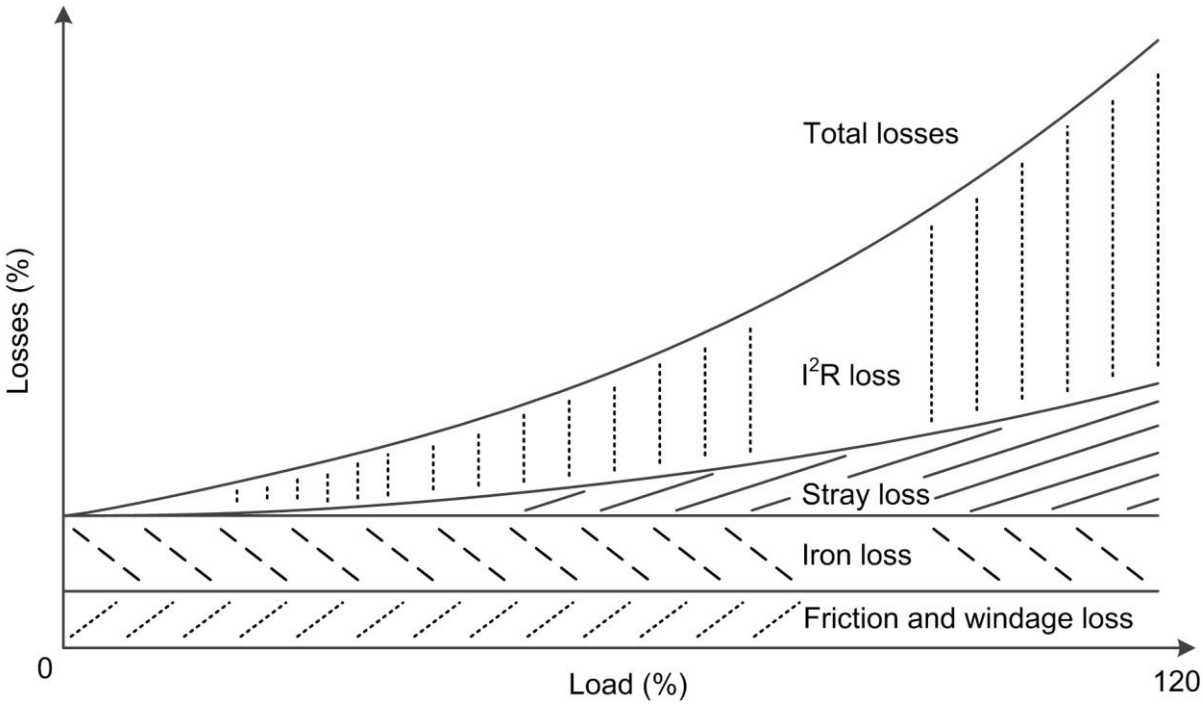

Figure 26: Respective motor losses with an increase in load (adapted from [14])

Hasanuzzaman et al [71] investigated the savings based on rewinding or replacing industrial motors. The efficiency of a rewound motor was shown to decrease by up to only one percent as the load rating of the motor increases. The replacement of standard motors with high efficiency motors (HEMs) showed a payback period of a half to two years. The HEMs' payback period could double (remaining within a two-year period) if operating conditions were reduced to 50% loading. Other sources showed a payback period of two to three years for the same strategy (where operating costs were inclusive) [14].

Ferreirra et al [72] similarly investigated the rewinding of squirrel-cage induction motors. Figure 27 represents a probable curve resulting from rewinding a motor. Here the motor is rewound to accommodate a lower load factor. As in typical designs, installations often have an unnecessarily high safety factor applied. This safety factor needs to be re-evaluated, where excess running costs result from high electricity consumption. Using the curve, the increase in efficiency and power factor is easily determined for the operating load. It was suggested that 30 to 50% of an equivalent HEMS motor be invested in the rewinding (for the operational loading), resulting in the realisation of a low-cost efficiency strategy.

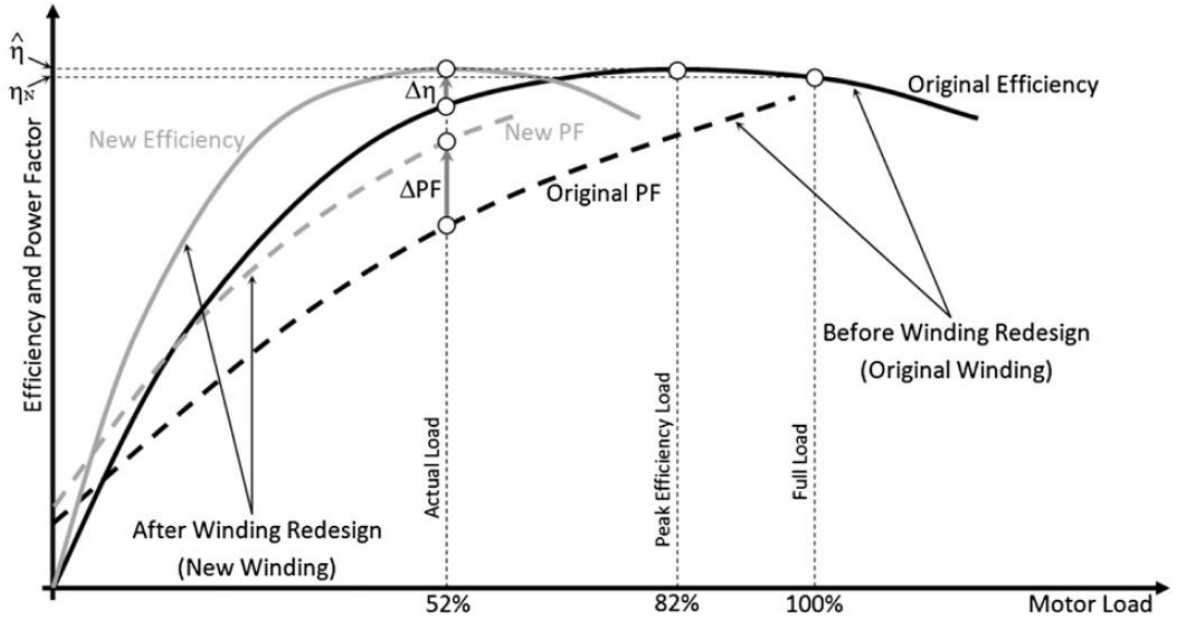

Figure 27: Motor efficiency and power factor as a function of motor load, before and after winding redesign [72]

Mckane et al [73] developed a methodology for determining the energy efficiency for industrial motors. The application of motor energy efficiency supply curves created a step curve to determine the cost-effective saving potential. As can be seen in Figure 28, the cost of conserved electricity is only viable for three to five strategies (all the strategies above the average unit-price line) on industrial pumps in developed countries. It was, however, determined that seven to nine strategies are cost-effective in developing countries. This is primarily due to lower labour and electricity costs.

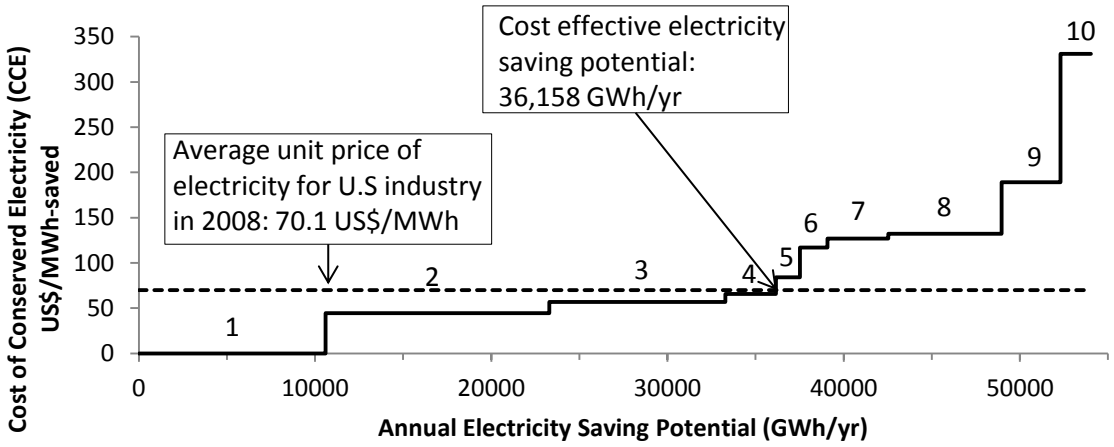

Figure 28: US pumping system efficiency supply curve (the cost-effectiveness of individual measures will vary, based on site-specific conditions) (Adapted from [73])

2.6 Need for Variable Speed Drive integration

2.6.1 Overview

The main function of a variable speed drive (VSD) is to alter the frequency of the voltage delivered to an electric motor. Motor torque is changed by altering the volts per hertz ratio (V/Hz). A new torque curve is created for any given frequency delivered by a VSD. This frequency range is anywhere between one and 50 Hertz. A constant maximum torque is achieved by keeping the ratio of applied motor voltage to supply frequency (V/Hz) constant. This is done by increasing the motor voltage directly with the frequency, which is commonly termed *constant volts per Hertz* control [9].

The use of VSD modules is implemented throughout commercial and industrial industries. This wide implementation of the technology is proof enough of its effectiveness. Its use varies from chillers used for HVAC purposes in large buildings to municipal pumping stations. The reliability of VSDs is demonstrated with successful implementation at national strategic points [10], [11]. On mines their application varies across conveyors, hoists, draglines and shovels, grinding mills, compressors, pumps and fans [12], [13].

VSDs offer a wide range of benefits other than the achievable energy savings. These include smoother start-ups (ramping up the motor speed), similar continuous control and planned stops, fast diagnostics of potential problems, continuous motor monitoring and motor protection through safety trips [15]. Softer start-ups, in addition, prevent start-up current spikes, which can typically be up to 500% or more than the motor running current [16]. The intelligent functions of these drives constantly increase and include processes such as an anti-jam feature on pumps, where the motor is placed in a series of forward and reverse runs to clean the pump impeller.

These drives are able to connect to networks via an Ethernet connection (or similar), or on some drives, even over wireless networks. This allows for remote monitoring and control. This results in simple monitoring and control and in less time being wasted on unnecessary site visits. Through the network, drives are able to calculate flows, monitor and even control according to specific set points [15].

2.6.2 Methods of speed variation and control

The concept of controlling the speed of a motor or its drive chain is not a recent development. Mechanical VSDs have been around for centuries, adapting to the modernisation of technology. These include belt drives, idler wheel drives, chain drives and gearboxes. Over time a means of hydraulic VSD have been implemented, mainly on turbines. Here the volume of oil in a shaft coupling determines the speed and torque that is transferred through the coupling [74]. The more recent control through electric VSDs has been implemented throughout industry.

Speed control through mechanical or hydraulic components adds to system inefficiencies. They also require the motor to operate at full speed all the time. These drives can also be noisy and difficult to maintain. Throttling the output of a full-speed motor has the same inefficiency effect as the other VSD mechanisms (mechanical and hydraulic) [8]. With all its benefits, it is estimated that less than 10% of pumps worldwide are equipped with VSDs [75]. The energy savings through electrical VSD control has thus a massive market to penetrate.

2.6.3 Electrical savings and payback period of installation

Motor savings achievable (%) through VSD control is determined by the cube of the motor speed. This is as the power draw is proportional to the cube of the motor speed (as previously indicated by the Affinity Laws). For example, a 20% reduction in motor speed will result in a 51.2% reduction in motor power (0.8^3) [74], [76].

$$S_{SR} = \left(1 - ES_{VSD}\right)^3 \tag{11}$$

The electrical energy consumption and savings can also be estimated using the following formulas [77]:

Load factor:

$$L = \frac{kW_a}{kW_r} \tag{12}$$

Electrical energy usage:

$$AEU = n \times P \times L \times hr \tag{13}$$

VSD energy savings:

$$AES_{VSD} = n \times P \times L \times hr \times S_{SR} \quad (14)$$

Or [13], [59]:

$$ES_{VSD} = n \times P \times hr \times S_{SR} \quad (15)$$

Payback period [78]:

$$PBP_{years} = \frac{C_{VSD}}{CS_{VSD}} \quad (16)$$

$$CS_{VSD} = (ES_{VSD})(ET) \quad (17)$$

2.6.4 Components of a VSD

The substantial advancements in electrical variable speed drive technology over the last decade have opened a window for effective control and energy efficiency. Most of these drives use pulse width modulation (PWM) to control the output frequency, voltage and current [74]. They consist of three main components, namely a rectifier, a regulator and an inverter. Figure 29 displays the systematic component layout of the components. Similarly, Figure 30 shows the circuit layout of the components.

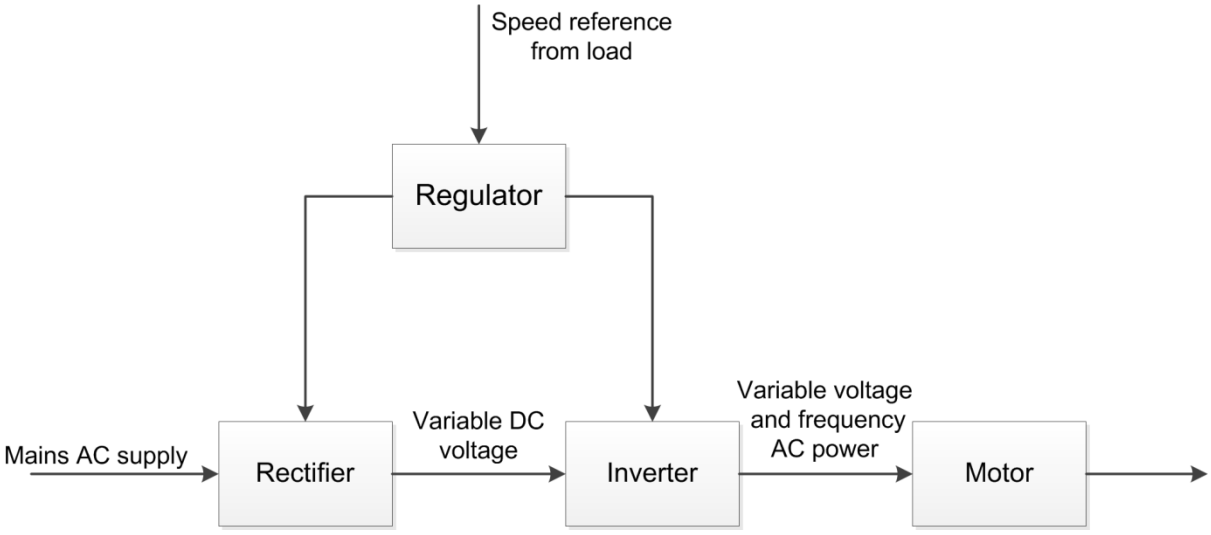

Figure 29: Components and control process of a VSD [14]

- **Rectifier [74]**

The rectifier is used to convert alternating (AC) current to direct current (DC). The two common medium voltage rectifier units are the diode and IGBT (insulated gate bipolar

transistor). The more common component in a rectifier is the diode rectifier, also known as the six-pulse width uncontrolled rectifier. Diode rectifiers have non-linear loads, where a non-sinusoidal current is received from the feeding line.

- **Regulator [74]**

A regulator acts as the control system for a VSD. It enables the exchange of data between the VSD and its peripherals, gathers and reports fault messages and subsequently activates the protective functions of the VSD (as previously mentioned).

- **Inverter [74]**

The inverter generates the AC current which is sent back into the electrical network. This is done by alternating the directions of a DC through the load. Most inverters have IGBT components. This structure results in a lack of parasitic body diode, which means that the IGBT requires a freewheeling diode to be placed across it. It is here that the PWM is used to control the output switches. This control results in pulses with a variable width, which constitutes a variable waveform.

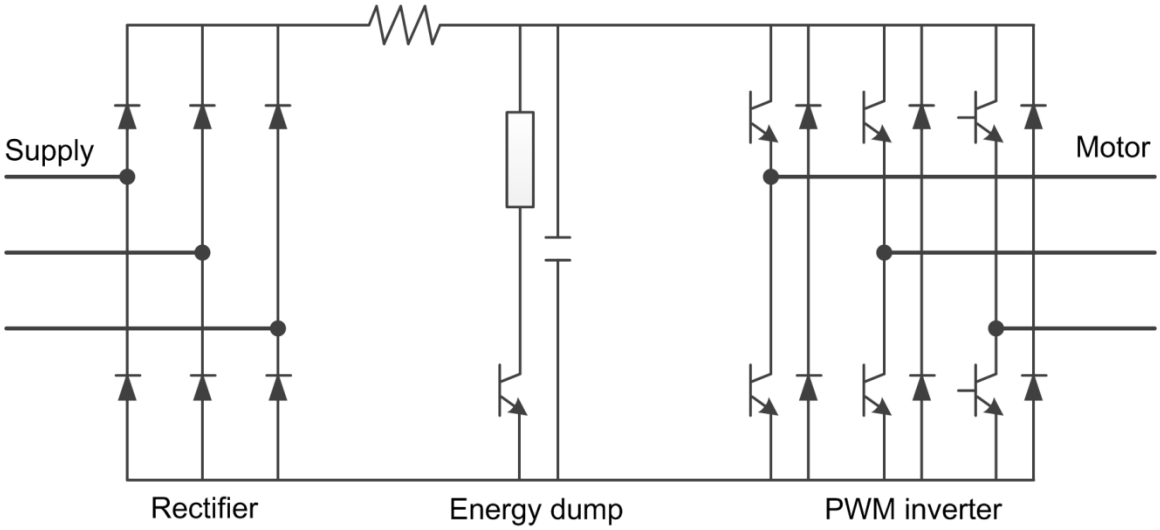

Figure 30: Common variable speed drive circuit [74]

2.6.5 VSDs and power factors

A common concern when installing VSDs into a system is harmonic distortion. This comes as a result of the non-linear load which consumes power in pulses [74]. This results in harmonic ripples being fed back into the power grid. Transmission losses result, as the grid must work harder to overcome this distortion. A bigger concern is apparent where other instrumentation is fed from the same electricity substation. As can be seen in Figure 31, the

higher the order of the harmonics, the more the current being fed decreases. This distortion is minimised by power factor correction (PFC) [78].

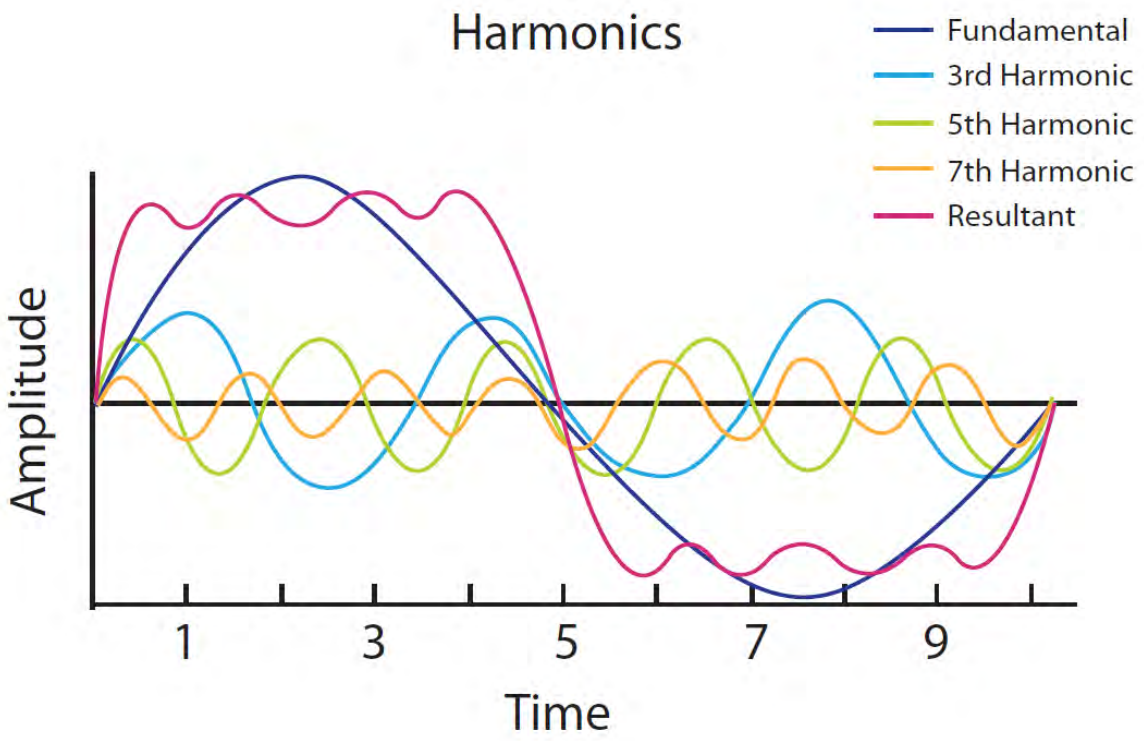

Figure 31: Fundamental (1st harmonic) current contribution at mains frequency (60 Hz), 3rd at 180 Hz, 5th at 300 Hz and 7th at 420 Hz [79]

The power factor is a dimensionless number that ranges from 0 to 1. It is the ratio of real/active power to apparent power (what is used by the device to the load present in the circuit) [14]. The power factor is an indicator of how efficiently electric power is being utilised. Mathematically the power factor is represented by equation 18 [14] and Figure 32. Typical harmonic suppression methods used for PFC include AC line reactors, DC inductors and active PFC [74]. Active PFC is the more versatile and sophisticated method for suppressing harmonics, which can raise a power factor (PF) up to 0.98 [79].

$$PF = \frac{Active\ power}{Apparent\ power} = \frac{P_r}{P_s} = \cos\theta \tag{18}$$

$$P_s = \sqrt{P_r^2 + P_q^2} \tag{19}$$

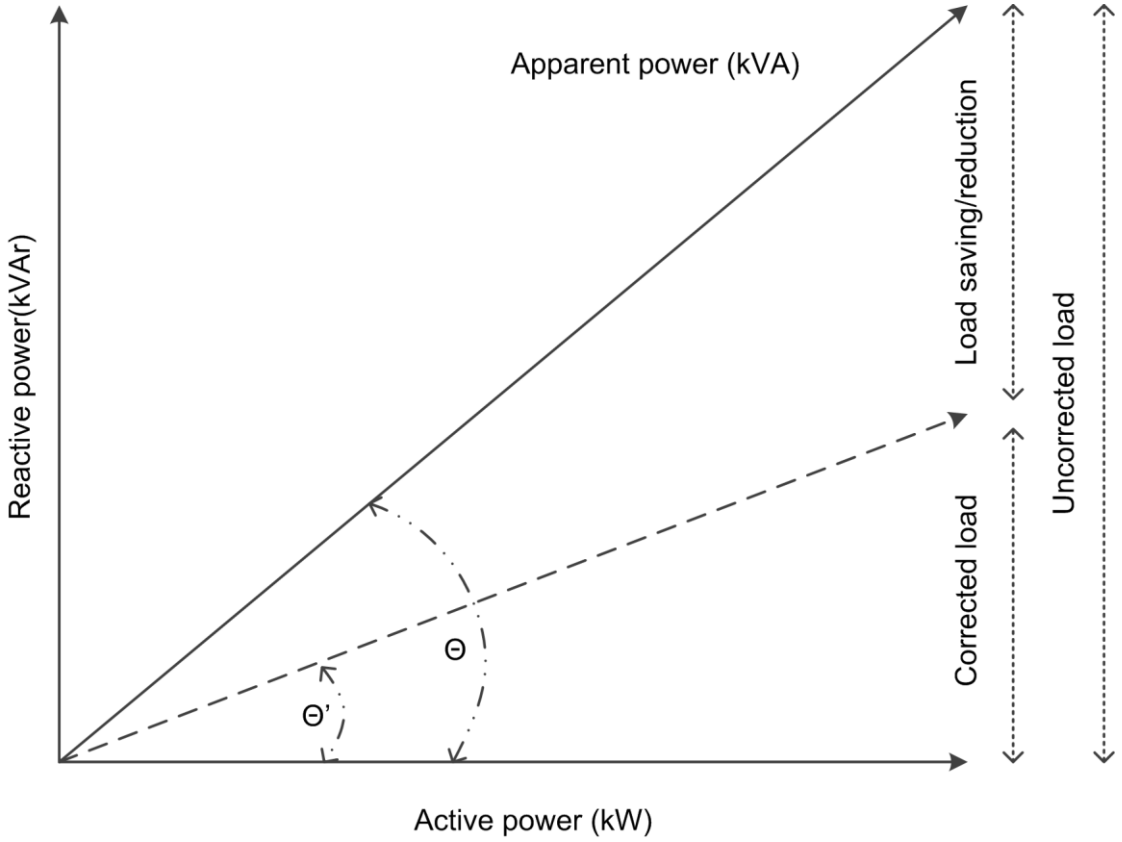

Figure 32: Illustration of the power factor components (adapted from [14], [80])

As a general rule the PFC installation should be placed as close as possible to the load which is being compensated [80]. It is also vital to not overcorrect a PF, as this may lead to over-voltage and insulation breakdowns.

It should be noted that the installation of a PFC unit is an investment, as is the installation of a VSD drive. The PFC unit will result in less electric energy being supplied by the utility to overcome the harmonic distribution. Less electricity costs will therefore be incurred over time [80]. A high power factor will also maximise the capacity of a power system, improve the voltage quality and reduce power losses [14].

2.6.6 Implementation strategies

Hartman [81] studied the concept of an “all-variable speed” plant. Here the chiller, its pumps and the cooling tower fans all had variable control capabilities. It was suggested that the life span and maintenance would be extended and reduced respectively for such a plant.

However, no data was available to support the claims. The potential electric energy reductions would range between 25% and 50%.

The possibility of converting a plant into an all-variable speed plant would require an analysis of the life-cycle costs [81]. Here the present plant's life cycle should be analysed and converted into a monetary value. This, compared to the potential savings, would determine the viability of such a retrofit. Another option is to install an integrated variable control plant when the life cycle of the existing plant ends. This would prove to be a viable option, as variable speed chillers are only slightly more expensive than constant speed alternatives.

The main difference between constant and variable speed plants is the peak chiller efficiency. With a constant speed plant the peak efficiency is reached at the maximum load, whereas an all-variable speed plant has its peak efficiency when all its components are operating at a partial load [81]. It was shown that an all-variable speed plant had a higher efficiency at all conditions, except for high outdoor wet-bulb temperatures and high load conditions. The main benefit, other than the obvious savings, is the redundancy that an all-variable speed plant provides. This not only protects the equipment from overloading, but also provides for additional cooling capacity during peak loading conditions.

Implementation of VSDs on chiller compressors was shown to have a poor payback period in South Africa, largely due to the high cost of medium-voltage VSDs. A potential payback period of 4.2 years exists within a large reduction in chiller loading. However, due to the large cooling demands on mines, this reduction is not realised. A typical reduced load could only realise a payback period of 15.5 years [82]. In addition, a minimum limit of 30 Hz should be applied on reciprocating compressors, as it could lead to noise, vibration and lubrication problems [83]. Throughout the development of variable speed compressor control the capital costs have remained high, while the control process has substantially improved [84].

Yu et al [10] optimised the condensing temperature control and varied the evaporator's chilled water flow rate of an air-cooled centrifugal chiller. The condensing temperature set point was adjusted according to ambient temperatures and chiller load. This led to a reduction of 16.3 to 21.0% in annual electricity consumption of a case study, resulting in a varied COP increase of 0.8 to 191.7%. It was noted that a minimum chilled water flow rate should be set, which would prevent water from freezing in the evaporator tubes, or scale building up in the tubes. This would, in addition, need to comply with the minimum tube

velocity and maximum rate of change of water flow. Such control was implemented for a 50 to 100% flow rate, and is adequate for a multiple chiller system.

As illustrated in Figure 33 and Figure 34, the COPs of a chiller operating at various ambient temperatures were higher across the range of part load ratios for the condenser temperature control. It is noticed that the COPs of both control methods increased when variable flow was applied to the chilled water. All cases had a constant chilled water-outlet temperature set point of 7 ˚C.

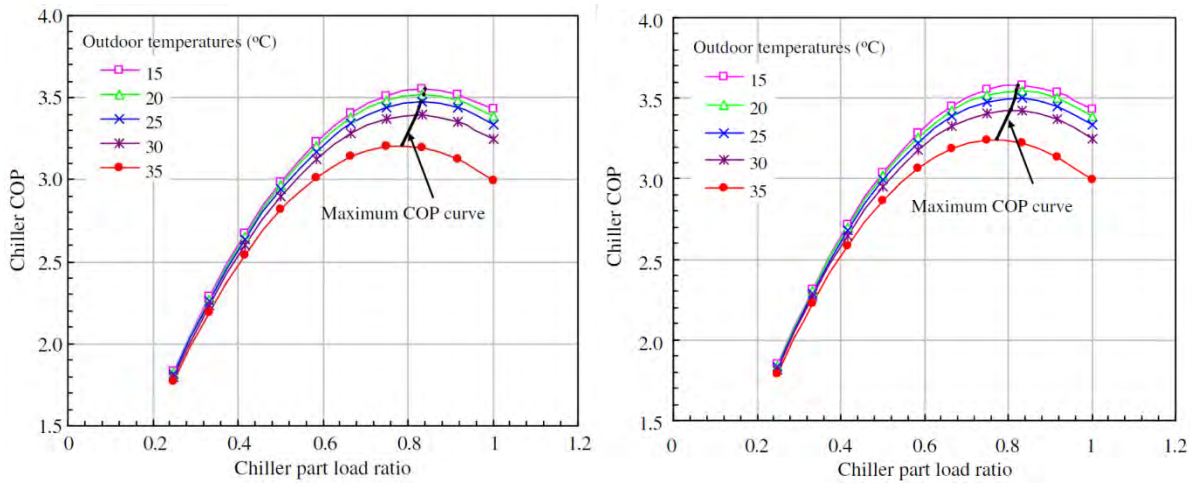

Figure 33: COPs of air-cooled chillers with head pressure control (left) and head pressure control with variable flow (right) [10]

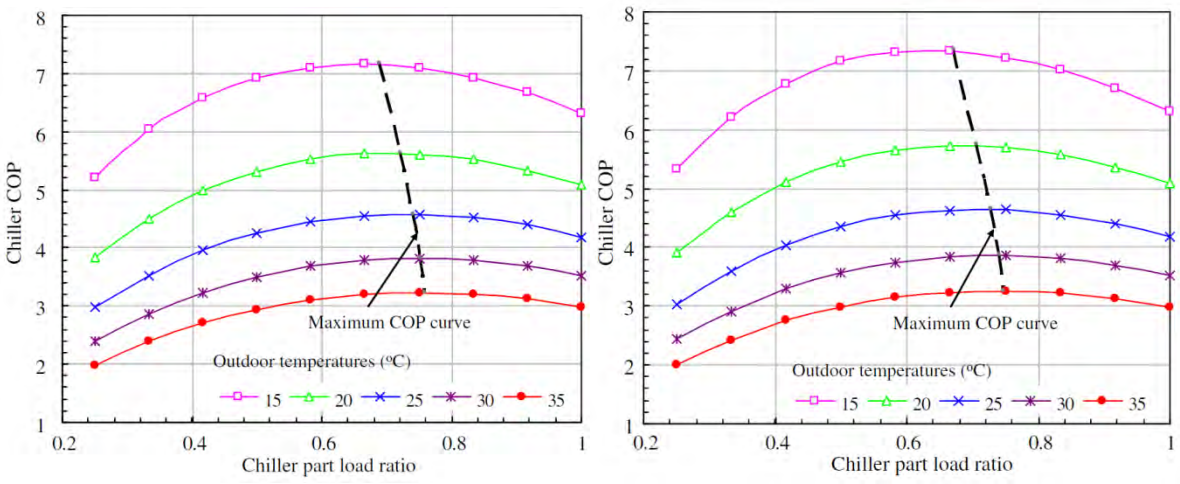

Figure 34: COPs of air-cooled chillers with condenser temperature control (left) and condenser temperature control with variable flow (right) [10]

Saidur et al [59] applied an energy audit on 16 buildings on a university campus. An estimated 51% of the entire electricity demand resulted from the combined HVAC system. By matching the system components with VSDs, a 68% saving could be reached on the chillers, with an additional 23.53 GWh of energy saved annually for the water supply pumps, condenser pumps and cooling tower fans. A 50% and 60% speed reduction was applied to the chiller and auxiliary components respectively. The highest energy savings and fastest payback period was found to exist within the auxiliary components' speed reductions.

A centrifugal pumping system is limited to the system pressure, thus a minimum motor rotation speed should be determined. This will also place a minimum limit on the frequency applied by a VSD. Should a pump operate at lower than the required rotation speed, the water would simply swirl within the tubes. This directly results in wasted energy and the overheating of the pump [85]. Preventing such operating conditions requires an open-loop VSD controller. As such a pump will be switched off if it no longer contributes to the flow in the system. Such a controller is best suited for a single-pump system (per stage or level).

Thirugnanasambandam et al [77] applied a 60% speed reduction on LT and HT motors used on a cement plant. Initial analysis revealed that motors were being operated at 3 to 16% of its load capacity. The speed reduction was realised by installing VSDs on the motors. An annual savings of 1 865.93 GWh and 4 600.39 GWh was estimated for the LT and HT motors respectively. Due to low levels of energy savings, it was found to not be economically viable to install both LT and HT capacitors to improve the power factor. As can be seen in Figure 35 and Figure 36, the efficiency and power factor relationships follow the same trend when plotted against the motor load.

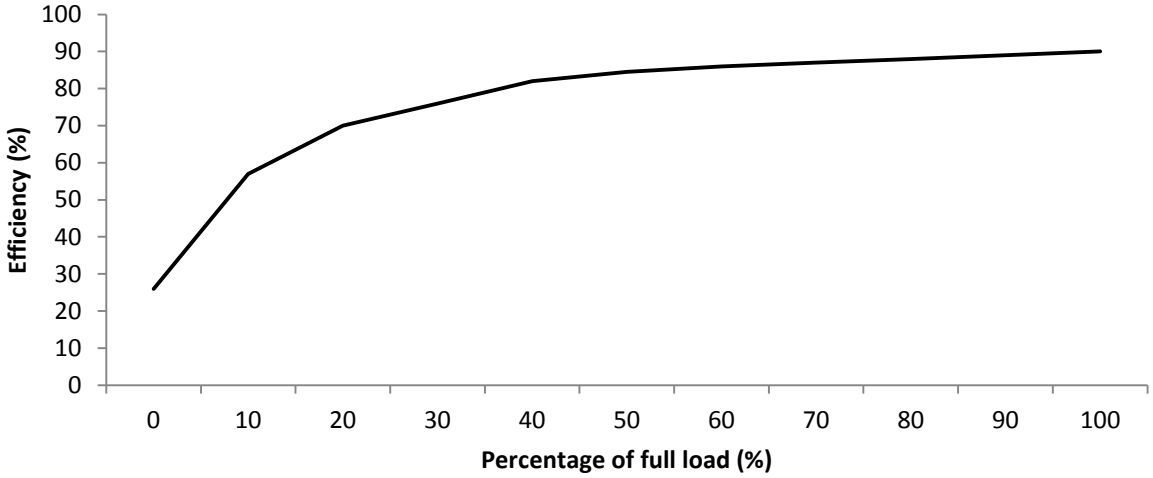

Figure 35: Relationship between motor loading and efficiency at partial loads [14], [71]

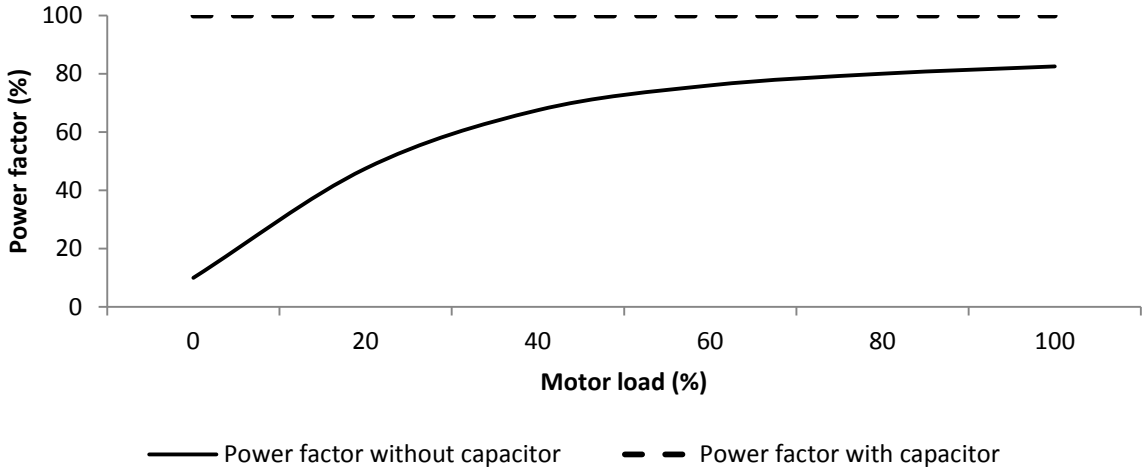

Figure 36: Power factor improvements by using capacitors for partial motor loads [86]

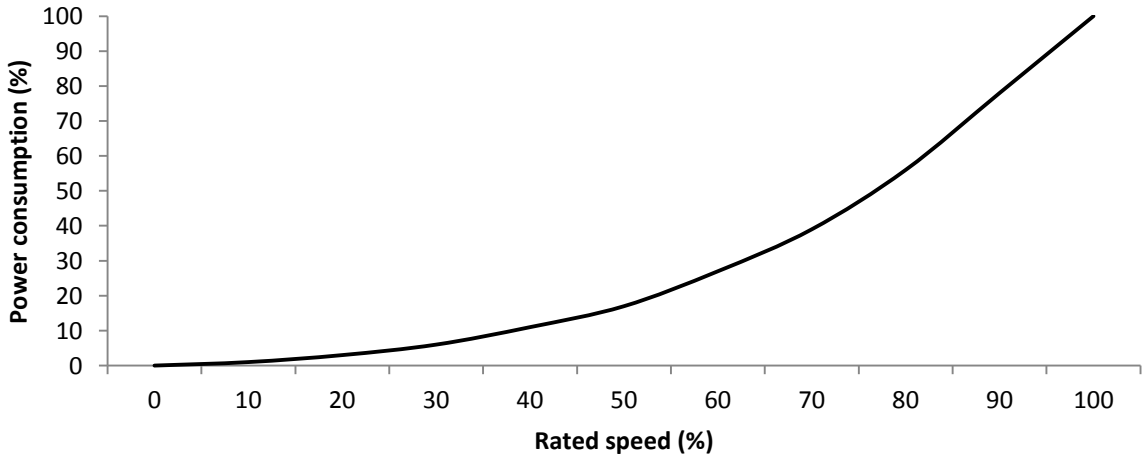

Figure 37: Relationship between motor power reduction and rated speed [86]

Saidur et al [86] realised a payback period of one to three years when implementing energy-efficiency strategies on larger motors through VSDs. The study also concluded that payback periods decrease as the rating of a motor increases. Similarly, an increase in speed reduction reduces the payback period. Saidur et al [78] concluded in another study (in a public hospital) that the quickest payback period of smaller motors is at 60% speed reduction. At this speed 33% of energy use can be reduced. Within the range of smaller motors the larger motors were observed to have a shorter payback period.

A national level integrated resource approach was analysed by Al-Mansour et al [87] in an industrial sector. His projections for an intensive strategy indicated that HEMs would have doubled in market share by 2010, up to 75% by 2015 and above 80% by 2020. It was concluded that Kyoto protocol targets were achievable within industry without loss in economic performance. The approach indicated that an average of 4% efficiency improvement was achievable by implementing HEMs. The larger portion of the Kyoto targets was, however, achievable with an efficiency increase of 32% through VSDs.

2.6.7 Installation costs of VSDs

Data obtained from mines A and B is shown in Table 5. This data reflects projects where electricity savings were achieved through the installation of VSDs on the auxiliary components of the chiller plants. As can be seen by the number of VSDs, the installation cost is linked more to the pumping infrastructure than the cooling capacity of the plant. The number of VSDs installed on the pumps is, in addition, site-specific and should be compared to the electricity savings achievable. The costs include all contract work related to the installation (site establishment, induction, PLC programming, installation, etc.).

Table 5: Cooling auxiliary installation costs

Mine	Cooling capacity of chiller plant (kW)	Evaporator pumps		Condenser pumps		Installation costs (Excl VAT)	VSDs installed	
A	39 000	6	110 kW	6	160 kW	R 2 847 684	6	110 kW
							3	200 kW
							3	75 kW
							2	70 kW
							1	55 kW
							1	40 kW
B	53 200	4	90 kW	5	185 kW	R 1 995 886	3	200 kW
							3	90 kW
							2	75 kW

Chapter 3 – Cascaded system energy and control audit

3.1 Introduction

A reasonable knowledge base of the respective principles and components has been developed through the analysis of various literature. This provides a platform for an analysis of now familiar systems and their auxiliaries. Throughout the chapter the chiller plant will be investigated and analysed. This will provide a data reference for later in the report and will highlight points where the system can be improved or modified.

A range of energy-saving projects have already been implemented at the case-study mine. These include underground pumping and surface fridge plant automation, control and optimisation. With the monitoring platforms installed on these projects, electronic data can be analysed to identify possible future projects.

It was decided during an initial investigation that March to May 2011 would be used for the energy audit. These months include a variety of operating conditions spread across about two seasons. A conclusive data set will thus be available. The data logged during these three months will be used as a reference baseline for the project. The baseline will serve as a tool to measure the success of the implemented electricity savings solution. Data for the entire period for all the required data sets is available for analysis.

3.2 Chiller plant variables and constraints

Throughout the implementation of a new system, or an integration of multiple systems, one should understand the functionality and limits that exist. A set of chillers exists on the case study's cooling plant, which is to be investigated. The network that it feeds and gets fed by needs to be separated as a functional system. Figure 38 illustrates the chiller plant, its piping and dam network that exist on the mine's surface operations. The orange illustrations indicate infrastructure which was implemented after an initial investigation.

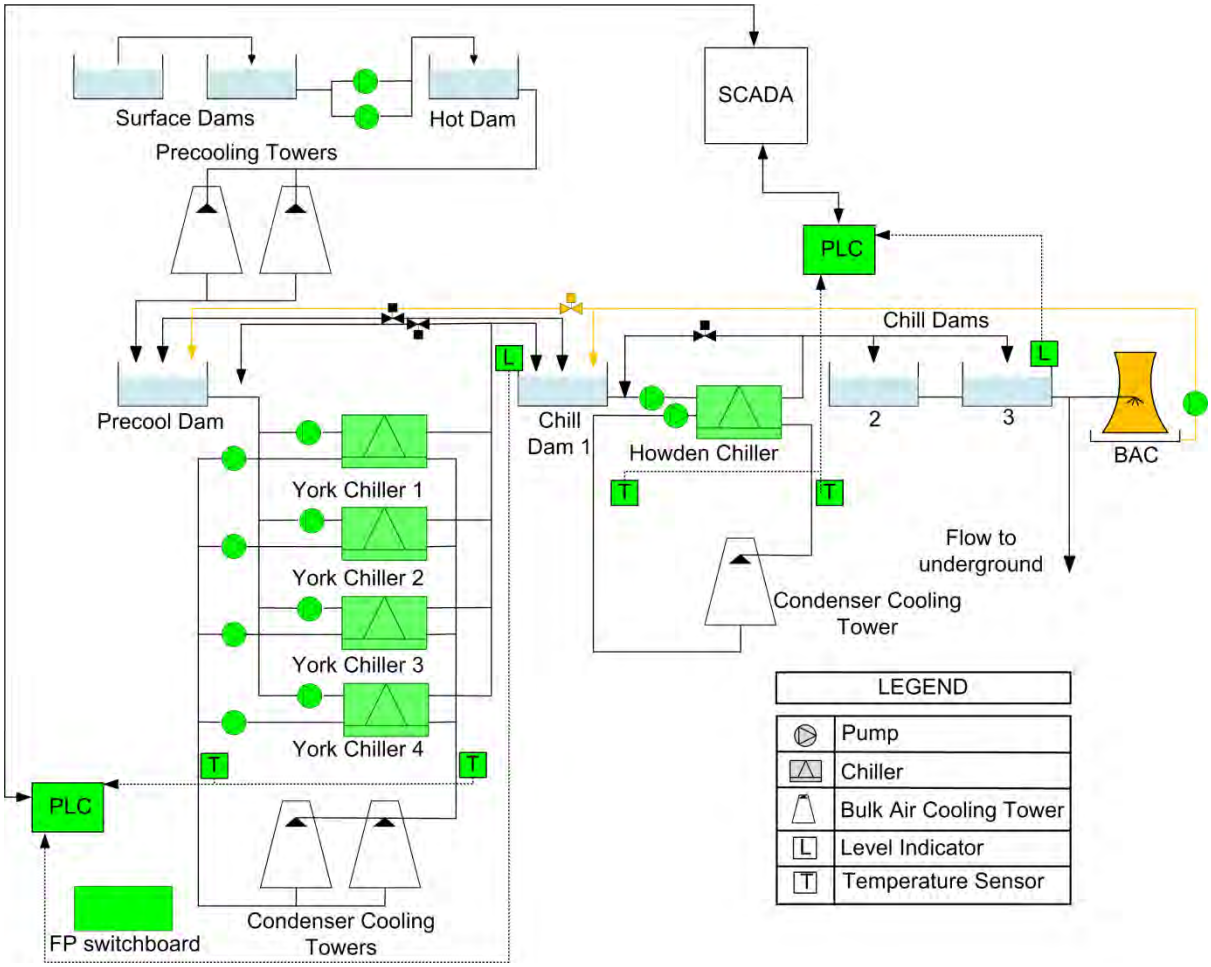

Figure 38: System layout prior to installation and post investigation

The general operating conditions are as follows: Hot water enters the surface hot dam at a temperature of 26 °C. From the hot dam the water is gravity-fed through precooling towers and pumped via sand filters into the precool dam. The average temperature in the precool dam is 20 °C. A total of 19 Ml/day is pumped from underground during an average summer and winter weekday.

The precooled water is pumped through four fridge plants in parallel to provide cold water at 8 °C in chill dam 1. From chill dam 1 water is pumped through an ammonia fridge plant to provide chilled water at 2.5 °C in chill dams 2 and 3. The combined nominal cooling capacity of the surface fridge plants is 26 MW. The combined COP of the surface fridge plants is 6 at nominal design conditions. From the chill dams (2 and 3) water is sent to the underground chilled dams.

The chiller system shown operates under a set of parameters. These parameters allow the plant to function under safe operating conditions. Conditions to be laid out were set during the design and installation of the original plant. Conditions, or parameters, will be classified into variables and constraints. Variables for this scope will be split into two groups, controllable and uncontrollable variables. Uncontrollable variables are ones that are set by the design limitations of each chiller and its components. They are maintained by PID loops that exist in each chiller's PLC. Controllable variables are ones that access to control will be provided for.

It is vital to be aware of all existing limitations. Knowledge of such information could assist in avoiding or analysing potential problems. Any of these limits could cause a chiller to 'trip', resulting in production loss of chilled water and possible damage to a plant. These safety controls are in place to prevent a plant from attaining permanent damage. Multiple trips on a single chiller will result in the chiller being 'locked', requiring the foreman to activate its operation after fault checking. Table 30 and Table 31 in Appendix C list the uncontrollable constraints of the York and Howden plants (here the uncontrollable values refer to the actual operational values, not the limits). These variables are more specific to the refrigeration process or its auxiliaries (gearbox, compressor, etc.).

All critical operational parameters on the chillers are monitored by instrumentation through a PLC to ensure the safe functioning. As these systems are already in place, no additional instrumentation is thus needed to monitor the operation of the respective chillers. These systems are checked and monitored by the plants operating staff. The parameters are listed in Table 30 and Table 31 in Appendix C.

Other variables that cannot be controlled and have a wide value range include the ambient air temperature and the precool dam temperature. Although the temperature of the water entering the precool dam can be lowered through the cooling towers, its drop in temperature across the cooling towers is still dependent on the ambient temperature.

The range of values listed in Table 6 and Table 7 are controllable. In the existing system the flows are controlled by valves. These flows in turn affect the respective heat transfer across the different chiller heat exchangers (condenser and evaporator). The PID loops in each chiller's PLC aim to maintain a set point value at each respective 'out temperature'. The respective condenser cooling towers aim to maintain low condenser water-inlet temperatures.

Table 6: York chillers' controllable variable ranges

York Chiller Constraints	High trip	High alarm	Low alarm	Low trip
Condenser water in temperature (˚C)	30	26	16	14
Condenser water out temperature (˚C)	33	32	20	20
Condenser water flow (ℓ/s)	330	320	280	260
Evaporator water in temperature (˚C)	25	22	12.5	11
Evaporator water out temperature (˚C)	16	12	4	3
Evaporator water flow (ℓ/s)	125	120	100	89

Table 7: Howden chillers' controllable variable ranges

Howden Chiller Constraints	High trip	Low trip
Condenser water in temperature (˚C)	30	12
Condenser water out temperature (˚C)	40	-
Condenser water flow (ℓ/s)	-	200
Evaporator water in temperature (˚C)	18	-
Evaporator water out temperature (˚C)	1.5	-
Evaporator water flow (ℓ/s)	-	200

The PID control loops for the evaporator water outlet temperatures are altered according to two seasons, namely summer and winter. The winter set points are functional for three to four months of the year, depending on ambient temperatures. As listed in Table 8, the York chiller's outlet set point is 8 ˚C in summer. This is due to the design restriction of the Howden chiller, which cannot operate with an evaporator inlet temperature lower than 8 ˚C (the Howden generally only operates in summer). This, however, reduces the loading on the York

chillers in the summer months, as the evaporator water outlet temperature will change from 5 ˚C to 8 ˚C.

The York chillers will still need to maintain their delta temperature, as the precool dam temperature will rise in summer. The York outlet temperature in winter indicates its lowest design outlet temperature. The respective temperature set points will result in the PID control changing the vane-angle set point of the compressors.

Table 8: Chiller evaporator PID control set points

Chillers' evaporator water outlet temperature	Summer	Winter
York	8 ˚C	5 ˚C
Howden	2.5 ˚C	Not operational

3.3 Electricity load defined by baselines

3.3.1 Overview

Through the analysis of a system and for the purpose of determining the availability of improvement, one must have a reference for determining the extent of success of said improvement. With the concept of VSD implementation on motors analysed, the primary result of such an installation would be reduced electricity consumption. As such an electricity-consumption baseline and variable data calculation formula are to be compiled.

3.3.2 Baselines

The electricity power data is separated into three sections: weekdays, Saturdays and Sundays. This separates the work and electricity tariff structures applicable to the mine. Figure 39 shows the baselines as separated by the three sections. As can be seen, the plant operation results in a more stable electricity consumption throughout the average weekday. During the weekends the consumption becomes very sporadic towards Sundays, indicating the periodic stopping and starting of machinery (due to operating schedules not being monitored by the foreman).

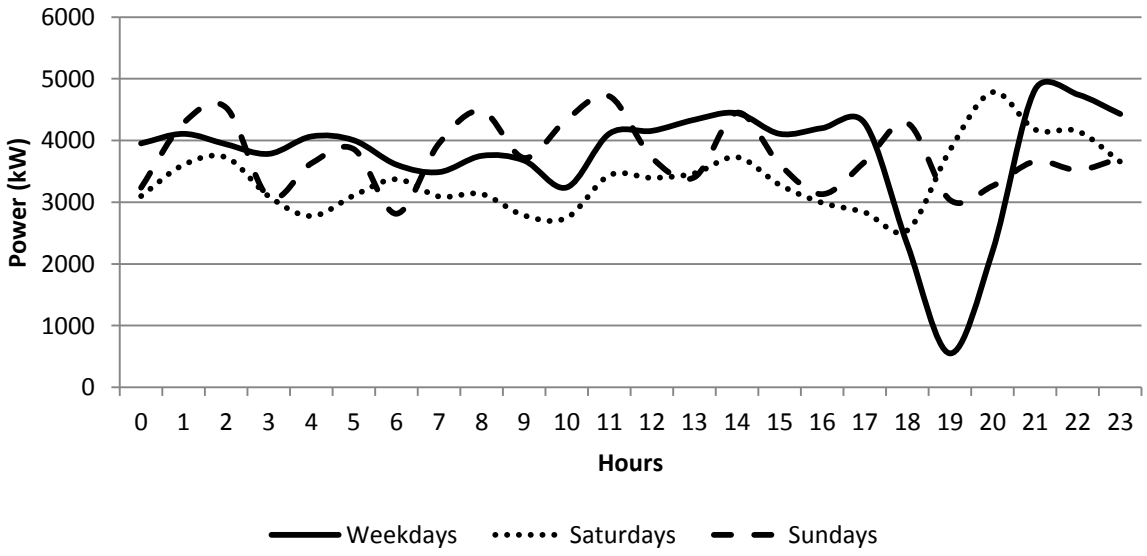

Figure 39: Average electricity demand for March to May 2011 compiled as baselines

Figure 40 to Figure 42 show the applicable baselines when plotted against the Megaflex tariff structure. As can be seen in Figure 40, an attempt is made to reduce power loading during the evening peak period. The halting of operations here shows room for improvement. It should be noted that reducing plant power consumption is just as important as selecting

the operational schedule of the plant. The sporadic operation on Sundays has no effect on the electricity cost of the plant. It does, however, show negligence towards the fatigue of the chillers through constant starting and stopping.

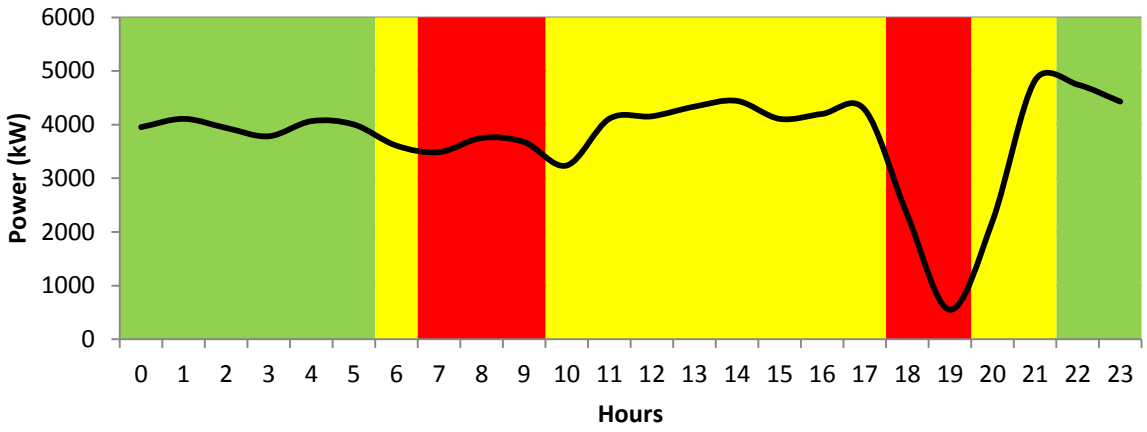

Figure 40: Average weekday baseline versus Megaflex tariff structure

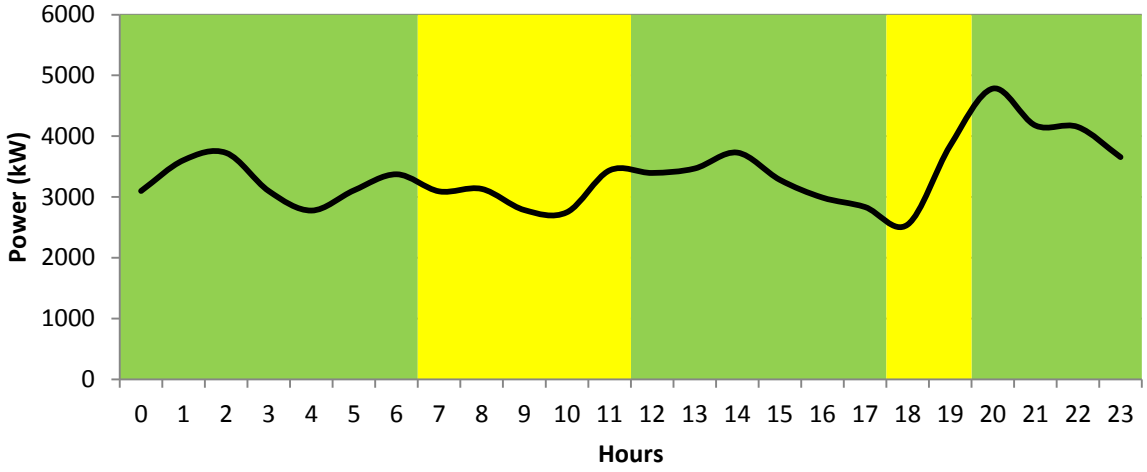

Figure 41: Average Saturday baseline versus Megaflex tariff structure

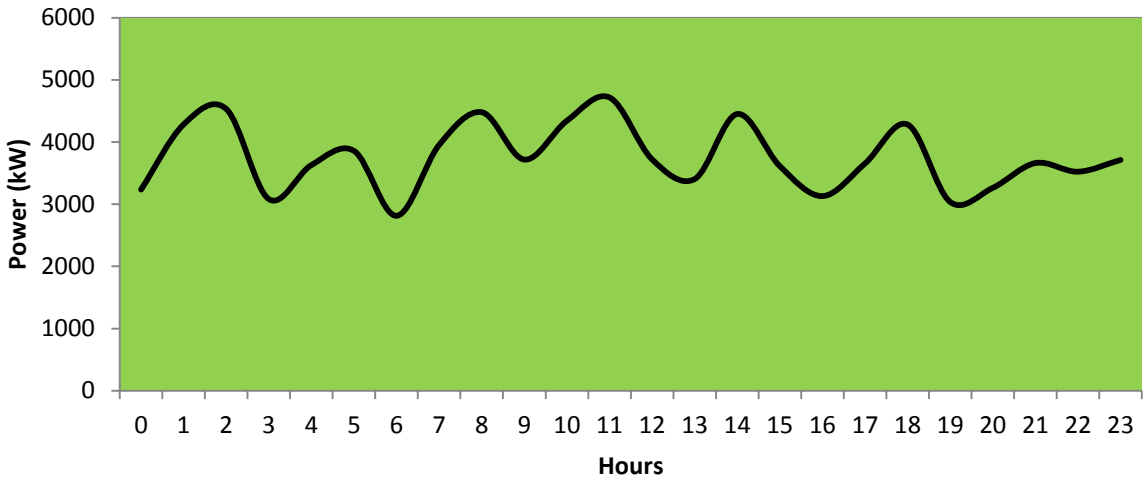

Figure 42: Average Sunday baseline versus Megaflex tariff structure

Power data for a year-on-year analysis is displayed in Figure 66 in Chapter 5.3. It is not displayed here, as no initial analysis is required.

3.3.3 Scaling of the baseline

The daily electricity consumption of the plant needs to be compared to the baseline post implementation of the project. As external variables affect the power consumption of the plant, they are used to determine what the baseline would have been on a specific day. Similarly these variables can be used to determine what a specific day's power profile would have looked like without any energy efficiency alterations to the plant. These variables fall into the category of how much power will be consumed to achieve the required cooling. In order to prevent biased scaling methods, a LINEST (Microsoft Excel) function is used to fit the variable data to the measured power data for the baseline period. A number of permutations of variables were considered. The one with the highest correlation (R^2) was selected. The equation obtained is as follows:

$$y = 0.002284a + 2301.297b + 6623.15c + 5550.693d - 120296.73 \quad (20)$$

$$R^2 = 0.77$$

This means that equation 20 has a 77 % correlation to the variables used to derive it.

Where y = daily electricity consumption of the plant (what it would have been)

	kWh/day
a = Flow rate leaving chill dam 3	litres/day
b = Ambient dry-bulb temperature	degrees Celsius
c = Precool dam temperature	degrees Celsius
d = Chill dam 3 temperature	degrees Celsius

The equation is based on average daily data for the three months of the baseline (March-May 2011). The following days were excluded from the data set:

- All weekends
- All public holidays
- Condonable data-loss days (7,8 and 21 April)

Any data presented or plotted, which is defined as having been calculated, is derived using equation 20, unless stated otherwise.

Data displayed in Figure 76, along with the calibration certificates shown in Figure 77 to Figure 79 in Appendix B, indicates the accuracy of the power (kW) data obtained from the system. All other data was obtained from data logged on the SCADA system.

Figure 43 shows the calculated baseline plotted against the actual baseline.

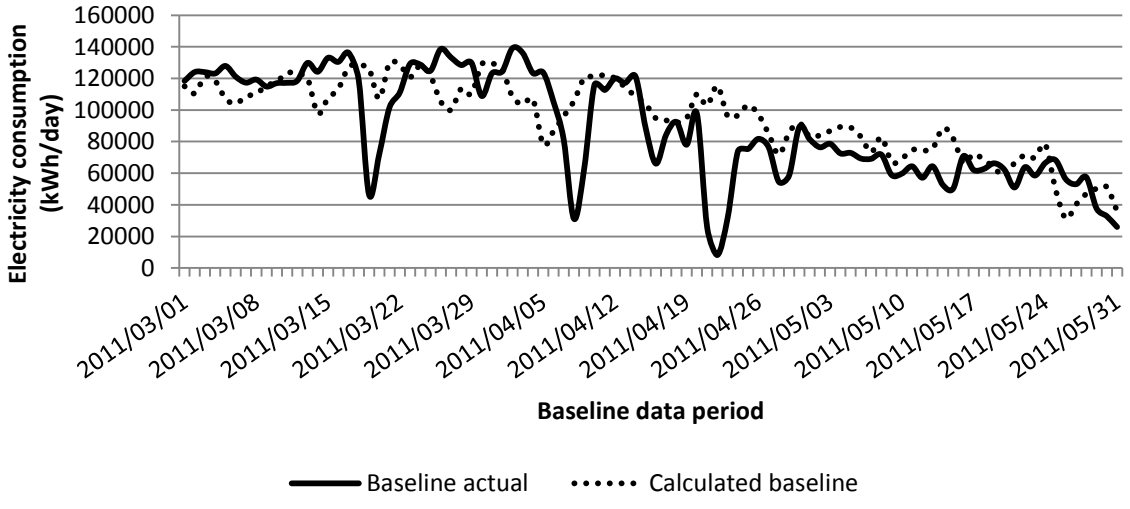

Figure 43: Baseline versus calculated baseline plot

This equation can thus be used to calculate what the electricity consumption (kWh) would have been per day. This will be done for each day during an assessment period. As can be

seen in Figure 43, the baseline covered both high and low electricity consumption periods. Equation 20 thus has a good accuracy range for any data to be assessed. It should be noted that this means of assessment will accurately indicate the respective power consumption for an increase in production (in the mine- and chilled water production).

Figure 44 shows the weekday baseline multiplied by a scaling factor to produce the average daily scaled baseline. The scaling factor is determined by dividing equation 20's output by the respective day's electricity consumption (kWh).

The scaling factor for Figure 44 is calculated as follows:

- Average hourly kWh for baseline period: 3 762.90 kWh
- Average hourly kWh of equation 20 for same period: 3 995.70 kWh

$$\frac{Calculated\ output}{Actual\ data} = \frac{3\ 995.70}{3\ 762.90} = 1.062$$

The scaling factor is thus 1.062.

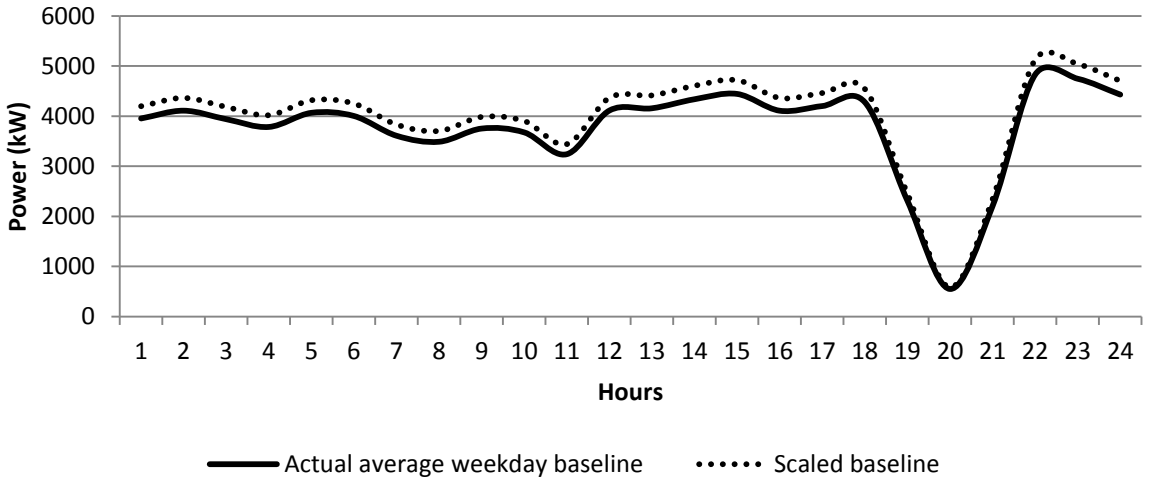

Figure 44: Weekday baseline plotted against the scaled baseline for the same period

3.4 System control strategy

The operating schedule of the chiller plant is a vital strategic optimisation point. Operation during the baseline period is to be analysed, indicating the possibility for improvement. A previous plant automation control system existed. It became redundant due to a lack of maintenance of mechanical components (Figure 45) and network links. This system started and stopped the chillers to maintain a set point level of the chill dams. The water flow through the plants was controlled with pneumatic valves.

Since the automated control was removed from the system, the plant has had no specific scheduling. The main reason for this is due to the lack of a constant service requirement (constant chilled water use underground). Chilled water is gravity-fed to the underground dams, where it is then used on the various mining levels. There is no system monitoring the underground flow, thus there is no means of determining the possibility of reduced consumption or wasted water (pipe leaks, etc.).

Figure 45: Non-functioning pneumatic control valve

A core focus of the plant scheduling is to fill the chilled water dams (chill dams 1, 2 and 3 in Figure 38). The York chillers maintain chill dam 1's level and draw water from the precool dam. The Howden chiller maintains chill dams 2 and 3, while drawing water from chill dam 1. Operators in the plant will manually switch individual plants on and off, ensuring that the dams never fall below critical levels (approximately 40% [2]). This operation focuses on flow through the plants. Since the automation stopped working, the flow through the plants has been controlled by manual valves (Figure 46).

[2] Danie Olwagen – Fridge plant foreman – Goldfields South Deep South shaft – September 2012

Figure 46: Manual water-flow control valve

While monitoring flow rates, the operators ensure that service delivery temperature requirements are met. Figure 47 indicates that the set points for the York and Howden chillers are 8 ˚C and 3 ˚C respectively. Figure 48, however, shows the different set point capabilities of the plant. As discussed, the Howden chiller cannot take in water colder than 8 ˚C. This can be seen in Figure 48, where chill dam 1's temperature remains constant and chill dam 3's temperature drops to about 1.5 ˚C in May 2011.

As discussed, the Howden chiller is switched off in winter months. The York chillers then produce chilled water at 5 ˚C. In the summer months the York and Howden chillers are set to

produce chilled water at 8 ˚C and 2.5 ˚C respectively. The data, however, indicates that these set points are not frequently achieved.

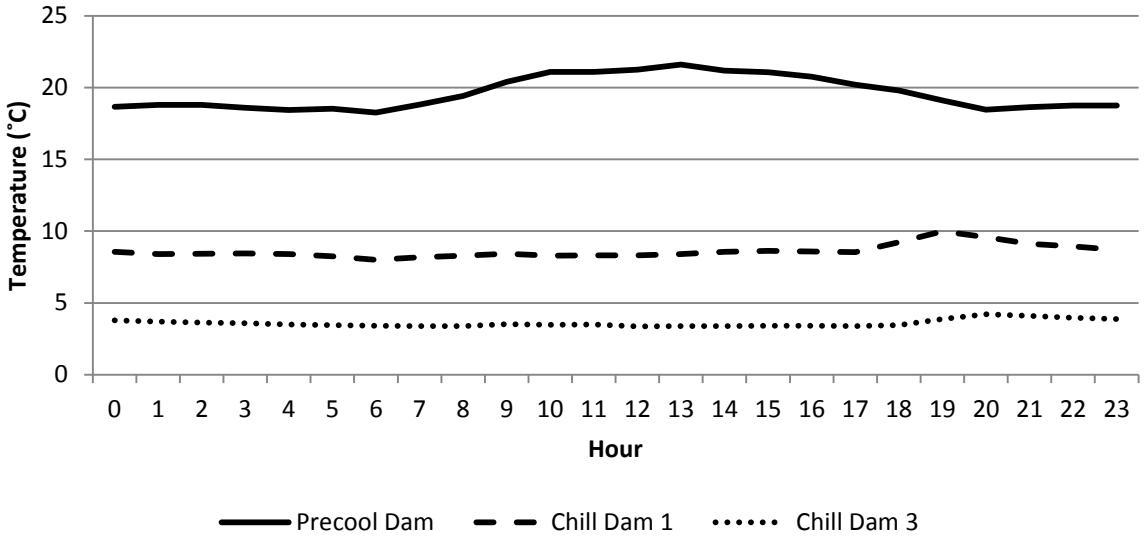

Figure 47: Average hourly storage dam temperatures during the baseline period

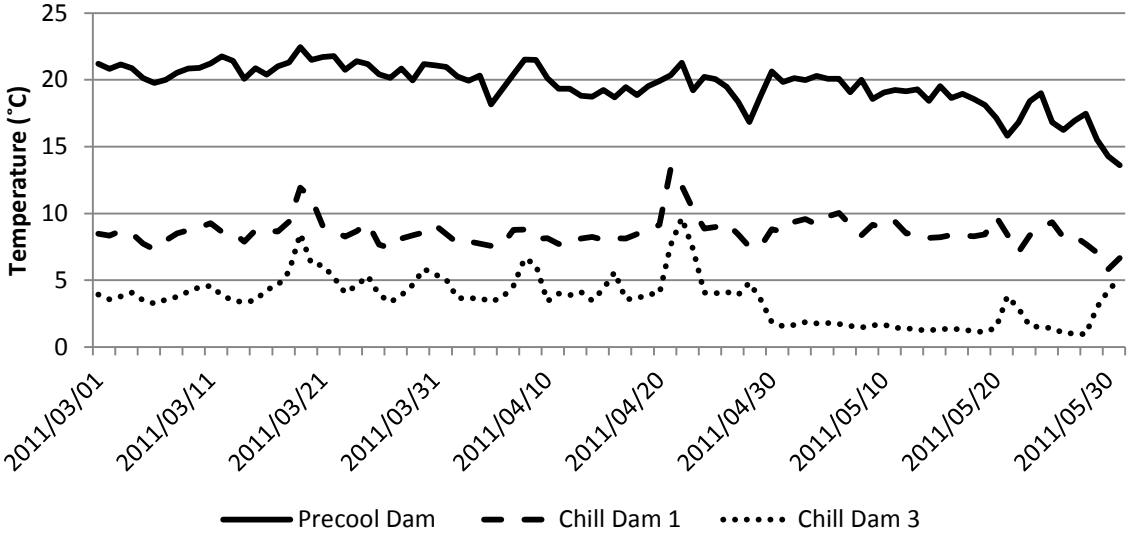

Figure 48: Average daily storage dam temperatures during the baseline period

From Figure 47 it can be seen that the temperature of the water entering the plant increases during the midday hours. This is due to the rise in ambient temperature during the day, as indicated in Figure 49. A result is less heat transfer to the ambient air in the precooling towers. This combination leads to the peak power consumption seen between 11:00 and 16:00. It should be noted that a correlation exists between ambient temperature and plant electricity consumption.

The spike in power consumption between 22:00 and 02:00 in Figure 49 is to 'catch up' on the cooling load that was reduced in the evening peak period from 18:00 to 22:00 (load-shifting). As previously discussed, the reduced load from 18:00 to 21:00 is due to the Megaflex tariff structure. Here the cost of electricity is more during national peak consumption hours.

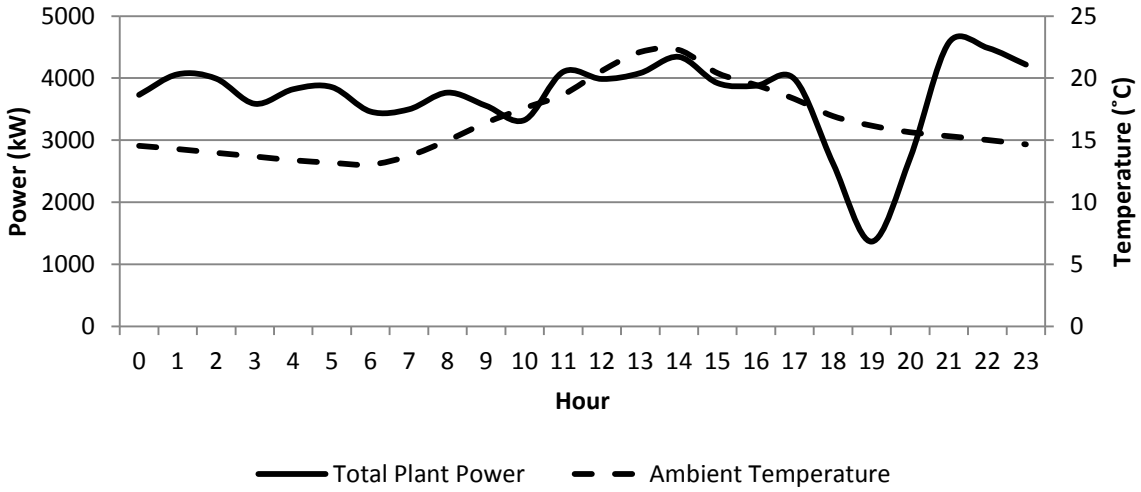

Figure 49: Baseline power profile plotted against average hourly ambient temperature over the same period

From Figure 80 to Figure 84 in Appendix D, it can be seen that a data cluster occurs above a COP of 7 at lower temperatures, indicating that the plant is operated more during the cooler temperatures of the day. This shows good logic, as less electricity load will be required to cool the water. This is also indicated by the COP values climbing above the 7 marker for all the chillers at lower temperatures. The reduced load is indicated by the ambient temperature drop from 03:00 to 10:00 in Figure 49.

3.5 Systems efficiency (COPs and SCOPs)

With the primary outcome of the case study being the difference in power (kW) and electricity consumption (kWh), one must consider whether any other means of evaluation exist. Here a reference data set will be compiled for each plant by means of its COP. The system will, in addition, be analysed as a group by means of various SCOPs. This data will illustrate individual and group efficiencies for the plant. From this data a good idea will be formed as to how effective the performance of the plant is. It is an ideal analysis that does not take into account how the plant is operated (scheduling). The data set will later be compared to similar data compiled during an assessment period. A good result will be indicated by an increased efficiency of all the components. The value of the COP and SCOP will therefore need to have risen.

Table 9 is derived by using equations 9 and 10. The c_p of water is 4.18 kJ/kg-K at 25 ˚C [42].It is assumed that this value remains constant throughout all calculations.

Table 9: Chiller plant's average COPs and SCOPs

Efficiencies	York 1	York 2	York 3	York 4	Howden	Cooling plant	Entire cooling load
COP	6.94	6.24	6.42	6.67	4.75	5.66	-
SCOP	5.64	5.03	5.22	5.41	3.76	4.54	6.06
COP Difference	1.30	1.21	1.21	1.26	0.99	1.12	-

As can be seen in Table 9, the York chillers have COPs above 6, indicating a high efficiency level. The Howden chiller, however has a COP of less than 5, showing poor efficiency for the stand-alone unit. The 'cooling plant' COP, lying below 6, indicates a good overall cooling load. The SCOP here includes the entire electricity load at the chiller plant, including the cooling towers, precool tower, pumps, etc.

Figure 50 to Figure 52 shows the average COPs and SCOPs of the various chillers during the baseline period. The data includes times when the machines were off, with an effective COP/SCOP of 0. This indicates the selection of chillers when operating the plant, as the data

includes the same total time period for each plant. As can be seen, York 2 is used the least of the remaining Yorks, York 3 is used the least during the day and York 4 is used the most overall.

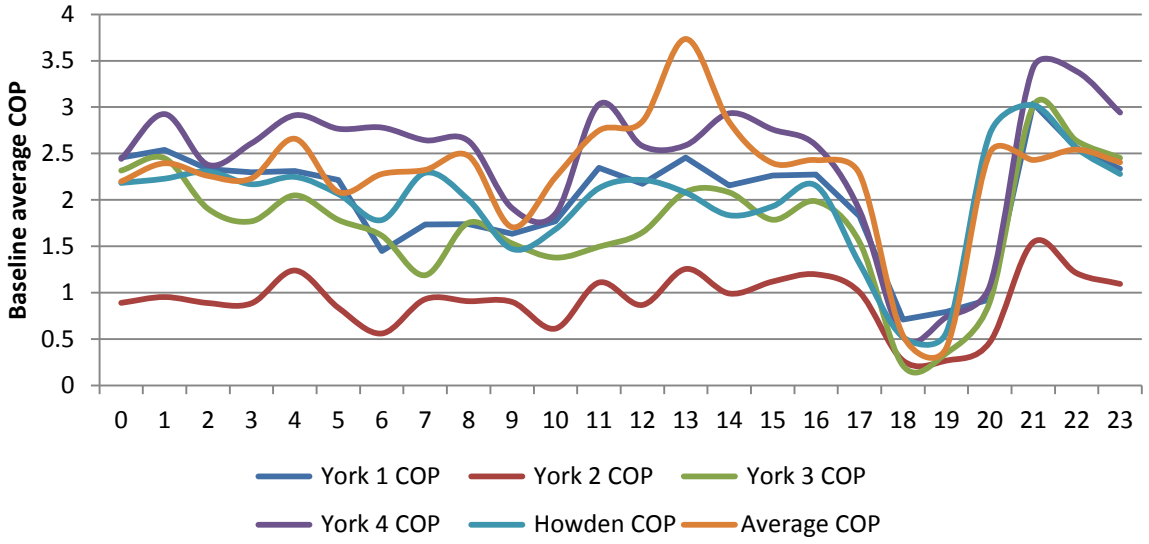

Figure 50: Average chiller COPs during the baseline period

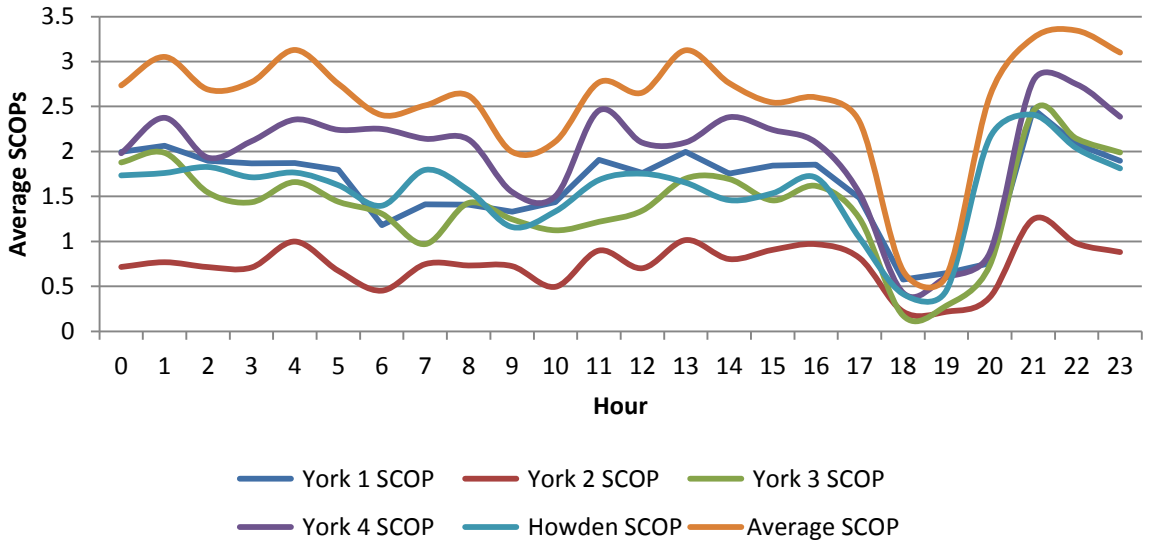

Figure 51: Average chiller SCOPs during the baseline period

When comparing Figure 50 and Figure 51 to Figure 52, it is noticed that, on average, York 2 is only used during lower ambient temperatures. From Table 9 it is noticed that York 2 has the lowest COP. However, with an average COP of above six, one is led to believe that there are other faults with this chiller, due to its limited use. The grouping of SCOPs at 15 ˚C in Figure 52 indicates the reduced cooling capacity required at lower temperatures.

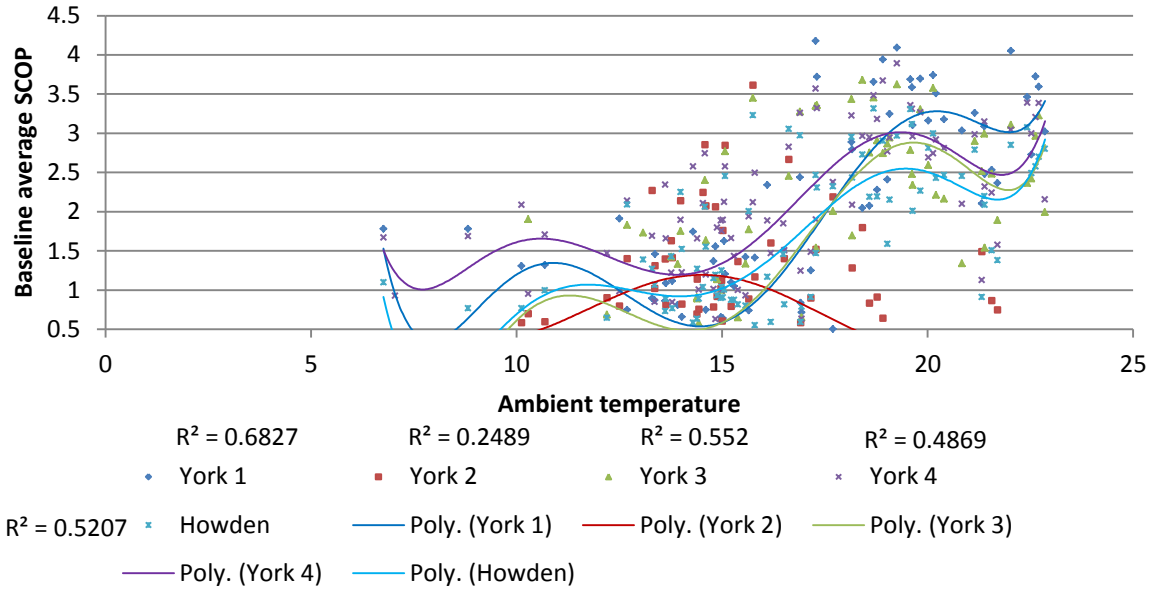

Figure 52: Average Daily SCOPs plotted against ambient temperature during the baseline period

3.6 Inclusion of BAC on the load

Just before the case study was implemented, a new load was placed on the chiller plant. As previously indicated the load came from a newly-installed BAC. The BAC has, since its implementation, drawn water from chill dams 2 and 3 to send cooled air down the mine-shaft. The system is set to return the water from the BAC to chill dam 1 in the summer months and to the precool dam in the winter months.

The electricity consumption of the BAC return pumps and the BAC fans will not be included in the savings analysis. There is no reference comparison as to their loading. The water usage of the system can, however, be included in the calculated savings comparison. This is due to water leaving the fridge plant and ambient temperature being included in equation 20's variable inputs.

From equation 20 the flow portion of the scaling can be estimated as $y = 0.002284a$ (kWh). This is illustrated in Figure 53. Data obtained indicated that the BAC consumed an additional 53% of the cooling plant's chilled water. The unknown portion of the power data is the circulation of water from the BAC to either the precool dam or chill dam 1. This is indicated by the grey area on the chart.

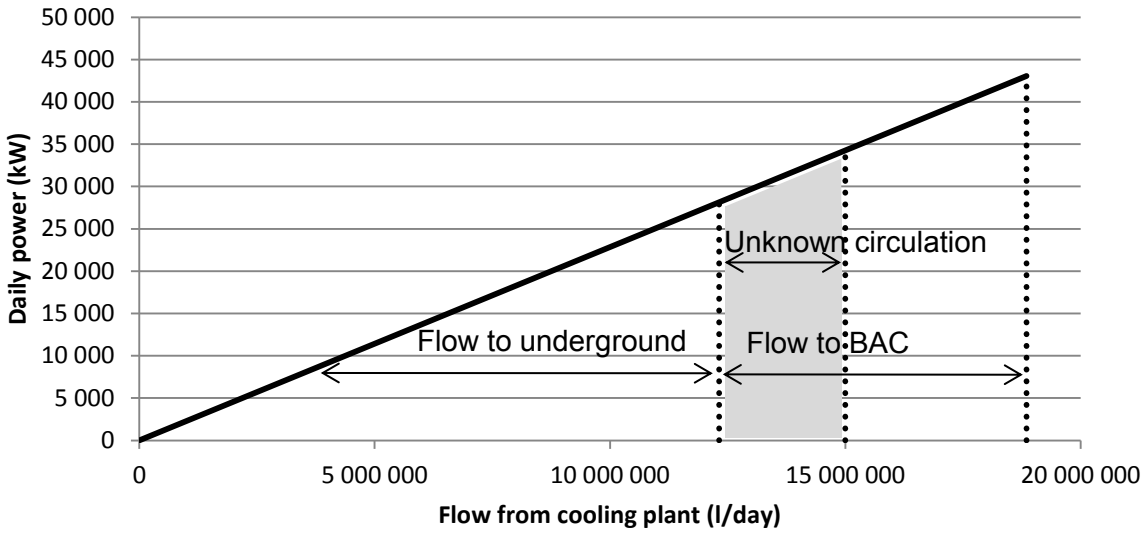

Figure 53: Illustration of power consumption of the chilled water consumers

Similarly to the baseline scaling, inclusion of this load will be estimated in terms of electricity usage. A calculated value will be provided to assist in year-on-year saving comparisons. This shall simplify a major outcome of this study. Figure 54 shows the new installations.

Figure 54: New BAC installed on case-study mine

3.7 Conclusion

System data collected from previous projects was analysed and a reasonable knowledge of the cooling system's technical information was developed. A reference electricity consumption was modelled in terms of independent energy drivers. This reference is in the form of a LINEST-derived equation (equation 20) and a power (kW) baseline. The outcome of the report can thus be validated.

System constraints and standard operating conditions were defined and analysed. This will provide a foundation for any control adjustments to be implemented. The need for separate seasonal service delivery conditions was noted. All necessary components of the cooling plant were reported. The potential of a new system can thus be analytically developed and implemented.

The addition of new infrastructure was discussed. This change in scope (with regards to chilled-water service delivery) will be separately analysed for the outcome of the study.

Chapter 4 – Implementation of intervention

4.1 Introduction

Throughout any design and/or implementation it is vital to note all stages of the completed work. This simplifies future work on the same, or a similar system. Notes should, in addition, be made as to problems encountered and solutions to overcome said problems. As previously stated, this case study should not negatively impact the service delivery of the mine. An improved service delivery should serve as a potential outcome of the case study. However, it should not result from a loss to the primary outcome of the case study.

This chapter focuses on the intended and resulting control implemented on the cooling plant. Potential energy savings of the system is also analysed. These savings are deduced by both a complete simulation model and calculations using the Affinity Laws. The calculations provide a validation of the simulation model. This will provide an estimate of the monetary return for the proposed implementation.

4.2 Proposed control

Mine cooling and ventilation is one of the most critical operations in deep-level mining. The complex operation of mine cooling and ventilation is dependent on a number of auxiliary equipment. These auxiliaries include medium voltage fans and pumps, as well as heat exchangers, evaporators, condensers and bulk air coolers. The proposed control will focus on optimising a selection of these auxiliaries.

The case study in question requires a means of implementing an energy-efficiency initiative. As present water-flow control is based on valve throttling, the pumps are using more power than required to produce the required flow rate. As discussed, automated valves previously installed on the chillers no longer operate due to a lack of maintenance. Manually-operated valves are thus being used to throttle the water. These valves are set to give the design flow rates of the chiller. As the water temperatures vary, the chiller compressor is not kept at optimal loading conditions.

As discussed in the literature, VSDs are widely used in industry to control the water flow. The VSDs are used to regulate the frequency of the voltage delivered to the motors. By regulating the frequency of the voltage, the speed at which the motor operates can be controlled, thus controlling the speed of the pumps. In addition, an energy-efficiency situation is created, where an electrical saving is measurable. Figure 55 illustrates where VSDs will be installed on the present chiller plant.

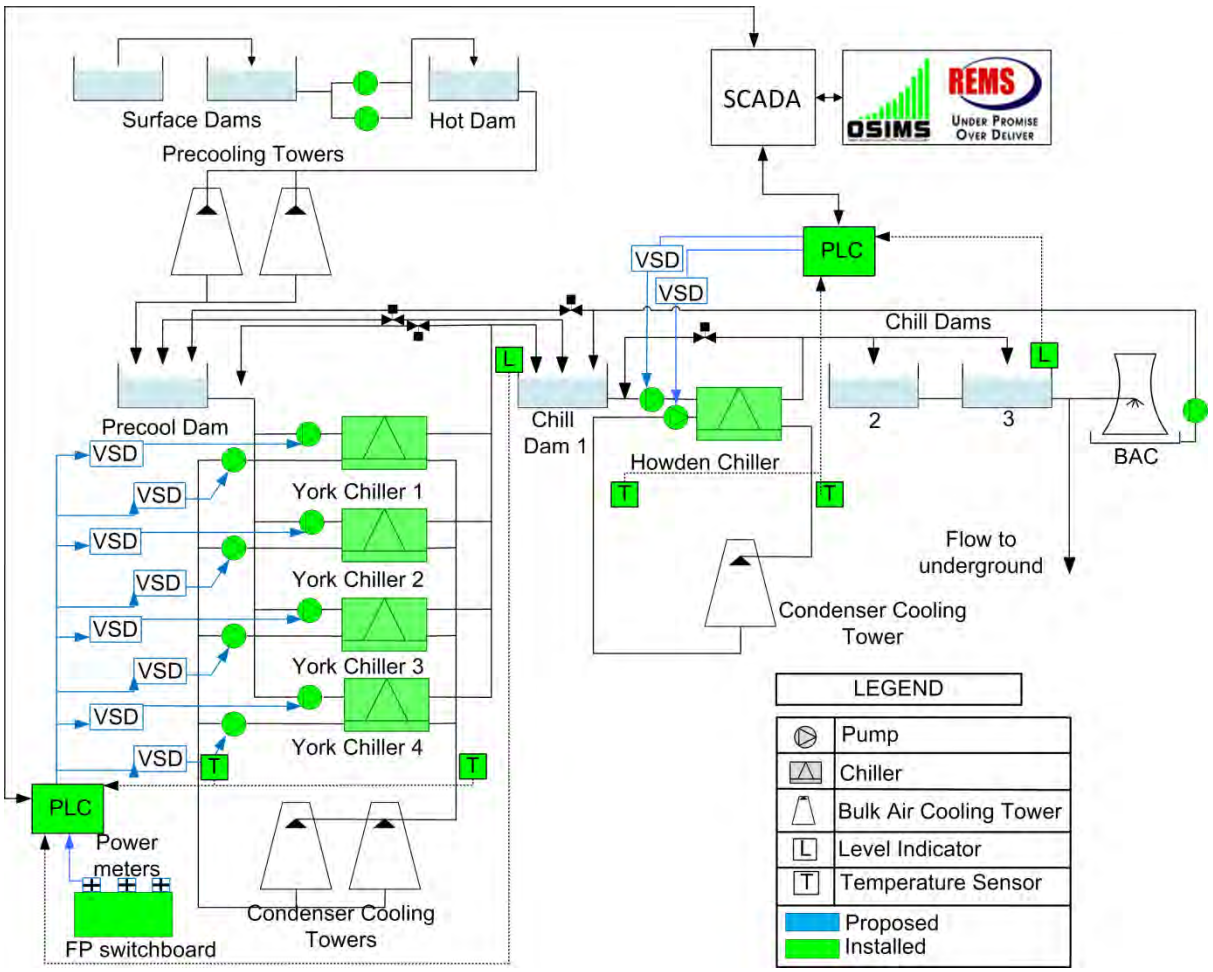

Figure 55: System layout with proposed control

As the present control is manually operated, inefficiency is created by both the wasted electric energy (physically restricting pump flow) and the lack of automated chiller flows (not extracting the optimum delta temperature). This creates the need for a more modern control method. This control can be implemented by installing VSDs for all the relevant pumps. These drives will be able to control the pressure, flow and automation requirements of the system [15]. This control is vital, as the variables of the system result in changes to the operational efficiency of the chillers.

In order to optimise these operations, the auxiliary equipment needs to be controlled by state-of-the-art intelligent controllers and technologies. The EMS previously discussed will automatically control and optimise all the necessary auxiliary equipment in order to reduce the electricity consumption. Figure 56 shows the control communication diagram implemented by EMS.

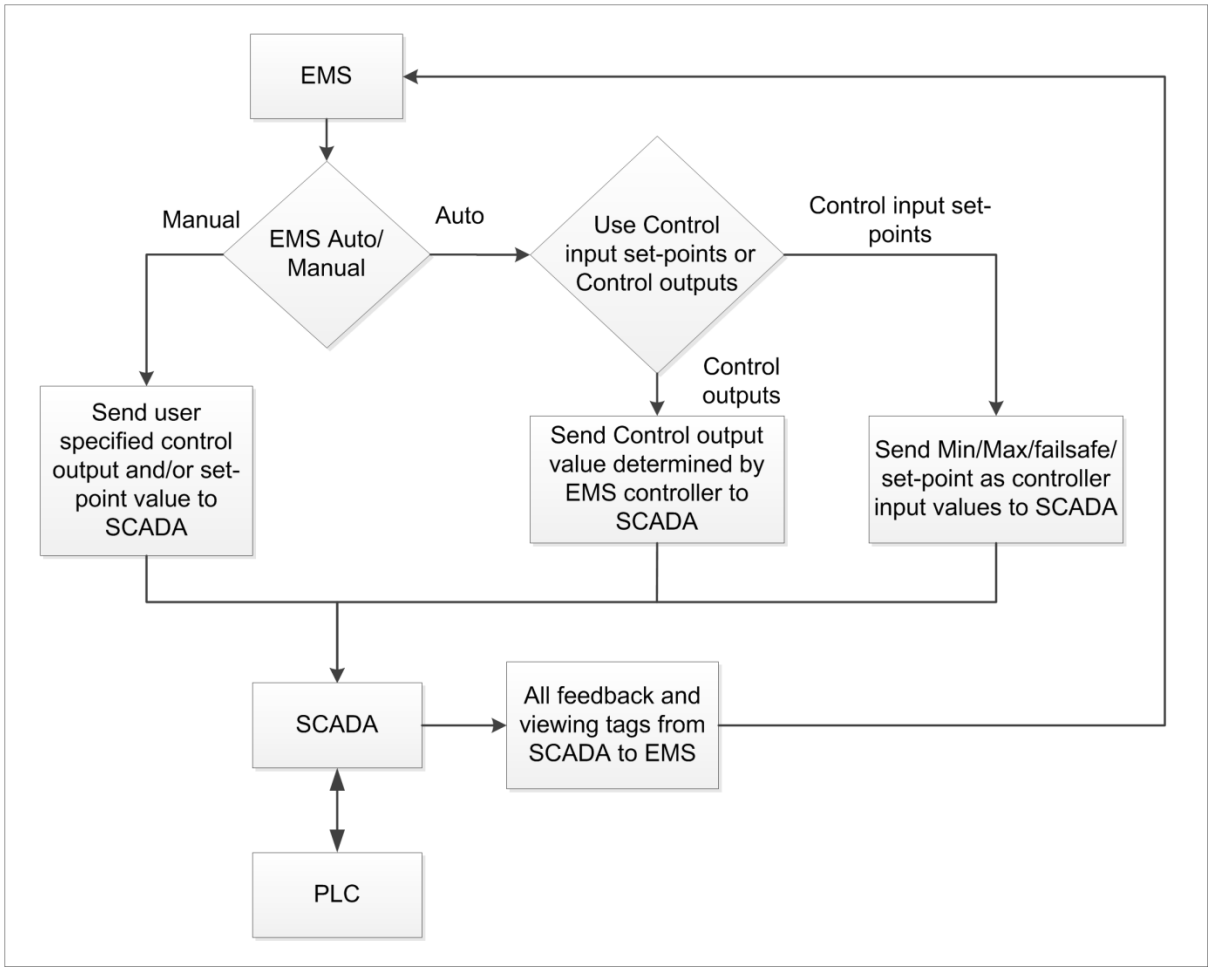

Figure 56: EMS control logic diagram

The control to be implemented in the system is a simple one. The VSDs will operate the flow rate of each pump according to set points laid out by the design of the chillers. This includes a maximum and minimum flow rate. The EMS will then vary this flow between specific frequency set points. These set points are to be determined during the commissioning phase of the implementation. Each chiller will be assessed to determine individual limits. This is due to the plants being in various stages of maintenance, resulting in varying amounts of scale build-up in the heat exchangers, and thus different flow capabilities.

The evaporator and condenser will have different control strategies. The condenser pump flow rate is to maintain a fixed temperature difference across the condenser. Evaporator pump flow rate is to maintain dam levels. These dams serve as a storage medium to supplement peak demand periods. The number of chillers in operation is therefore not always dependent on the demand. This further allows for the electricity load to be shifted away from peak electricity demand periods. Figure 57 and Figure 58 show the evaporator and condenser control communication diagrams.

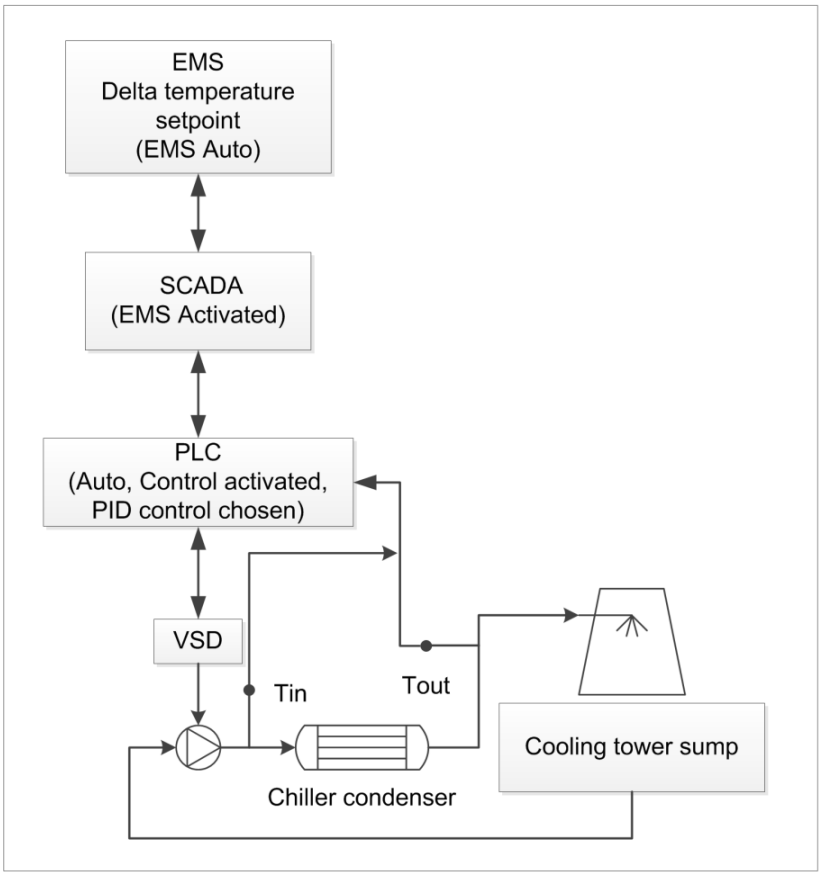

Figure 57: Condenser water-flow control logic diagram

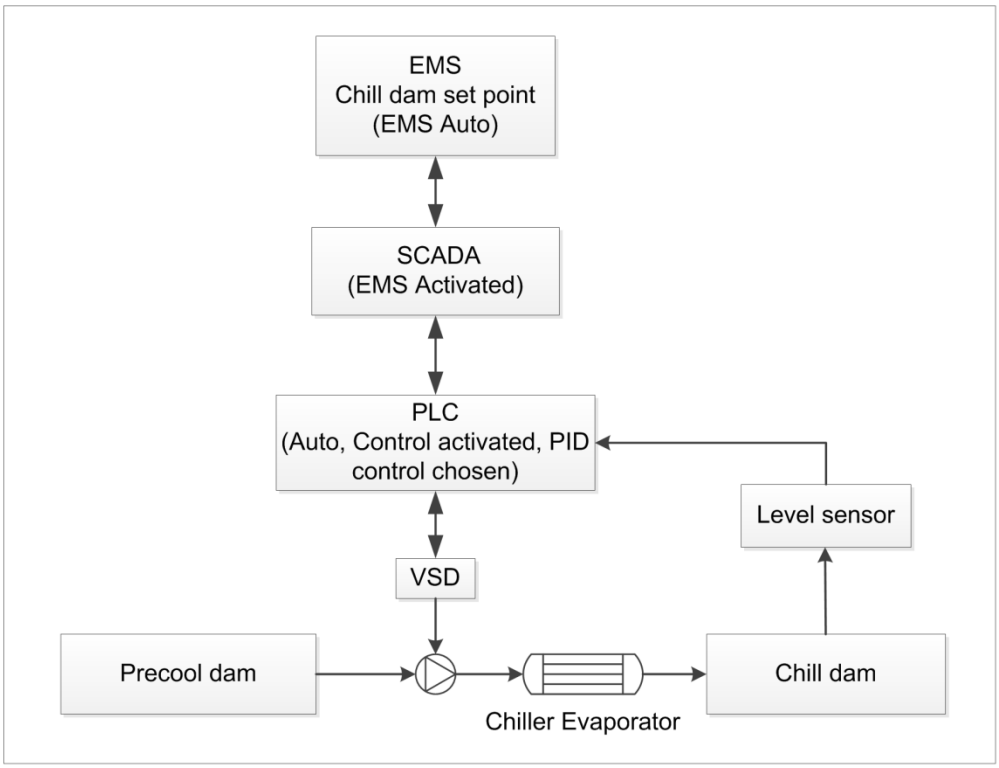

Figure 58: Evaporator water-flow control logic diagram

Due to heat loss experienced by the water in cooling towers, both condenser and evaporator flow temperatures are dependent on ambient temperatures. The need for variable flow is therefore critical in optimising each chiller. A common circulation loop is also present in the evaporator pipeline. This pipeline has a restricted flow, controlled by a pneumatic valve. The valve is controlled by a PLC block which ensures a constant outlet temperature into the storage dam. More circulation is therefore allowed if the outlet temperature of each stage of the cooling plant is too high. The control strategy includes limiting the valve to a minimum open position, as less pumping will be required during the cooling process. This valve does, however, have a minimum flow rate, as it does not have a complete seal.

The most important part of the automated control is how the operator will be affected. The simplicity of the system allows for the operator's work structure to remain. The plant and pumps will be started and stopped exactly as it would have been done previously. This prevents any possible altering of system parameters by an operator, or additional work. As has been previously witnessed, changing the scope of work for mine staff is not welcomed. This control will thus not negatively affect anyone at the mine.

It is important to set the control set point to which the evaporator water flow rate is controlled to below the maximum dam level. This would be below the dam level where operators would switch off chillers to prevent overflowing. The VSDs would thus reduce the flow and maintain the dam level. As the dams are generally filled to 90%, a good set point would be 85%.

4.3 Proposed savings

4.3.1 Overview

The case study requires a large capital investment to realise the electricity savings. A marker thus needs to be set to determine the potential investment and return. Achievable savings are to be determined by two methods. The first utilises a full simulation model and the respective system parameters, and the second utilises the Affinity Laws. The simulation model is to be designed in Process Toolbox.

4.3.2 Process Toolbox simulation

The cooling plant was modelled in Process Toolbox. Two models were developed. One model adapted to the cooling plant as described in the baseline, the other, as expected, post VSD installation. Figure 105 and Figure 106 in Appendix F show partial screen shots of the models (these initial models do not include the BAC, as its design and service delivery was not known).

The first model was verified utilising a random day in the baseline period (2011/04/12). An additional day (2011/04/11) was used to balance out the mass and energy profile, as the model can take up to a 24-hour period to converge. The variables, as measured on these days and utilised for the model verification, are shown in Table 32 in Appendix F. These variables include the running status of the respective plants, the ambient drybulb temperature and the flow to underground (service delivery).

By placing these variables into the simulation, with plant specific restrictions already implemented, the simulation could be validated. Plant specific restrictions applicable to the model include detail such as chiller compressor power, precooling and condenser cooling tower fan power, evaporator and condenser pump power and plant water flow limits. These restrictions have been listed through Table 6 and Table 7 in Chapter 3.2 and in Table 30 and Table 31 in Appendix C. The power output profile of the simulation (results) is compared to the actual power profile of the two days in Figure 59.

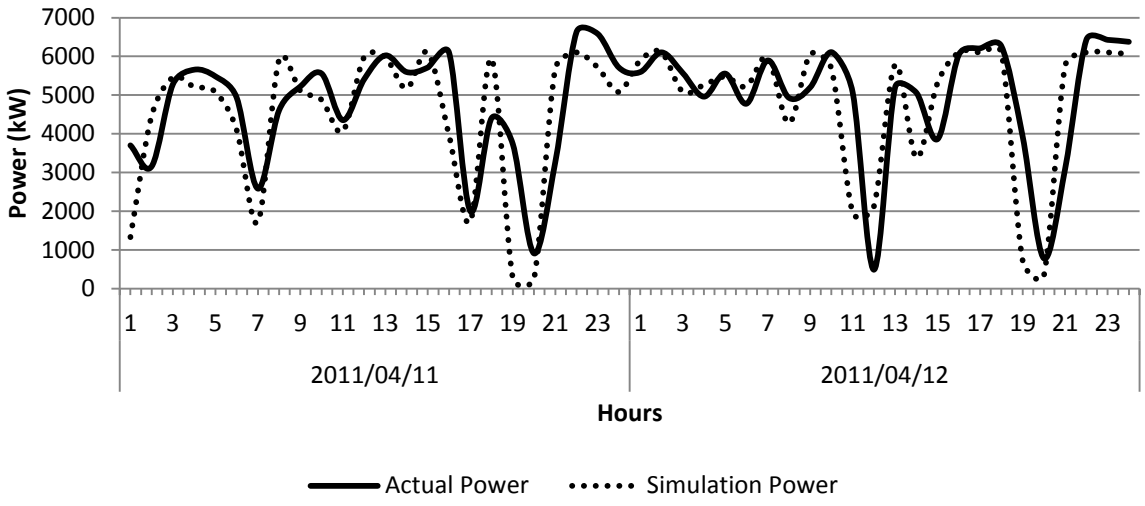

Figure 59: Simulation model verification based on data from 2011/04/11 and 2011/04/12

The average percentage error as shown by the output power profile of the simulation was 2.51%, as compared to the actual power profile of the second day. It was thus shown that the model is very accurate. The phase difference seen in Figure 59 was due to the average actual power only being logged every half hour, whereas the simulation provided instantaneous power results.

As the accuracy of the model was verified, the model is suitable to determine the potential savings of the system. The models were simulated according to the four seasons (summer to spring) to determine the yearly potential savings. It thus indicates the potential for an implementation budget. The tariffs utilised in the simulation are indicated in Table 2 and Table 3. These simulated power profiles are shown in Figure 60. Average electricity results and savings and weekday monetary cost savings are displayed in Table 10 and Table 11 respectively.

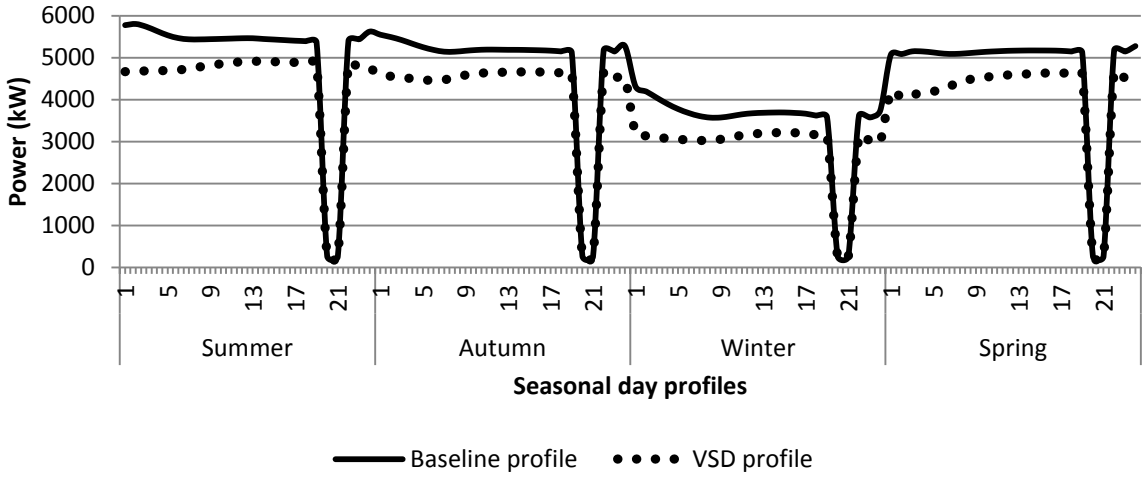

Figure 60: Seasonal simulation power profiles

Table 10: Average weekday simulated cooling plant power and respective operating costs

Season	Simulation power output (kW)		2011/2012 tariff structure costs (R)		2012/2013 tariff structure costs (R)	
	Baseline	VSD	Baseline	VSD	Baseline	VSD
Summer	5 064	4 414	43 453	38 248	50 017	44 025
Autumn	4 814	4 214	41 328	36 470	47 571	41 979
Winter	3 445	2 879	59 458	50 684	68 445	58 345
Spring	4 737	4 098	40 806	35 625	46 970	41 007

Table 11: Average weekday simulation savings (baseline minus VSD)

Season	Simulation power difference (savings) (kW)	2011/2012 tariff structure costs (R)	2012/2013 tariff structure costs (R)
Summer	649	5 205	5 991
Autumn	600	4 857	5 591
Winter	565	8 773	10 100
Spring	638	5 180	5 962
Average	**613**	**6 004**	**6 911**

As indicated in Table 11, the average daily electrical savings are 613 kW throughout the year. This translates to a 13.6% savings. Analysing the weekday cost savings across the two tariff structures shows the increase in return to be expected per year. This shows the importance of implementing the energy-efficiency improvement strategy as soon as possible.

Any increase in service delivery will, in addition, immediately show a reduced cost profile (relative to the increased service delivery).

The expected yearly savings based on present service delivery is indicated in Table 12. Here the year was broken into the four seasons, each containing 13 weeks (totalling 52 weeks). As can be seen, the change in yearly tariffs will already result in an inflated saving of R 300 000 from the investigation period to the post implementation period.

Table 12: Expected yearly savings based on simulations

	2011/2012 tariff structure cost savings	2012/2013 tariff structure cost savings
Weekday	R 1 561 169.44	R 1 797 032.92
Saturday	R 219 893.02	R 253 104.18
Sunday	R 195 509.61	R 225 023.51
Total	**R 1 976 572.07**	**R 2 275 160.61**

4.3.3 Verification calculations

Use of the Affinity Laws provides an accurate simplified analysis to determine the potential electricity savings of the system. It thus gives an indication of the possible best-case savings achievable by utilising the correct constraints. These savings are to be realised on the respective evaporator and condenser pumps.

Table 13: Estimated savings utilising the Affinity Laws

Parameters and Results	York evaporators	York condensers	Howden evaporator	Howden condenser
Q_1 (ℓ/s)	180	350	330	330
Q_2 (ℓ/s)	125	280	250	250
P_1 (kW)	55	132	200	200
Number of pumps	4	4	1	1
P_2 (kW)	18.42	67.58	86.96	86.96
Individual pump savings (kW)	36.58	64.42	113.04	113.04
Total pump savings (kW)	146.32	257.66	113.04	113.04
Combined achievable savings (kW)	**630.07**			

As indicated in Table 13, the average daily savings could amount to 630kW per day. This is dependent on the daily scheduling of the plant. It is, however, a good benchmark for verifying the results of the simulation. An example of how the values in Table 13 were obtained is shown in Appendix G.

4.4 Implementation

Implementation of such a large case study requires many aspects related to project management. The most important components of these are time- and budget management. Of these, the choice of installed components and contractor selection is crucial. One should analyse quotes, delivery and installation dates, as many aspects are related to monetary exchange rates.

As the initiative is a DSM project, the allocation of funding is fixed, thus a set installation cost needs to be set. Three contractors were requested to quote for the installation, resulting in the complete operation and control of the case study. The quote had to cover the entire infrastructure required to gain the effective savings and monitor the system. All instrumentation quoted on was prescribed by the client. No product supplier selection matrix was required.

An important factor to consider is the delivery time of VSDs, which can take between 12 and 16 weeks to be shipped to site. This time frame is also largely dependent on whether or not the VSDs need to be placed in enclosures. The quotes received were as follows:

Table 14: Contractor comparison

Quoting company	Cost of full installation (R) (Excl VAT)	Implementation period (weeks)	Installation period (weeks)	Previous experience with ESCOs
Company A	1 633 910.00	30	10	Yes
Company B	3 290 791.21	20	10	No
Company C	1 305 510.00 (Excluding VSD supply)	32	12	No

The implementation period indicated includes sourcing of respective components, shipping, installation, etc. With the installation time of company A and B being the same, the choice of contractor was chosen to be company A, due to the large cost difference. In addition, Company A's costs will show a payback period of less than a year based on Table 12. Company C was not considered, as they were not willing to carry the risk of the VSD order. This would also have raised their costs far beyond Company A's.

The implementation period took longer than company A specified. As the implementation was started early (to cover expected possibility of delays), the case study was still

implemented and completed by the end of the 'winter' months of the year. As such, one would still expect to see better kWh savings resulting from the case study operating in the summer months. The most notable factor resulting from the VSD installations was the reduced noise in the cooling plant.

Figure 61 and Figure 98 to Figure 100 in Appendix E show the custom control and optimisation platform built in EMS. The four pages developed in the program display an overview of the chiller plant, a data logging and trending page and the evaporator and condenser control pages respectively. The program allows one to automate the plant's auxiliaries, or to manually override various set points during operations. The staff at the chiller plant thus only need to adjust set points if required for a specific operating period.

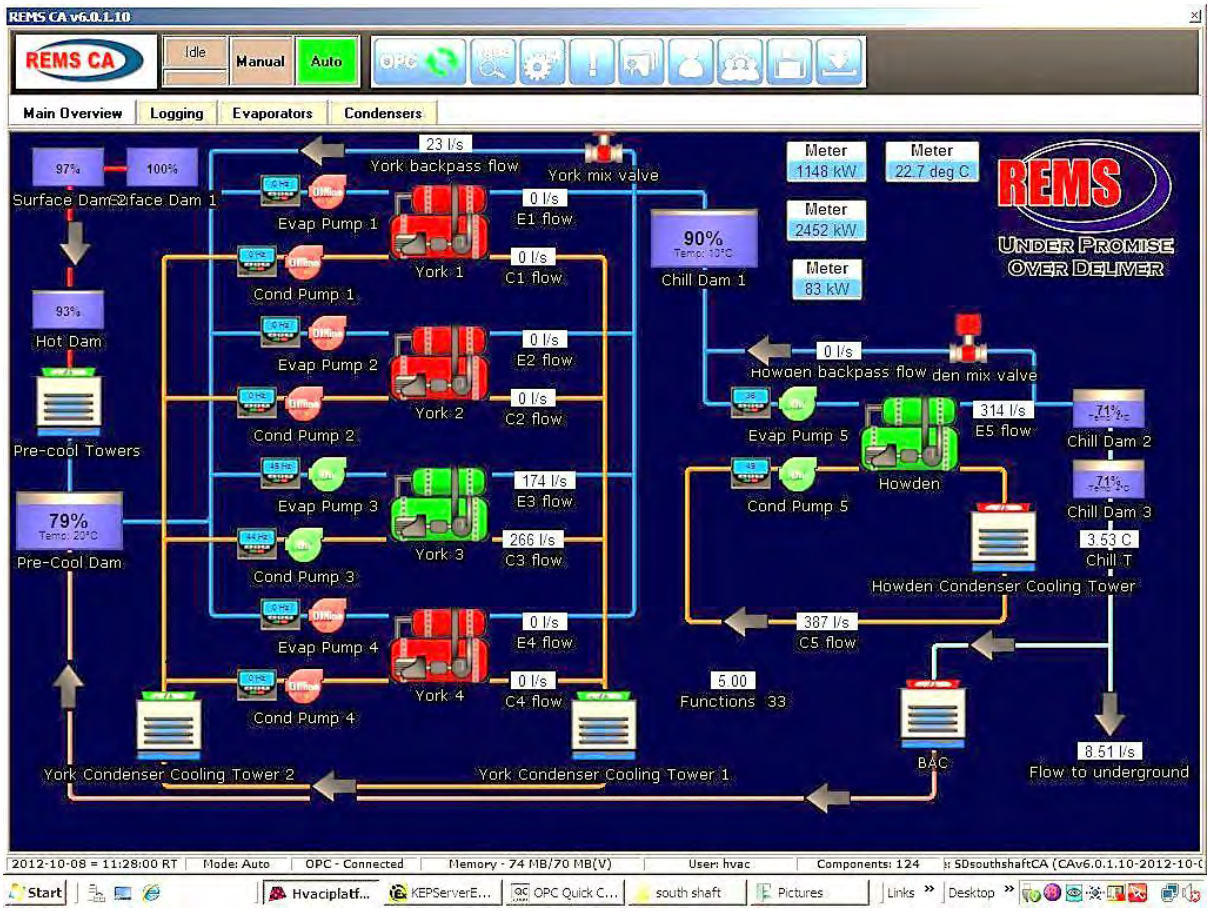

Figure 61: EMS print screen – main overview of chiller plant and auxiliaries

As mentioned in Chapter 3.2, the plants critical operation parameters are monitored by the plant operators. All necessary data is available on the SCADA system. As such it is not necessary for these conditions to be monitored in the EMS platform, specifically as controllable operational parameters are not exceeded by the implementation.

4.5 Resulting control

As expected, each chiller had different set points relating to its flow versus frequency limits. As discussed in the previous chapter, different temperature set points were required from each stage of the plants. These were separated as winter and summer set points. The main purpose of this was the evaporator water design inlet temperature of the Howden chiller. The implementation did not alter the standard control as implemented by the fridge-plant foremen. Table 15 and Table 16 show the set points that were determined when testing for minimum and maximum flow rates and the respective frequencies.

Table 15: Evaporator VSD frequency control set points

	York 1	York 2	York 3	York 4	Howden
Control	Closed loop PID	Closed loop PID	Closed loop PID	Closed loop PID	Closed loop PID
Feedback input signal	Chill dam 1 level	Chill dam 1 level	Chill dam 1 level	Chill dam 1 level	Chill dam 3 level
Set point	90%	90%	90%	90%	90%
Minimum VSD frequency	20Hz	20Hz	20Hz	20Hz	30Hz
Maximum VSD frequency	40Hz	45Hz	45Hz	40Hz	50Hz

Table 16: Condenser VSD frequency control set points

	York 1	York 2	York 3	York 4	Howden
Control	Closed loop PID	Closed loop PID	Closed loop PID	Closed loop PID	Closed loop PID
Feedback input signal	Condenser cooling tower sump level	Condenser cooling tower sump level	Condenser cooling tower sump level	Condenser cooling tower sump level	Condenser cooling tower sump level
Set point	90%	90%	90%	90%	90%
Minimum VSD frequency	20Hz	20Hz	20Hz	20Hz	20Hz
Maximum VSD frequency	45Hz	46Hz	47Hz	45Hz	49Hz

Table 17 shows the optimum frequency set points where the maximum delta temperature across the evaporator was achieved. As shown, York 3 was able to operate at a much higher flow rate than its three counterparts. These evaporator set points should be a permanent control condition should a constant condenser delta temperature be maintained, along with a constant precool dam temperature. The only condition that could cause the need for a change in flow rate would be if the Howden evaporator inlet temperature is too

high or too low. It was found that an increment of one Hertz on a York evaporator pump had an average flow-rate change of 4 ℓ/s.

Table 17: Optimum respective VSD set points as per implementation

Chiller	Evaporator pump optimum-frequency set point (Hz)	Condenser pump optimum-frequency set point (Hz)
York 1	40	45
York 2	32	46
York 3	45	40
York 4	32	45
Howden	36	49

As previously indicated the chillers are in various stages of maintenance. A result is different levels of scale build up in the heat exchanger tubes (evaporator and condenser). The varied frequency set points indicated in Table 17 are likely due to pumping pressure resulting from these blocked tubes. A solution to this problem could be increased maintenance and cleaning of the tubes.

Pump operating hours were reduced through a combination of increased evaporator water flow rates and reduced recirculation flow. It is expected that this will result in additional electricity savings.

4.6 Conclusion

A proposed control philosophy was presented. This philosophy is based on information detailed in the literature. The philosophy is intended to provide optimal savings with minimal losses to the system.

Electricity savings were verified through utilisation of both a Process Toolbox simulation baseline model and the Affinity Laws. The model was based on the proposed control philosophy, system layout and operating conditions for an entire year. The model was verified based on a random data set of actual operating conditions. Potential daily electricity savings of the baseline cooling plant can be conservatively given as 600 kW, based on both analyses. This would translate to an annual reduced load of 5.26 GWh.

The electricity savings is expected to result in a yearly payback of R2 275 000, based on Eskom's 2012/13 Megaflex tariff structure. Based on installation costs of Company A, the payback period for the case study is expected to be 8.6 months (0.72 years).

The intervention was implemented successfully. All the operational requirements were met. The plant operators, where necessary, were shown how to operate the EMS platform. A remote login to the server was created in the operator's office for this purpose. The ability to control the respective flows by the plant operators would result in less future assistance being required for minor temporary operational changes.

The control range of the plant differed with the presented control philosophy during implementation. As expected, each plant had different set points. It was found that the York chillers' evaporator flow rates could be largely increased with minor changes to the delta temperature. Reducing the recirculation flow rate, however, caused a slight increase in evaporator water delta temperature across all the Yorks.

As the intervention has been implemented and outcomes predicted, the system needs to be analytically reviewed to determine the success of the case study.

Chapter 5 – Cooling system performance post implementation

5.1 Introduction

With the implementation of the energy-efficiency intervention, a detailed analysis is required to determine the outcome. In this chapter the change in efficiency of the plant will be investigated. Electricity and monetary savings are to be determined. These results will be combined to indicate the payback period of the case study.

The impact of the addition of the BAC to the system will be interpreted through both equation 20 and a year-on-year data-trending comparison. The total monetary savings will not be compared to the original baseline power profile, due to this change in service delivery. Instead the cost savings will be analysed according to the power profile of the assessment period.

Once all relevant data post implementation has been analysed, a detailed discussion of the results will be presented. The discussion will include an analysis of new data and a comparison with the data presented in chapters 3 and 4. The extent of success achieved through the intervention will be realised and presented.

VSD and control savings will not be presented separately. Electricity and monetary savings will be presented as the total savings. This is due to the energy-efficiency improvement being a combination of the total implementation.

5.2 Subsequent systems COP

Through the installation and control of the VSDs it was expected that the respective coefficients of performance would increase. A small increase in COP is an indication of a large increase in efficiency. Table 18 below shows the average COPs and SCOPs during the assessment period.

Table 18: Respective COPs and SCOPs after implementation of the case study

Efficiencies	York 1	York 2	York 3	York 4	Howden	Cooling plant
COP	7.92	-	8.29	6.72	7.60	8.53
SCOP	7.01	-	7.96	5.52	5.48	6.84
COP to SCOP difference	0.91	-	0.33	1.19	1.71	1.69

The change in COP/SCOP of York 2 could not be evaluated, as it was offline for maintenance over the entire assessment period.

A partial increase in the COP/SCOP is the result of a higher average evaporator temperature. This can be seen in Table 19 and Table 20. The average water temperatures of each evaporator are shown in Table 19. These results increased due to the reduced recirculation flow across the chillers. The overall average evaporator temperatures are also shown to have increased in Table 20, due to an increase in average precool dam temperature and an increase in service-delivery temperature (decreased average chill dam 3 temperature).

Table 19: Average evaporator temperatures

	York 1 (˚C)	York 2 (˚C)	York 3 (˚C)	York 4 (˚C)	Howden (˚C)
Baseline period	12.81	-	13.23	11.34	5.51
Assessment period	13.96	-	13.69	14.34	6.17

Table 20: Average dam temperatures

	Precool dam temperature (˚C)	Chill dam 3 temperature (˚C)
Baseline period	19.60	3.59
Assessment period	20.97	2.65

Figure 62 shows the SCOPs of each chiller plotted against ambient temperature during the assessment period. As seen in Table 18, York 1 and 3's SCOPs were much higher than the rest of the chillers. This was mostly due to the high water-flow rate through the evaporator (approximately 160 ℓ/s), and due to it being utilised more than the other chillers. Irrespective of the flow, the temperature difference across York 3 was also on average 1 ˚C higher than the other Yorks. This indicated that it had a greater efficiency.

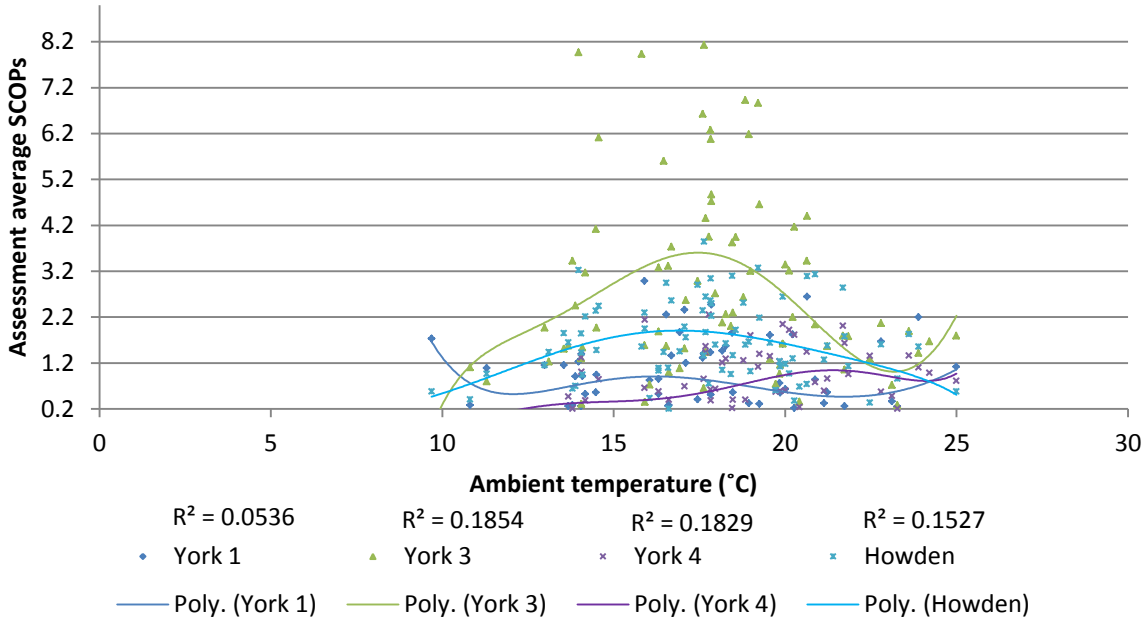

Figure 62: Chiller SCOPs plotted against ambient temperature during assessment period

The data here again includes times where the machines were off with an effective SCOP of 0. This indicates the selection of chillers when operating the plant, as the data includes the same total time period for each plant.

5.3 Electricity savings achieved

The savings achieved, as discussed, is to be determined by utilising equation 20 and the respective variables from the assessment period. Figure 63 shows the output of equation 20, utilising these variables. The variable data is available in Table 27 in Appendix A.

The area between the solid- and dotted lines in Figure 63 represents the electricity savings achieved over the assessment period (calculated assessment minus assessment actual). This area is represented in Table 25 in Appendix A. In summation, the electricity savings achieved amounted to 4.2 GWh over the three-month period, or an average power saving of 2.3 MW daily. This translates to a total saving of 47.12%, as calculated below. The values in the equation are obtained from Figure 64.

$$Total\ savings = \frac{Average\ calculated\ assessment - Average\ assessment\ actual}{Average\ calculated\ assessment}$$

$$= \frac{4.91 - 2.59}{4.91} = 47.12\%$$

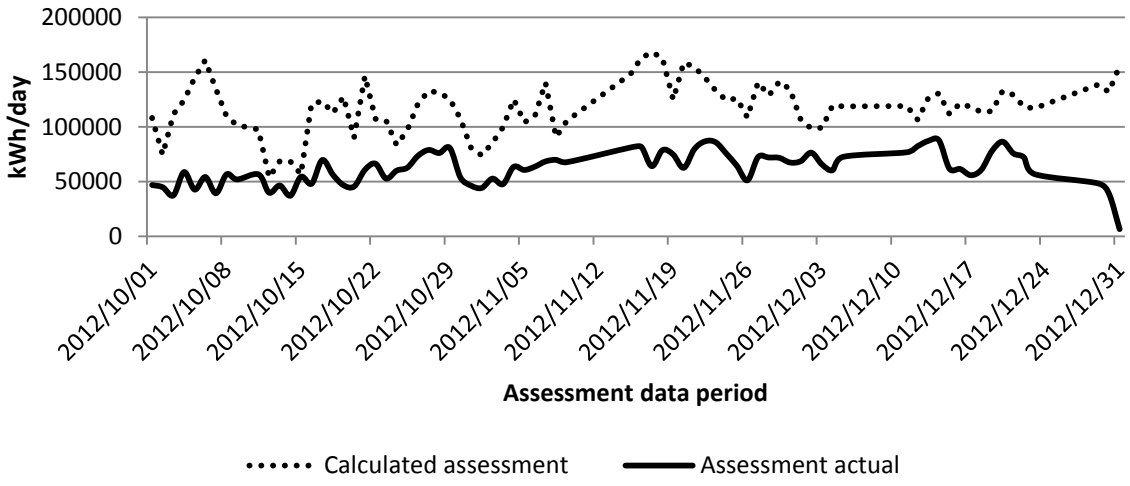

Figure 63: Actual and calculated assessment period's power consumption

Figure 64 shows the scaling used to determine the cost savings for the case study. The scaling here again utilises a scaling factor from the average daily power data to determine cost savings. Time-of-use savings for that period is determined by applying the scaling factor to the assessment power profile (the hourly cost savings based on that period's time-of-use is thus determined). The multiple cost savings are shown in Table 26 in Appendix A. The savings relative to Figure 64 is R 23 290 per average day. This translates to a saving of R 2 142 770 over the assessment period of 92 days.

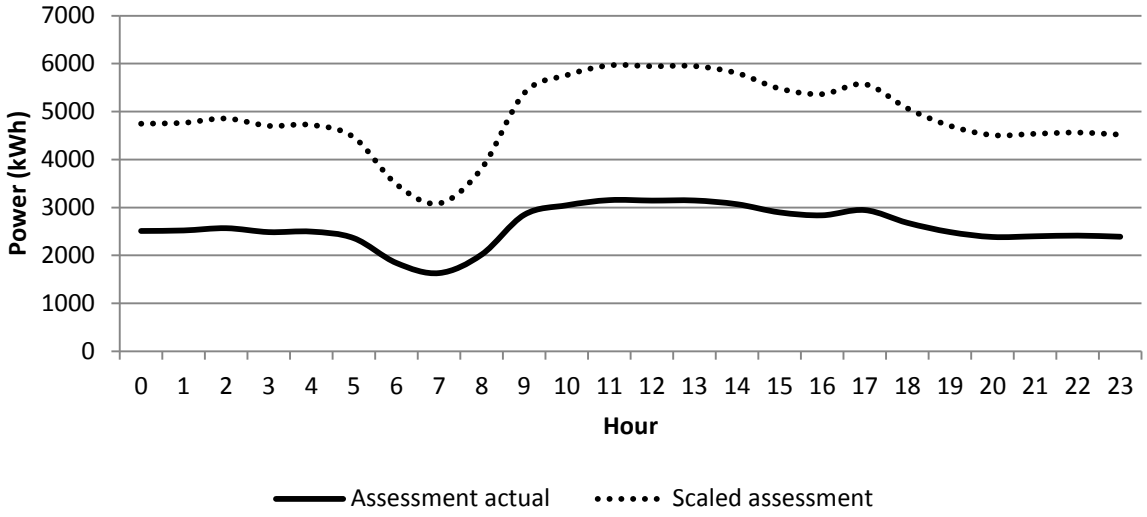

Figure 64: Actual and scaled assessment period average hourly power consumption

From Figure 65 it can be seen that the assessment period had an average day power profile operating almost entirely under the baseline power profile. This, compared with the increased production and ambient temperature differences between the two periods, is proof enough of the effectiveness of the case study.

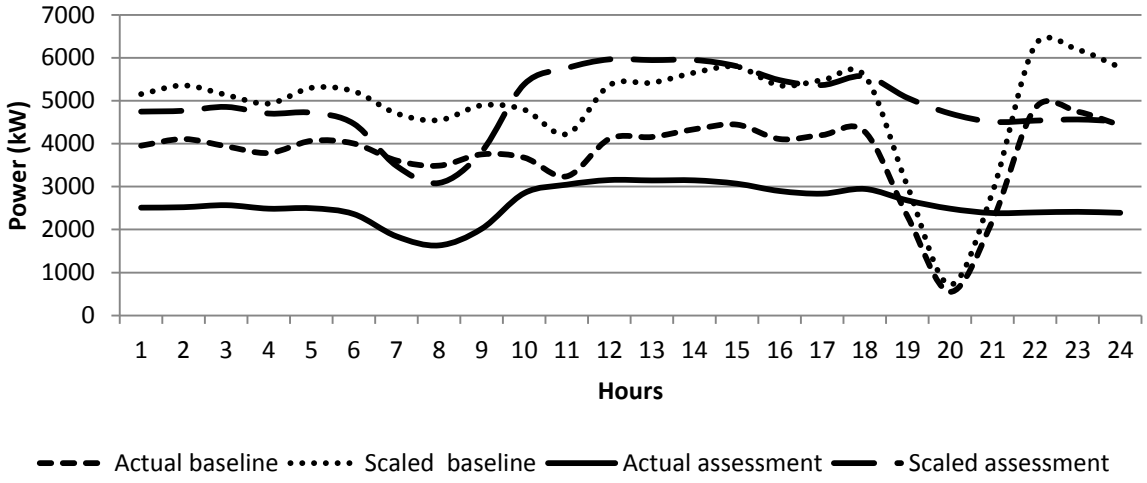

Figure 65: Average weekday baseline and assessment period cooling plant power and scaled plots

When comparing the scaled assessment to the scaled baseline in Figure 65, the main difference noticed is the evening peak load shift from the baseline period. The daily cost saving, as analysed by the scaled baseline, is R 21 522. If the assessment was completed in the winter months, this saving would have been much smaller due to the evening peak costs. This shows the need to revert to evening peak load shifting. As discussed, this

analysis will not be continued, due to the service-delivery changes resulting from the inclusion of the BAC in the assessment period.

An alternative means of assessment would be to compare the power data from the same period in 2011. This data is represented in Figure 66. As can be seen, the average power in 2012 is consumed more constantly, where it is noticed that the chiller plant was switched on and off as was needed during 2011. The difference between the two years' power data is shown in Table 28 in Appendix A. In summary, an average daily difference or savings of 0.24 MW is seen (as per Figure 66 and Table 28). The difference in savings as per the calculated (equation 20) and year-on-year analysis is due to the following reasons:

- 53% additional cooling load flow (flow to underground with addition of BAC flow as discussed in chapter 3.6)
- Increased service delivery temperatures (precool and chill dam 3 temperatures)

With these additional loads on the cooling plant, a year-on-year saving was still realised. It thus shows the effectiveness of having installed the VSDs and implementation of the respective control strategies.

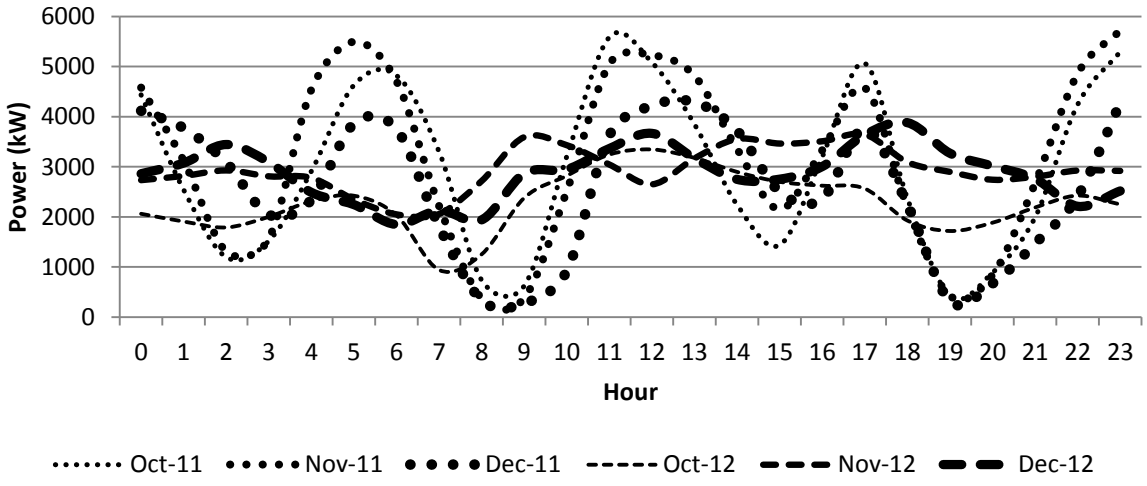

Figure 66: 2011 and 2012 October to November average weekday cooling plant power comparison

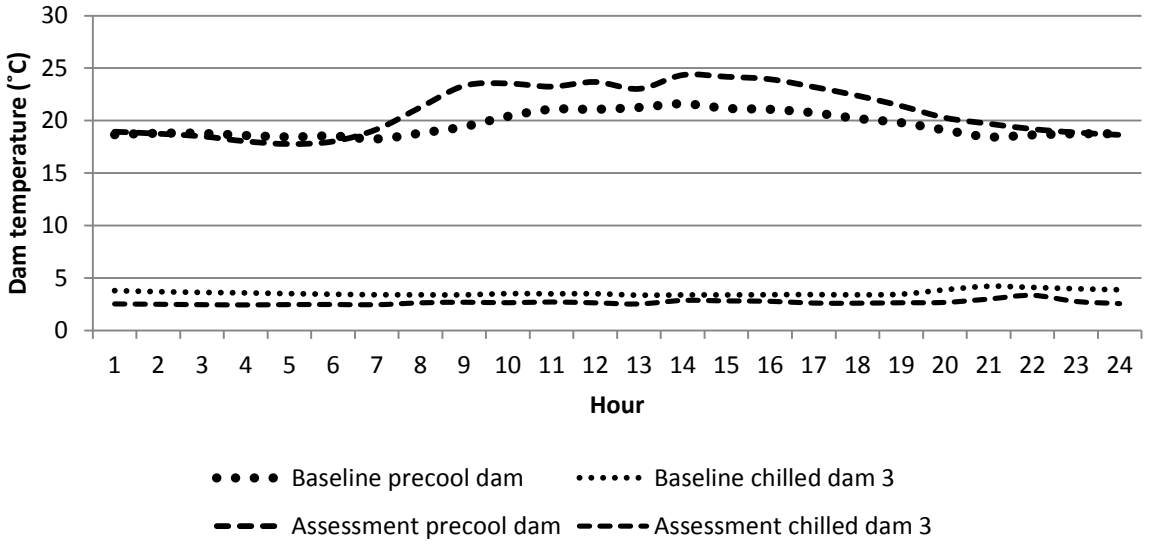

Figure 67: Average weekday assessment and baseline period hourly storage-dam temperatures

As can be seen in Figure 67 and Figure 68, the implementation not only maintained service delivery temperatures, but it improved the overall output of the plant. The increased difference between the two dam temperatures over the assessment period in Figure 67 is an indication of increased loading experienced by the plant.

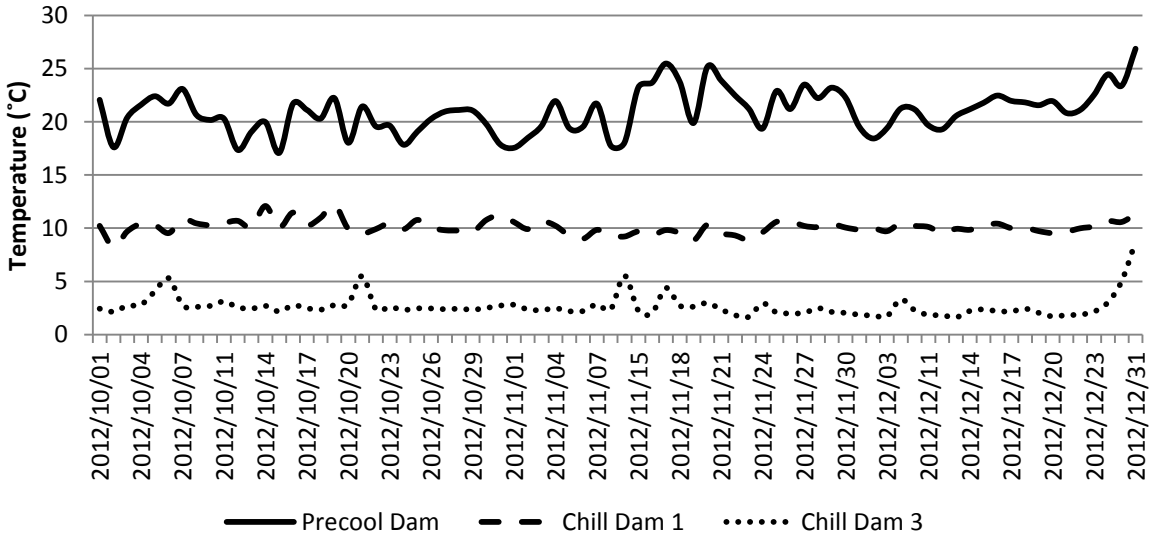

Figure 68: Average daily assessment period storage-dam temperatures

5.4 Analysis of BAC on load and efficiency

As previously discussed, a BAC (post energy audit) was installed, drawing an additional load from the chiller plant. As data collected for the baselines did not include this load, an additional analysis needs to be done. This additional data serves to provide a more accurate year-on-year analysis. As discussed, the targeted electricity savings were already in excess of the target. Any savings determined here is therefore merely a supplementary interpretation. Figure 69, below, displays useable data analysed to accurately obtain a kW output equation. The raw data is displayed in Table 29 in Appendix A. The equations obtained represent each month of the performance assessment period. The data used was to achieve an R^2 value above 0.85 where possible.

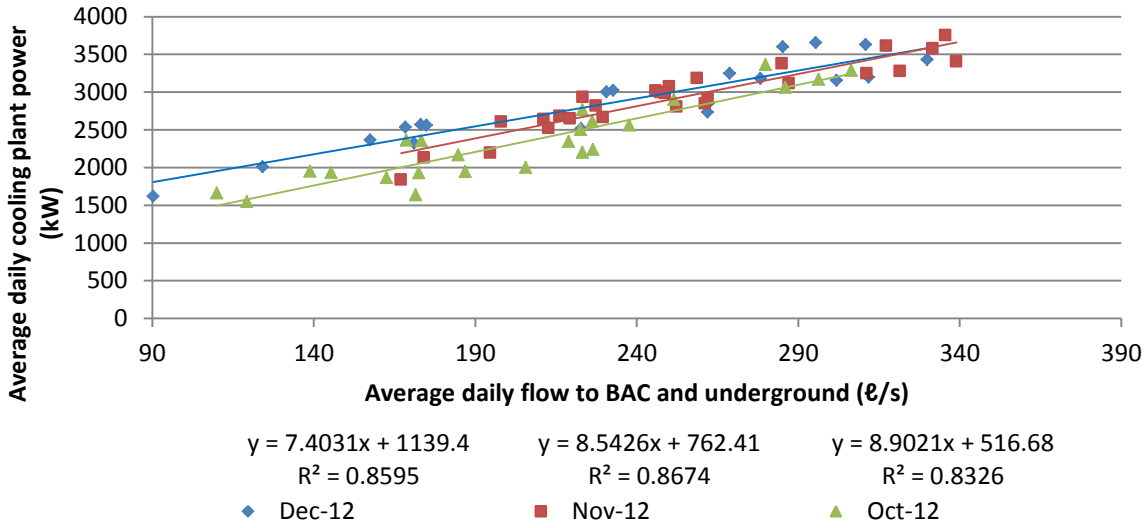

Figure 69: Trended power versus flow data for October to December 2012

Oct 12: $$y = 8.9021x + 516.68 \quad (21)$$

Nov 12: $$y = 8.5426x + 762.41 \quad (22)$$

Dec 12: $$y = 7.4031x + 1139.4 \quad (23)$$

The results in Table 21 were obtained by utilising equations 21 to 23 from Figure 69, with the average daily data from Figure 70 to Figure 72. It should be noted that the equations seem to be accurate, as each has a correlation (R^2) value of above 0.8. These high correlation values are the basis for utilising a proportional load assumption when applying these equations to obtain the values in Table 21.

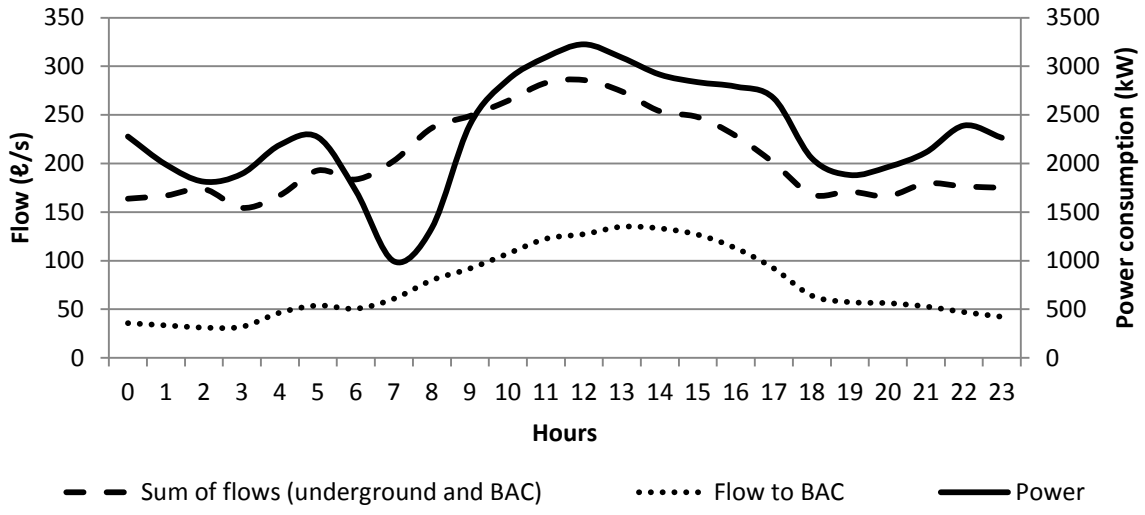

Figure 70: Average daily power and flow averages for October 2012

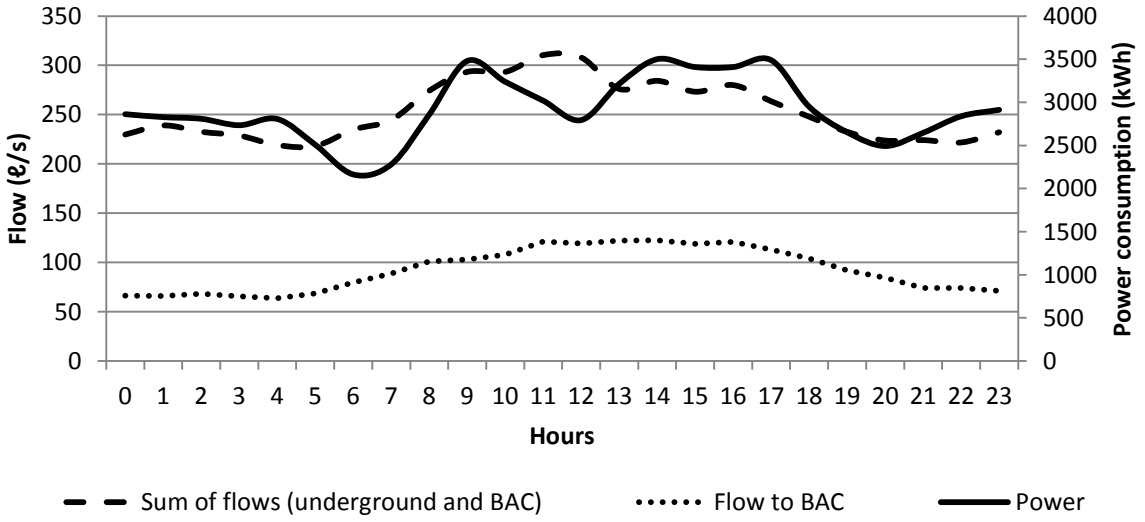

Figure 71: Average daily power and flow averages for November 2012

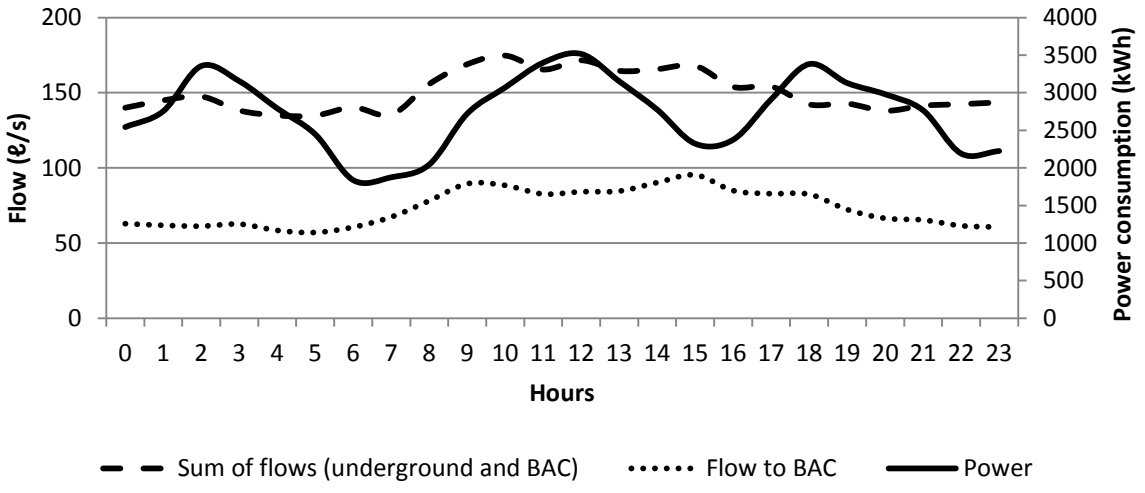

Figure 72: Average daily power and flow averages for December 2012

Table 21: Trended power data based on chilled water flow to the BAC for the year-on-year analysis

Hour	October (kW)	November (kW)	December (kW)	Average (kW)
0	835	1 329	1 604	1 256
1	814	1 326	1 596	1 246
2	794	1 345	1 592	1 244
3	801	1 324	1 602	1 243
4	931	1 307	1 571	1 270
5	995	1 347	1 561	1 301
6	967	1 442	1 587	1 332
7	1 058	1 518	1 637	1 405
8	1 228	1 625	1 717	1 523
9	1 335	1 642	1 801	1 592
10	1 471	1 684	1 793	1 650
11	1 607	1 797	1 751	1 718
12	1 649	1 781	1 762	1 731
13	1 717	1 806	1 765	1 763
14	1 702	1 807	1 807	1 772
15	1 644	1 777	1 844	1 755
16	1 520	1 795	1 767	1 694
17	1 336	1 727	1 752	1 605
18	1 086	1 650	1 749	1 495
19	1 027	1 546	1 674	1 416
20	1 018	1 483	1 631	1 377
21	987	1 394	1 622	1 335
22	936	1 394	1 594	1 308
23	893	1 370	1 588	1 284
Average	**1 181**	**1 551**	**1 682**	**1 471**

As can be seen by the calculated values in Table 21, the BAC water usage represents a large additional load on the chiller plant (1 471 kW). This data indicates that the year-on-year power consumption difference (electricity savings) should actually be as shown in Table 22 (1 712 kW). It should be noted that the load indicated in Table 21 is based on the power data from the assessment period.

Table 22: Realistic year-on-year power difference (Actual minus BAC power trending, electrical savings 2011-2012)

Hour	October (kW)	November (kW)	December (kW)	Average (kW)
0	3 207	3176	2 861	3 129
1	1 446	1629	2 293	1 874
2	2 00	-275	1 235	511
3	3 20	78	556	393
4	1 530	3069	1 422	2 006
5	3 203	4494	3 178	3 611
6	3 757	4101	3 491	3 757
7	3 417	1677	1 317	2 190
8	710	-716	113	27
9	-419	-1570	-789	-944
10	1 860	771	-230	766
11	3 948	3804	2 015	3 266
12	3 386	4358	2 315	3 420
13	2 386	3456	2 886	2 916
14	1 045	1608	2 777	1 773
15	383	464	1 591	787
16	2 097	1617	1 120	1 601
17	3 834	2654	1 878	2 836
18	1 528	747	117	940
19	-267	-928	-1 279	-724
20	20	-414	-713	-296
21	791	1263	331	824
22	2 753	3329	1 792	2 570
23	3 942	4173	3 348	3 811
Average	**1 883**	**1 776**	**1 401**	**1 712**

This analysis needs to similarly be completed utilising equation 20. Placing the variables with only flow to the BAC into equation 20 shows this higher load as shown in Figure 73. This separates the power used by the BAC and the underground flow. A more accurate approach could be to determine the power consumed for the chilled water flow to underground. This is shown in Figure 74. The BAC load here is the area between the dotted and dashed plots. In comparison to Table 21, this is a much smaller load with an average daily BAC cooling plant load consumption (power) of 628.8 kW.

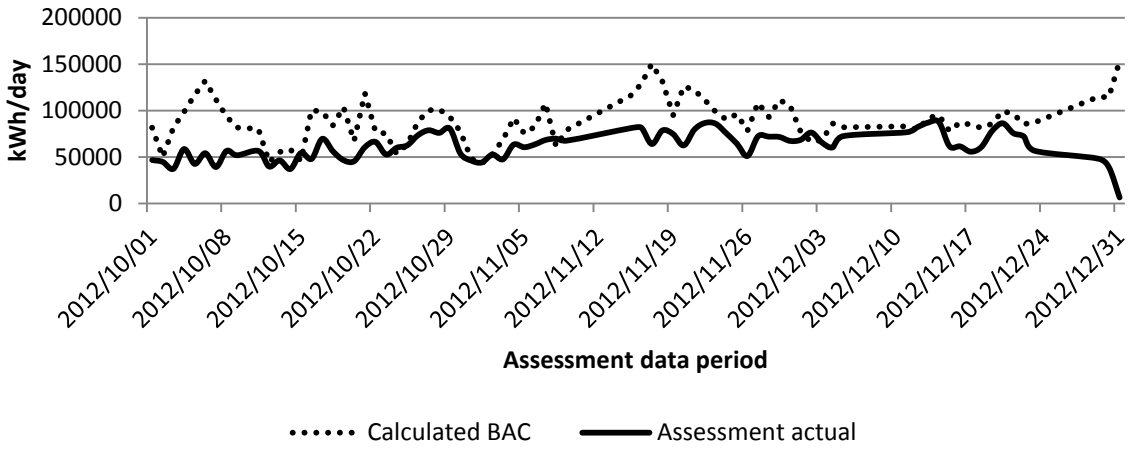

Figure 73: Calculated cooling load utilised by the BAC

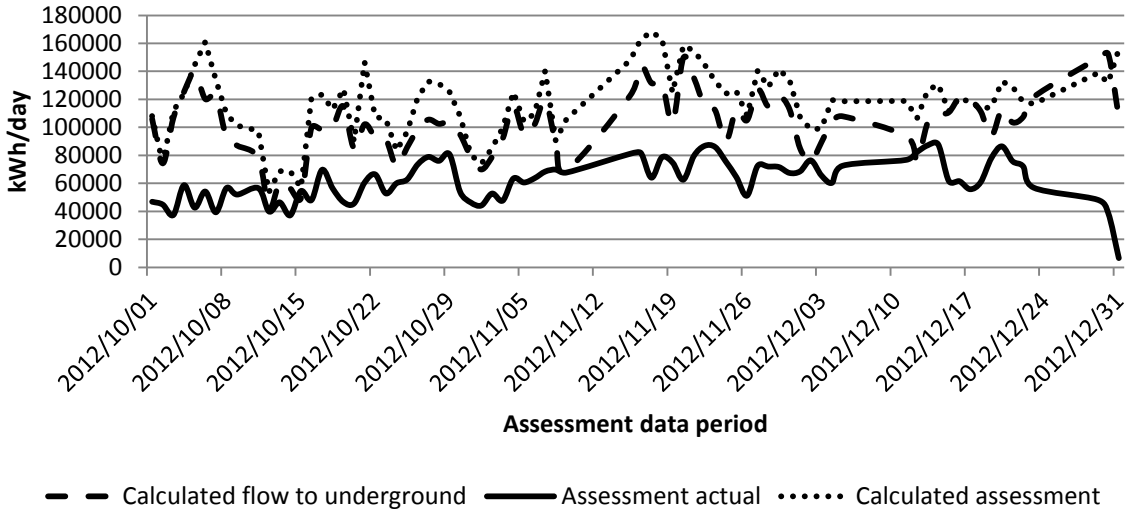

Figure 74: Calculated cooling load used by the chilled water sent underground and the total chilled water consumption (assessment)

Both the year-on-year and scaled baseline comparisons can be illustrated as the difference in power used to adjust the dashed plots in Figure 75 to the dotted plots (difference in chilled water flow). An additional illustration of this power difference is shown in Figure 67.

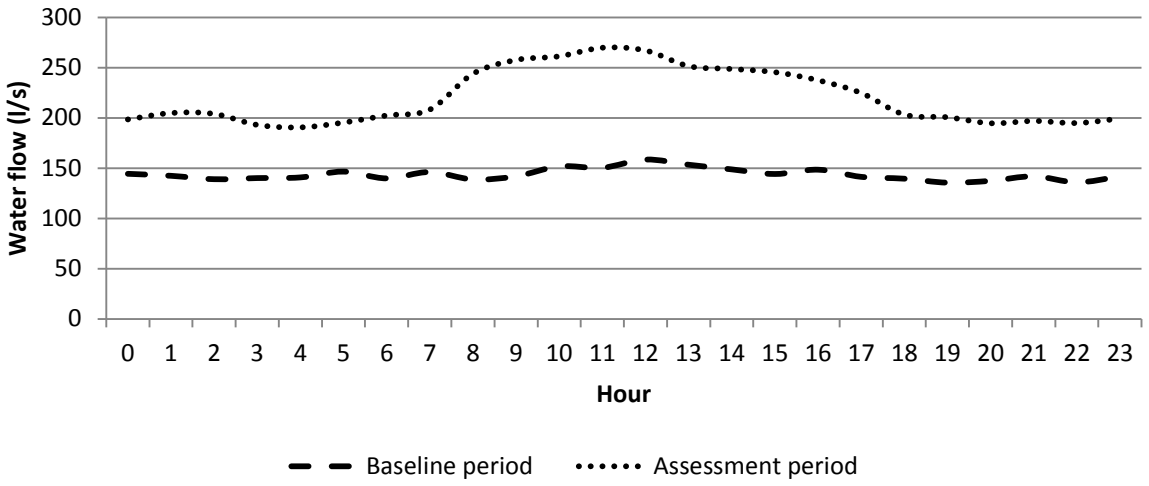

Figure 75: Baseline and assessment period service flow comparison

Summary of results:

Year-on-Year analysis:

- Average daily BAC load = 1.47 MW
- Average daily savings = 1.71 MW (0.24+1.47)

Calculated analysis:

- Average daily BAC load = 0.63 MW
- Average daily savings = 1.68 MW (2.31-0.63)

This indicates that the average daily savings approximates 1.7 MW. It is noted that the similarity of this data could be a data anomaly; however, findings will be based on these results being correct.

5.5 Interpretation of results

A point should be noted from the addition of the BAC on the chiller plant cooling load; the power data trended to adjust the year-on-year data is based on power consumption utilising the VSDs. As discussed, assuming no VSDs were present on the plant, said cooling load would thus most likely have been higher. This should be indicated in Figure 73. It is, however, obvious here that a low chilled water flow (consumption) does not provide an accurate analysis utilising the equation 20 (one third of the total flow cannot result in such a large portion of the total power consumption). It is thus reasonable to assume that the values from Table 21 are derived from the more accurate approach.

Through the analysis of the BAC on the loading of the cooling plant, it was seen that both means of savings verification produced the same outcome. The BAC loading, however, differed extensively in the two analyses. The calculated analysis showed the BAC loading to be 0.63 MW where the trended loading averaged at 1.47 MW. A difference is expected here; however, not as seen by the results. Both analyses indicated an average savings of 1.7 MW (33.6%) (excluding the BAC loading). These analyses include the calculated analysis and year-on-year trending. Findings will be based on these results being correct.

From Figure 75 it can be seen that the service-delivery flow rate to underground increased from the baseline to the performance assessment period. This is clear in the morning and evening periods when there was no flow to the BAC. It is this additional flow, coupled with the decreased chill dam 3 temperature, that partially results in the additional savings. This occurs as more power would be required to process the additional water through the plant, thus more pump savings would result. The decreased temperatures sent underground would, in addition, require more plant power, thus the calculated analysis would increase. The last portion of the additional savings resulted from the reduced recirculation of water through the plant. As less water is recirculated, less pumping costs are incurred, as the same volume of water does not pass through a pump more than once.

Based on these stated reasons it is reasonable to assume that the 1.7 MW saving was achieved on the cooling plant, as described in the baseline. It is thus also reasonable to assume that the savings difference of 0.6 MW (1.7 to 2.3 MW) is based on the same principles applied to the water consumed by the BAC.

Considering the installation costs incurred by the contractor, the payback period can be calculated using equation 16. As the case study was not analysed over an entire year, the

average daily savings is used to determine the PBP. An assumed average month of 30 days was used in the conversion of the PBP to years. As can be seen in Table 23, the PBP just exceeds two months, which is extremely short. It is noted that additional savings were incurred due to the installation of the BAC. The savings calculated for the year-on-year analysis, including BAC flow trends, show a longer payback period (less than four months), but this is still extremely economically viable.

Table 23: PBP realised from case study

	Installation costs (R)	Daily savings (R)	PBP (days)	PBP (years)
Calculated savings	1 633 910.00	23 290	70	0.2
Year on year savings with BAC trending analysis	1 633 910.00	15 022	108	0.3

An increase in efficiencies from the audit to the assessment period (COP/SCOP) is indicated in Table 24. As can be seen, the COPs and SCOPs increased across all the chillers (although only marginally for York 4).The large increase in efficiency for York 1 and 3 is largely due to the increase in evaporator water flow rate. The increase in Howden COP is largely due to the increase in evaporator water delta temperature.

Table 24: Increase in COP/SCOP from audit to assessment

Efficiencies	York 1	York 2	York 3	York 4	Howden
COP	0.98	-	1.87	0.05	2.85
SCOP	1.37	-	2.74	0.11	2.13

5.6 Conclusion

The intervention showed an increase in efficiency of individual plants, along with increased group efficiencies. The increase in COP and SCOP averaged 1.4 and 1.6 (23.2% and 31.7%) respectively. The increase in COP resulted from increased water flow rates through the evaporator, coupled with an increase in average evaporator temperature range. Additionally, reduced load on the chiller compressors was experienced. The SCOP's increase was from a combination of the COP increases and the reduced load on the water pumps.

Electricity consumption of the plant was shown to have a reduced power demand of 2.3 MW through the calculated assessment analysis. This translates to a saving of 4.2 GWh over the three-month assessment period. A return of R 23 290 per average weekday resulted from the reduced loading, leading to a saving of R 2 142 770 over the assessment period (92 days). Electricity demand only showed a reduction of 0.24 MW when comparing year-on-year data. The payback period realised is 2.3 months (0.2 years).

As analysed through equation 20 and the trended data, disregarding BAC service delivery, an average common saving of 1.7 MW is achieved. As per the initial investigated cooling plant, the following led to this saving: increased flow rates through various pumps, thus reduced pump and chiller running hours; reduced recirculation flow, thus reduced pump and chiller running hours; increased flow to underground, thus increased power demand; reduced water temperature sent underground, thus increased power consumption. All these, coupled with the energy efficiency improvement through the VSD installations, would have resulted in a decreased power consumption. These facts all lead to the conclusion that the saving of 1.7 MW that produces a payback period of 3.6 months (0.3 years) is accurate.

An average of 0.24 MW saving is seen when comparing the power of the same period from the previous year. With the BAC added to the service delivery of the plant, coupled with the service-delivery temperatures, enough proof that energy efficiency was improved is shown. Plant data could, however, not be compared for the year-on-year analysis due to data loss.

Power consumption of the cooling plant was shown to be less sporadic than the previous year. This indicates an improved control and utilisation of chiller scheduling.

Chapter 6 – Conclusion

6.1 Summary of work done

By analysing the past and present electricity situation in South Africa, a need for potential energy efficiency was defined. The availability of the DSM structure and its related literature identified a market gap to fulfil the need defined.

Through a study of various documents, a thorough knowledge of the respective components and concepts related to the case study was obtained. This knowledge formed the foundation for the implementation of an energy-efficiency case study. Not only did it provide a means of implementation, but it also provided a means of analysing the success of the case study. Additional knowledge not directly used on the case study would provide insight into alternative improvements that could be implemented.

The cooling plant was analysed to provide insight into control methods and process limitations. Data gathered through electronic mediums was analysed to indicate technical operating aspects of the system. These aspects would provide a baseline for comparison post implementation of the case study. Specific data was processed to form a scaling methodology, creating the ability to compare post implementation data of various operating conditions. The change in scope through the addition of a BAC to the cooling plant load was noted.

Projected results of the case study were evaluated by both a simulation and verification calculation set. Here it was indicated that the cooling plant had a potential for daily reduced electricity demand of an average 600 kW (13.6%). This electricity saving would show a saving of R2 275 000 per year based on the 2012/2013 Eskom Megaflex tariff structure. Contractor and capital installation costs would lead to a payback period of 8.6 months (0.7 years), based on the predicted return.

Negligible issues resulted from the installations. Control results on the VSDs varied per plant. Frequency operating ranges were determined per plant in addition to optimal evaporator water-delta temperature flow-rate frequencies. Control was commissioned through the EMS.

Savings realised in the assessment period through utilising equation 20 amounted to a daily average of 2.3 MW (47.1%). This showed a daily saving of R 23 290, resulting in a payback

period of 2.3 months (0.2 years). Year-on-year power comparisons showed a daily saving of 0.24 MW. Removing BAC trended cooling-load use from the year-on-year power data showed a daily saving of 1.7 MW (33.63%). A similar result was achieved when applied to equation 20. These analyses showed a daily saving of R15 022, resulting in a payback period of 3.6 months (0.3 years).

Throughout the dissertation it has been shown that the energy efficiency of the cooling plant was improved. Given the various operational changes, it is concluded that the resulting control did lead to an energy-efficiency improvement, even though the means of data scaling were not conclusive. The energy-efficiency improvement of the system ranges between 13.6% and 47.1%, depending on service delivery analysed.

The case study has shown that it is a worthy investment to install VSDs on water pumps in a mine cooling plant. The minimum energy-efficiency improvement proposed would have resulted in a payback period of less than a year. As a payback period of three years is still deemed to be acceptable, an increase in inflated installation costs would need to triple before one could consider such an implementation to be not viable.

6.2 Recommendations

As per the assessment, the main operational difference noticed was the absence of a load shift in the evening peak periods. The first step to realise reduced operating costs from the cooling plant is to re-establish a load-shifting operating schedule. An optimal load shift would include reduced consumption in both the morning- and evening peak periods. Countering this lost cooling load would require the entire plant to operate in the evening off-peak period.

Such an operating structure will result in a load shift energy-neutral schedule to a load shift energy-efficiency schedule because the evening ambient temperatures would allow for reduced load to be placed on the chillers. The capacity of the extent to which this can be implemented needs to be investigated through the cooling capacity of the precool towers and the storage capacity in the chilled water dams. The main return from this system will be seen by the client, due to reduced tariff structures where Eskom would see a minimal reduced loading.

Prediction capabilities should be investigated with reference to the controlling program. This could result in the plant only operating in the most efficient and cost-effective periods of the day. Additionally, operators would be able to plan minor maintenance schedules without interfering with the plant's scheduling. This will result in less downtime of components in the plant.

The potential for additional energy efficiency of the plant includes two noticeable opportunities.

1 The potential for power factor correction in the system. The aim would be to minimise the reactive power leaving the plant. As a result, the apparent power would converge towards the real power across the main power incomers.

2 The potential for installation of HEMs. All of the motors in the plant are old and have been rewound at least once. The potential in return through improved efficiency should be weighed against the LCCs of the present infrastructure and the cost of new infrastructure.

References

[1] Eskom, 2013. Capacity expansion. Available from: http://www.eskom.co.za/c/21/ capacity- expansion/. [accessed 18 April 2013].

[2] Eskom, 2012. Integrated results presentation for the year ended 31 March 2012. Available from: http://www.eskom.co.za/content/Eskomresults31Mar2012media_ presFINAL~3.pdf [accessed 20 April 2013].

[3] Eskom, 2010. The energy efficiency series, Towards an energy efficient mining sector. Available from: http://www.eskomidm.co.za/wp-content/themes/eskom/pdfs/ Industrial/Mining/121040ESKD%20Mining%20Brochure_paths.pdf [accessed 20 April 2013]

[4] Bluhm, S. and Biffi, M., 2001. Variations in ultra-deep, narrow reef stoping configurations and the effects on cooling and ventilation. *The Journal of The South African Institute of Mining and Metallurgy*, 3: 127-134. Available from: http://www.saimm.co.za/ Journal/ v101n03p127.pdf. [accessed 25 April 2013].

[5] Department of Minerals and Energy, 1996. No. 29 of 1996: Mine health and safety act, 1996. Available from: http://www.info.gov.za/view/DownloadFileAction?id=70869 [accessed 20 August 2013].

[6] Department of Minerals and Energy, 2008. Mine health and safety amendment bill. http://www.bullion.org.za/MediaReleases/Downloads/mine-health-and-safety.pdf [accessed 20 August 2013].

[7] ASHRAE, 2011. *HVAC Applications.* Atlanta: American Society of Heating, Refrigeration and Air conditioning Engineers.

[8] ABB, 2008. Energy efficiency makes a difference. Available from: http://www05.abb. com/global/scot/scot201.nsf/veritydisplay/cd6d14453239c791c125750800332bd2/$fil e/energy_efficiency_makes_difference_191108.pdf. [accessed 11 February 2012].

[9] Ozdemir, E., 2004. Energy conservation opportunities with a variable speed controller in a boiler house. *Applied Thermal Engineering*, 24: 981-993.

[10] Yu, F.W. and Chan, K.T., 2008. Improved energy performance of air cooled centrifugal chillers with variable chilled water flow. *Energy Conversion & Management,* 49: 1595-1611.

[11] DeBenedictis, A., Haley, B., Woo, C.K., Cutter E., 2013. Operational energy-efficiency improvement of municipal water pumping in California. *Energy,* 53: 237-243.

[12] TMEIC GE, 2011. Drive solutions for the global mining industry. Available from: http://www.tmge.com/upload/library_docs/english/TMEIC_GE_Solutions_for_the_Mining_Industry_lo-res_1306357296.pdf. [accessed 17 October 2012]

[13] Saidur, R., Rahim, N.A. and Hasanuzzaman, M., 2010. A review on compressed-air energy use and energy savings. *Renewable and Sustainable Energy Reviews,* 14: 1135-1153.

[14] Saidur, R., 2010. A review on electrical motors energy use and energy savings. *Renewable and Sustainable Energy Reviews,* 14: 877-898.

[15] World Pumps, 2009. Intelligent drives on the rise again. Available at: http://www.worldpumps.com/downloads/ [accessed 17 October 2012].

[16] Nored, M.G., Hollingsworth, J.R. and Brun, K., 2009. Application guideline for electric motor drive equipment for natural gas compressors. Gas Machinery Research Council, Southwest Reasearch Institute, US.

[17] U.S. Energy Information Administration, not dated. Independent statistics and analysis. Available from: http://www.eia.gov/cfapps/ipdbproject/iedindex3.cfm?tid=2&pid=2&aid=2&cid=r6,&syid=2006&eyid=2010&unit=BKWH [accessed 3 July 2013].

[18] NUS Consulting Group, 2012. Utility cost management. *2011-2012 International electricity and natural gas report and price survey*. Available from: http://www.kraftaffarer.se/meralasning/2012E&GSurvey.pdf [accessed 17 April 2013].

[19] Inglesi-Lotz, R. and Blignaut, J.N., 2011. South Africa's electricity consumption: A sectoral decomposition analysis. *Applied Energy*, 88: 4779-4784.

[20] The World Bank, not dated. South Africa. Available from: http://data.worldbank.org/country/south-africa#cp_surv [accessed 3 July 2013].

[21] Statistics South Africa, 2011. Statistical release P0302. Mid-year population estimates 2011. Available from: http://www.statssa.gov.za/publications/P0302/P03022011.pdf [accessed 20 April 2013].

[22] Index mundi, 2011. South Africa – Industrial production. Available from: http://www.indexmundi.com/g/g.aspx?c=sf&v=78 [accessed 20 August 2013].

[23] Etzinger, A., 2013. Southern African institute of steel construction, Steel Future. Steel Future conference 5& 6 March 2013 Sandton Sun Hotel conference centre. Available from: http://saisc.co.za/mail/steelfuture-presentation/25-AndrewEtzinger_presentation.pdf [accessed 20 August 2013].

[24] Fin24, 2008. Mines get Eskom breather. Available from: http://www.fin24.com/Economy/Mines-get-Eskom-breather-20080318-2 [accessed 15 April 2013].

[25] Hindustan times, 2012. Power grid failures a 'wake up call' for aspiring India. Available from: http://www.hindustantimes.com/India-news/NewDelhi/Power-grid-failures-a-wake-up-call-for-aspiring-India/Article1-906410.aspx [accessed 14 March 2013].

[26] Mehdudia, S., 2012. Day two: 21 States plunge into darkness as 3 grids collapse. The Hindu. Available from: http://www.thehindu.com/news/national/day-two-21-states-plunge-into-darkness-as-3-grids-collapse/article3707135.ece [accessed 14 March 2013].

[27] Thomas, S. 2008. Eskom may be forced to cut mines' power. Mail & Guardian. Available from: http://mg.co.za/article/2008-03-18-eskom-may-be-forced-to-cut-mines-power [accessed 18 April 2013].

[28] Statista, 2013. Global platinum mine production 2010-2012 by country. Available from: http://www.statista.com/statistics/273645/global-mine-production-of-platinum/ [accessed 20 October 2013]

[29] Goldsheet, 2012. Gold production history. Available from: http://www.goldsheetlinks.com/ production.htm [accessed 20 October 2013]

[30] Eskom, 2013. Kusile Power Station Project. Available from: http://www.eskom.co.za/ c/ article/58/kusile-power-station/. [accessed 18 April 2013].

[31] Eskom, 2013. Medupi Power Station. Available from: http://www.eskom.co.za/c /article/ 57/medupi-power-station/. [accessed 18 April 2013].

[32] Department of Energy, Republic of South Africa, 2012. Renewable Energy Independent Power Producer Procurement Programme. Available from: http://www.ipprenewables.co.za/ [accessed 20 August 2013].

[33] Eskom, 2013. Guide to Independent Power Producer (IPP) processes. Available from: http://www.eskom.co.za/c/73/info-site-for-ipps/ [accessed 20 August 2013].

[34] de Almeida, A.T., Fonseca, P. and Bertoldi, P., 2003. Energy-efficient motor systems in the industrial and in the services sectors in the European Union: characterisation, potentials, barriers and policies. *Energy*, 28: 673-690.

[35] Eskom, 2013. Tariffs and charges. Available from: http://www.eskom.co.za/c/53/ tariffs-and-charges/ [accessed 19 October 2013]

[36] Eskom, 2012. Tariffs & Charges Booklet 2011/12, Tariffs & Charges Booklet 2012/13. Available from: http://www.eskom.co.za/c/article/141/tariff-history/ [accessed 13 April 2013].

[37] Statistics South Africa, 2013. Quarterly labour force survey: quarter 1 (January to March), 2013 press statement. Available from: http://www.statssa.gov.za/news_ archive/Docs/QLFS_Press_statement_Q1_2013.pdf [accessed 24 August 2013]

[38] Wang, S.,Ren, T., Zhang, T., Liang, Y. and Z. Xu, 2012. Hot environment - estimation of thermal comfort in deep underground mines. *In:12th Coal Operators' Conference, University of Wollongong & the Australasian Institute of Mining and metallurgy*, 2012, 241-248. Available from: http://ro.uow.edu.au/cgi/viewcontent.cgi?article= 2073&context=coal. [accessed 04 May 2013].

[39] Stanton, D.J., 2004. Development and testing of an underground remote refrigeration plant. *In: International Platinum Conference 'Platinum Adding Value'.* The South African Institute of Mining and Metallurgy, 2004. Available from: http://www.saimm.co.za/ Conferences/ Pt2004/187_Stanton.pdf. [accessed 4 May 2013].

[40] Thomaz, C., 2009. Cooling solution for Africa's deep-level mines. *Mining weekly*. Available from: http://www.miningweekly.com/article/cooling-solution-for-africas-deep-level-mines-2009-07-10. [accessed 25 April 2013].

[41] IDE Technologies, 2010. Vacuum Ice Maker (VIM) for deep mine cooling. Available from: http://www.ide-tech.com/files/990b0fa01310a9c82f841f2183e9ebcb/page/2009/10/Mine%20Cooling%20%20Data%20Info%20-%20SR%20-%2020.10.2010%20(E).pdf [accessed 25 April 2013].

[42] Borgnakke, C., and Sonntag, R.E., 2009. *Fundamentals of Thermodynamics, SI Version*. 7th Edition. Hoboken: John Wiley & Sons.

[43] Cengel, Y.A., 2006. *Heat and Mass Transfer: A Practical Approach*. 3rd Edition. New York: McGraw-Hill.

[44] Srikhirin, P., Aphornratana, S. and Chungpaibulpatana, S., 2001. A review of absorption refrigeration technologies. *Renewable and Sustainable Energy Reviews*, 5: 343-372.

[45] Ansbro, J., Jonson Controls, not dated. Packaged Ammonia Chillers with Variable Frequency Drives. Avalable from: http://ec.europa.eu/clima/events/docs/0007/johnson_controls_ammonia_slides_en .pdf. [accessed 02 April 2014]

[46] ASHRAE, 1996. *HVAC Applications.* Atlanta: American Society of Heating, Refrigeration and Air conditioning Engineers.

[47] Irfan, H., Engpedia, not dated. Heat exchanger: Types of heat exchanger – shell, tube, plate, spiral. Available from: http://www.enggpedia.com/chemical-engineering-encyclopedia/93-machines-equipment/1854-heat-exchanger-types [accessed 24 August 2013]

[48] Techno Service, 2009. Gasket: Plate heat exchangers. Available from: www. technoserviceco.com/gasket.htm [accessed 24 August 2013].

[49] BPMA, 2004. Variable speed driven pumps, best practice guide. Birmingham: British Pump Manufacturers association. Available from: http://www.bpma.org.uk/ filemanager_net/files/gpg344_variable_speed_best_practice_for_pumps.pdf [accessed 14 September 2013].

[50] Wilson, S. Pump affinity laws for centrifugal pumps. *Grundfos White paper*. Available from: http://www.grundfos.com/content/dam/CBS/global/whitepapers/Whitepaper% 20-% 20Affinity%20Laws.pdf. [accessed 14 September 2013].

[51] The Engineering Toolbox. Pump Affinity Laws. Available from: http://www. engineeringtoolbox.com/affinity-laws-d_408.html. [accessed 14 September 2013].

[52] World Pumps, 2010. Energy savings begin at pump. Available at: http://www. worldpumps.com/downloads/ [accessed 17 October 2012].

[53] Kaya, D., Yagmur, A.E., Yigit S.K., Canka Kilic, F., Eren S.A. and Celik, C., 2008. Energy efficiency in pumps. *Energy Conversion and Management*, 49: 1662–1673

[54] Lee, T.S., Liao, K.Y. and Lu, W.C., 2012. Evaluation of the suitability of empirically-based models for predicting energy performance of centrifugal water chillers with variable chilled water flow. *Applied Energy,* 93: 583-595.

[55] Lu, Y., Chen, J., Liu T. and Chien M., 2011. Using cooling load forecast as the optimal operation scheme for a large multi-chiller system. *International Journal of Refrigeration*, 34: 2050-2062.

[56] Navarro-Esbrı´, J., Berbegall, V., Verdu, G., Cabello, R. and Llopis R., 2007. A low data requirement model of a variable-speed vapour compression refrigeration system based on neural networks. *International Journal of Refrigeration,* 30: 1452-1459.

[57] Romero, J.A., Navarro-Esbrí, J. and Belman-Flores, J.M., 2011. A simplified black-box model oriented to chilled water temperature control in a variable speed vapour compression system. *Applied Thermal Engineering,* 31: 329-335.

[58] Ma, Z., Wang, S., Xu, X. and Xiao, F., 2008. A supervisory control strategy for building cooling water systems for practical and real time applications. *Energy Conversion and Management,* 49: 2324-2336.

[59] Saidur, R., Hasanuzzaman M., Mahlia, T.M.I., Rahim, N.A. and Mohammed, H.A., 2011. Chillers energy consumption, energy savings and emission analysis in an institutional buildings. *Energy,* 36: 5233-5238.

[60] Yao, Y., Lian, Z., Hou, Z. and Zhou, X., 2004. Optimal operation of a large cooling system based on an empirical model. *Applied Thermal Engineering,* 24: 2303-2321.

[61] Tirmizi, S.A., Gandhidasan, P. and Zubair, S.M., 2012. Performance analysis of a chilled water system with various pumping schemes. *Applied Energy,* 100: 238-248.

[62] Manske, K.A., Reindl, D.T. and Klein, S.A., 2001. Evaporative condenser control in industrial refrigeration systems. *International Journal of Refrigeration,* 24: 676-691.

[63] Yu, F.W., and Chan, K.T., 2006. Modelling of the coefficient of performance of an air-cooled screw chiller with variable speed condenser fans. *Building and Environment,* 41: 407-417.

[64] Yu, F.W. and Chan, K.T., 2010. Economic benefits of optimal control for water-cooled chiller systems serving hotels in a subtropical climate. *Energy and Buildings,* 42: 203-209.

[65] Kairouani, L. and Nehdi, E., 2006. Cooling performance and energy saving of a compression–absorption refrigeration system assisted by geothermal energy. *Applied Thermal Engineering,* 26: 288-294.

[66] Pelzer, R., Mathews, E.H. and Schutte, A.J., 2010. Energy efficiency by new control and optimisation of fridge plant systems. *In: Proceedings of the industrial and commercial use of energy (ICUE) conference.* 28-30 July 2010 Cape Town. Available from: http://timetable. cput.ac.za/_other_web_files/_cue/ICUE/2010/PDF/Paper%20-%20EH%20Matthews.pdf. [accessed 7 June 2010]

[67] Yu, F.W. and Chan, K.T., 2008. Optimization of water-cooled chiller system with load-based speed control. *Applied Energy,* 85: 931-950.

[68] Navarro-Esbrı´, J., Ginestar, D., Belman, J.M., Milián V. and Verdú, G., 2010. Application of a lumped model for predicting energy performance of a variable-speed vapour compression system. *Applied Thermal Engineering,* 30: 286-294.

[69] Tian, J., Feng, Q. and Zhu, R., 2008. Analysis and experimental study of MIMO control in refrigeration system. *Energy Conservation and Management,* 49: 933-939.

[70] Bellas, I., Tassou, S.A, 2005. Present and future applications of slurries. *International Journal of Refrigeration,* 28: 115-121.

[71] Hasanuzzaman, M., Rahim, N.A., Saidur, R. and Kazi, S.N., 2011. Energy savings and emissions reductions for rewinding and replacement of industrial motor. *Energy,* 36: 233-240.

[72] Ferreira, F.J.T.E. and de Almeida, A.T., 2012. Induction motor downsizing as a low-cost strategy to save energy. *Journal of Cleaner Energy,* 24: 117-131.

[73] Mckane A. and Hasanbeigi A., 2011. Motor systems energy efficiency supply curves: A methodology for assessing the energy efficiency potential of industrial motor systems. *Energy Policy,* 39: 6595-6607.

[74] Saidur, R., Mekhilef, S., Ali, M.B., Safari, A. and Mohammed H.A., 2012. Applications of variable speed drive (VSD) in electrical motors energy savings. *Renewable and Sustainable Energy Reviews,* 16: 543-550.

[75] ABB, 2012. ABB Technology Guide: Variable-speed drive. Available from: http://www02.abb.com/db/db0003/db002698.nsf/ca7e93ab03030d22c12571380039e8fc/aa5853d43c2ad412c125720300632f74/$FILE/Tech+Guide_Drive.pdf [accessed 11 February 2012]

[76] Turkel, P.M. and Solomon, S., 1999. Understanding variable speed drives (Part 2) Available from: http://ecmweb.com/basics/understanding-variable-speed-drives-part-2. [accessed 11 February 2012].

[77] Thirugnanasambandam, M., Hasanuzzaman, M., Saidur, R., Ali, M.B., Rajakarunakaran, S.,Devaraj D. and Rahim N.A., 2011. Analysis of electrical motors load factors and energy savings in an Indian cement industry. *Energy,* 36: 4307-4314.

[78] Saidur, R., Hasanuzzaman M., Yogeswaran S., Mohammed H.A. and Hossain, M.S., 2010. An end-use energy analysis in a Malaysian public hospital. *Energy,* 35: 4780-4785.

[79] Schillinger, D., 2011. Variable speed technology improves power factor, boosts grid reliability. Danfoss Commercial Compressors. Available from: http://danfoss.com/ commercialcompressors [accessed 30 January 2013].

[80] NHP, 2007. Power factor correction. Available from: http://www.nhp.com.au/files/ editor_upload/File/Power%20Quality/Introduction-to-Power-Factor-Correction.pdf [accessed

[81] Hartman, T.P.E., 2002. *All-variable speed centrifugal chiller plants: Can we make our plants more efficient?* Available from: http://www.automatedbuildings.com.news. mar02/art/hrtmn/hrtmn.htm [accessed 15 October 2012]

[82] Du Plessis, G.E., Liebenberg, L. and Mathews, E.H., 2013. The use of variable speed drives for cost-effective energy savings in South African mine cooling systems. *Applied Energy,* 111: 16-27.

[83] Widell, K.N. and Eikevik, T., 2010. Reducing power consumption in multi-compressor refrigeration systems. *International Journal of Refrigeration,* 33: 88-94.

[84] Qureshi, T.Q. and Tassou, S.A., 1996. Variable-speed capacity control in refrigeration systems. *Applied Thermal Engineering,* 16: 103-113.

[85] Zhang, H., Xia, X. and Zhang, J., 2012. Optimal sizing and operation of pumping systems to achieve energy efficiency and load shifting. *Electric Power Systems Research,* 86: 41-50.

[86] Saidur, R., Rahim, N.A., Ping, H.W., Jahirul M.A., Mekhilef, S. and Masjuki H.H., 2009. Energy and emission analysis for industrial motors in Malaysia. *Energy Policy,* 37: 3650-3658.

[87] Al-Mansour, F., Merse, S. and Tomsic, M., 2003. Comparison of energy efficiency strategies in the industrial sector of Slovenia. *Energy,* 28: 421-440.

Appendix A – Additional savings data

Table 25: Respective daily savings over the assessment period

Date	Daily energy savings (kWh)	Average daily power savings (kW)
2012/10/01	61 149	2 547
2012/10/02	29 675	1 236
2012/10/03	74 325	3 096
2012/10/04	65 615	2 733
2012/10/05	10 189	4 245
2012/10/06	10 666	4 444
2012/10/07	94 830	3 951
2012/10/08	52 537	2 189
2012/10/09	49 297	2 054
2012/10/11	40 968	1 707
2012/10/12	13 800	575
2012/10/13	22 374	932
2012/10/14	31 342	1 305
2012/10/15	2 314	96
2012/10/16	72 999	3 041
2012/10/17	53 697	2 237
2012/10/18	56 326	2 346
2012/10/19	80 765	3 365
2012/10/20	4 533	1 855
2012/10/21	85 883	3 578
2012/10/22	41 029	1 709
2012/10/23	53 132	2 213
2012/10/24	23 270	969
2012/10/25	34 089	1 420
2012/10/26	47 851	1 993
2012/10/27	53 913	2 246
2012/10/28	55 222	2 300
2012/10/29	44 751	1 864
2012/10/30	53 943	2 247
2012/10/31	33 955	1 414
2012/11/01	29 804	1 241
2012/11/02	32 504	1 354
2012/11/03	51 846	2 160
2012/11/04	61 766	2 573
2012/11/05	43 483	1 811
2012/11/06	46 386	1 932
2012/11/07	71 982	2 999
2012/11/08	20 614	858
2012/11/09	37 895	1 578

2012/11/15	66 975	2 790
2012/11/16	81 101	3 379
2012/11/17	104 093	4 337
2012/11/18	84 422	3 517
2012/11/19	50 029	2 084
2012/11/20	96 113	4 004
2012/11/21	74 902	3 120
2012/11/22	58 148	2 422
2012/11/23	47 137	1 964
2012/11/24	48 555	2 023
2012/11/25	61 394	2 558
2012/11/26	57 123	2 380
2012/11/27	68 168	2 840
2012/11/28	56 593	2 358
2012/11/29	69 921	2 913
2012/11/30	66 749	2 781
2012/12/01	38 340	1 597
2012/12/02	21 961	915
2012/12/03	33 508	1 396
2012/12/04	59 160	2 465
2012/12/05	46 165	1 923
2012/12/11	42 115	1 754
2012/12/12	24 087	1 003
2012/12/13	39 198	1 633
2012/12/14	42 912	1 788
2012/12/15	49 954	2 081
2012/12/16	59 664	2 486
2012/12/17	62 163	2 590
2012/12/18	52 638	2 193
2012/12/19	36 229	1 509
2012/12/20	46 378	1 932
2012/12/21	53 324	2 221
2012/12/22	46 162	1 923
2012/12/23	60 006	2 500
2012/12/29	90 341	3 764
2012/12/30	92 980	3 874
2012/12/31	149 074	6 211
Sum/Average	**4 216 246**	**2 311**

Table 26: Average daily cost savings of case study implementation

Hour	Electricity tariff (c/kWh)	Baseline actual (kW)	Baseline cost (R)	Assessment actual (kW)	Assessment cost (R)	Scaling factor	Calculated assessment (kW)	Assessment savings (kW)	Cost savings (R)
0	28.69	3 952	1 134	2 510	720	1.89	4 746	2 236	641
1	28.69	4 107	1 178	2 520	723	1.89	4 765	2 245	644
2	28.69	3 938	1 129	2 567	736	1.89	4 855	2 287	656
3	28.69	3 783	1 085	2 486	713	1.89	4 701	2 215	635
4	28.69	4 065	1 166	2 496	716	1.89	4 720	2 224	638
5	28.69	4 002	1 148	2 359	676	1.89	4 461	2 102	603
6	41.04	3 607	1 480	1 841	755	1.89	3 481	1 640	673
7	66.98	3 487	2 336	1 631	1 092	1.89	3 085	1 453	973
8	66.98	3 751	2 512	2 017	1 351	1.89	3 815	1 797	1 204
9	66.98	3 674	2 461	2 847	1 907	1.89	5 384	2 536	1 699
10	41.04	3 239	1 329	3 045	1 250	1.89	5 759	2 713	1 113
11	41.04	4 111	1 687	3 153	1 294	1.89	5 962	2 809	1 152
12	41.04	4 155	1 705	3 143	1 290	1.89	5 944	2 800	1 149
13	41.04	4 336	1 779	3 145	1 290	1.89	5 948	2 802	1 150
14	41.04	4 442	1 823	3 067	1 258	1.89	5 800	2 733	1 121
15	41.04	4 107	1 685	2 897	1 189	1.89	5 478	2 581	1 059
16	41.04	4 200	1 723	2 836	1 164	1.89	5 364	2 527	1 037
17	41.04	4 277	1 755	2 945	1 208	1.89	5 569	2 624	1 077
18	66.98	2 312	1 548	2 679	1 794	1.89	5 067	2 387	1 599
19	66.98	550	368	2 487	1 666	1.89	4 703	2 216	1 484
20	41.04	2 203	904	2 384	978	1.89	4 509	2 124	871
21	41.04	4 826	1 980	2 399	984	1.89	4 536	2 137	877
22	28.69	4 745	1 361	2 413	692	1.89	4 563	2 149	616
23	28.69	4 429	1 270	2 389	685	1.89	4 519	2 129	610
Sum	**42.33**	**90 309**	**36 558**	**62 267**	**26 141**	**-**	**117 744**	**55 477**	**23 290**

Table 27: Variable data used to compile the assessment period calculated plot

Date	BAC flow from chiller plant (ℓ/s)	Flow to underground (ℓ/s)	Litres per day total	Ambient DB Temperature (˚C)	Precool Dam Temperature (˚C)	Chill Dam three Temperature (˚C)
2012/10/01	2.61	133.18	11732570	18.17	22.07	2.44
2012/10/02	16.72	124.41	12193619	16.61	17.62	2.16
2012/10/03	27.71	149.70	15328374	20.42	20.37	2.71
2012/10/04	30.09	130.25	13854018	23.61	21.60	2.81
2012/10/05	63.45	140.60	17630074	23.27	22.41	4.07
2012/10/06	134.15	146.94	24286491	22.80	21.70	5.30
2012/10/07	53.99	113.82	14499476	23.11	23.08	2.75
2012/10/08	86.62	79.94	14390692	19.73	20.64	2.61
2012/10/09	83.79	98.84	15779059	16.05	20.17	2.70
2012/10/11	83.43	87.78	14792521	14.06	20.30	3.11
2012/10/12	55.56	45.38	8721766	10.81	17.35	2.56
2012/10/13	50.68	66.60	10132845	11.30	19.09	2.44
2012/10/14	46.32	51.53	8454361	9.69	19.95	2.70
2012/10/15	54.49	55.49	9502861	13.10	17.08	2.17
2012/10/16	100.12	102.50	17506588	18.41	21.70	2.75
2012/10/17	124.98	124.90	21589142	17.68	21.12	2.48
2012/10/18	73.72	143.90	18802944	18.48	20.30	2.34
2012/10/19	65.32	119.62	15978448	21.14	22.22	2.78
2012/10/20	99.43	116.38	18646527	14.09	18.03	2.87
2012/10/21	137.09	141.55	24074504	17.07	21.44	5.50
2012/10/22	78.00	152.47	19912673	17.10	19.56	2.39
2012/10/23	65.53	155.55	19101627	16.59	19.64	2.59
2012/10/24	59.29	150.82	18152972	13.55	17.82	2.32
2012/10/25	56.24	168.64	19429742	14.17	19.08	2.47
2012/10/26	113.92	168.30	24383170	16.53	20.27	2.46
2012/10/27	139.66	164.07	26241995	17.85	20.96	2.39
2012/10/28	143.43	151.23	25458144	17.45	21.10	2.43
2012/10/29	115.79	162.25	24022760	16.68	21.06	2.35
2012/10/30	71.69	152.55	19374602	16.93	19.76	2.50
2012/10/31	8.82	162.19	14774881	14.49	17.86	2.72
2012/11/01	8.34	157.05	14289563	12.98	17.55	2.80
2012/11/02	30.64	161.74	16622121	13.89	18.49	2.36
2012/11/03	43.17	156.85	17282024	16.31	19.63	2.30
2012/11/04	42.58	167.27	18130370	19.56	21.94	2.48
2012/11/05	45.70	147.08	16656176	19.84	19.40	2.20
2012/11/06	58.04	138.03	16939755	21.74	19.53	2.21
2012/11/07	95.31	164.59	22455013	21.69	21.70	2.84
2012/11/08	97.12	145.00	20919451	14.05	17.74	2.37
2012/11/09	91.85	132.47	19381396	13.68	18.04	5.53

2012/11/15	122.46	161.68	24549913	19.93	23.24	2.26
2012/11/16	162.08	173.07	28957358	21.23	23.68	2.03
2012/11/17	138.28	89.91	19716347	21.84	25.49	4.38
2012/11/18	158.98	160.09	27568081	20.88	23.75	2.72
2012/11/19	119.15	151.20	23357906	19.85	19.86	2.62
2012/11/20	29.14	165.02	16775056	25.00	25.16	2.98
2012/11/21	82.12	164.06	21269266	23.89	23.88	2.36
2012/11/22	143.13	170.39	27087573	19.25	22.47	1.83
2012/11/23	141.53	175.02	27350214	17.83	21.22	1.67
2012/11/24	150.23	171.79	27821961	15.81	19.37	2.93
2012/11/25	64.23	150.81	18579738	17.60	22.89	2.09
2012/11/26	17.53	152.70	14707481	18.94	21.19	2.00
2012/11/27	81.61	161.73	21024626	20.01	23.49	2.03
2012/11/28	58.49	179.25	20540664	17.85	22.20	2.49
2012/11/29	93.85	153.04	21331309	20.64	23.22	2.13
2012/11/30	102.56	145.69	21449324	20.22	22.28	2.04
2012/12/01	109.53	148.89	22327202	15.90	19.52	1.86
2012/12/02	113.09	163.08	23860854	13.97	18.43	1.79
2012/12/03	95.12	156.94	21777470	13.80	19.38	1.73
2012/12/04	49.07	169.70	18901670	16.31	21.25	3.32
2012/12/05	42.30	185.80	19707665	17.82	21.17	2.30
2012/12/11	126.82	181.02	26597908	16.46	19.67	1.85
2012/12/12	144.80	136.75	24326054	14.48	19.28	1.82
2012/12/13	134.74	174.23	26694683	17.63	20.54	1.62
2012/12/14	113.24	179.50	25292732	17.68	21.17	2.22
2012/12/15	-0.31	170.40	14695767	17.78	21.78	2.37
2012/12/16	-0.27	171.25	14771918	20.27	22.47	2.21
2012/12/17	-0.30	168.60	14541693	20.63	21.96	2.18
2012/12/18	-0.30	162.44	14008789	18.99	21.83	2.44
2012/12/19	93.98	143.39	20508631	14.56	21.57	2.04
2012/12/20	105.55	168.29	23659724	19.21	21.94	1.71
2012/12/21	131.18	166.29	25701538	18.56	20.81	1.83
2012/12/22	62.65	164.80	19651717	18.84	21.11	1.88
2012/12/23	-0.27	149.80	12919400	20.12	22.55	2.16
2012/12/29	3.25	120.43	10685364	24.21	24.45	3.04
2012/12/30	0.00	88.92	7682687	22.47	23.39	5.04
2012/12/31	0.00	9.31	804615	20.71	26.87	8.74

Table 28: Year-on-year power difference (supposed electricity savings 2011-2012)

Hour	October difference (kW)	November difference (kW)	December difference (kW)	Average savings (kW)
0	2372	1847	1256	1873
1	632	303	696	628
2	-593	-1620	-356	-732
3	-481	-1245	-1045	-849
4	599	1761	-149	736
5	2207	3146	1617	2309
6	2789	2658	1903	2424
7	2358	158	-320	785
8	-517	-2341	-1604	-1496
9	-1754	-3212	-2590	-2537
10	388	-912	-2023	-883
11	2341	2006	264.	1547
12	1736	2576	552	1688
13	668	1649	1121	1153
14	-656	-199	969	1
15	-1261	-1313	-253	-968
16	576	-178	-647	-93
17	2498	927	125	1230
18	442	-903	-1631	-554
19	-1294	-2474	-2953	-2140
20	-998	-1898	-2344	-1674
21	-196	-131	-1291	-511
22	1817	1934	197	1261
23	3049	2802	1760	2527
Average	**701**	**225**	**-281**	**241**

Table 29: Raw power and chilled water flow data

	Average daily cooling plant power (kW)	Average daily flow to BAC and underground (ℓ/s)
2012/10/01	1951.5	138.8
2012/10/02	1865.9	162.6
2012/10/07	1637.3	171.5
2012/10/08	2360.3	168.7
2012/10/09	2165.1	184.7
2012/10/10	2561.9	237.6
2012/10/11	2355.8	173.3
2012/10/12	1660.1	110.0
2012/10/13	1934.5	145.4
2012/10/14	1546.7	119.3
2012/10/16	2002.0	205.6
2012/10/17	2902.7	251.5
2012/10/18	2344.1	218.9
2012/10/19	1944.4	186.9
2012/10/22	2764.7	223.2
2012/10/23	2199.7	223.2
2012/10/24	2500.5	222.6
2012/10/25	2611.9	226.3
2012/10/26	3062.2	286.0
2012/10/27	3285.7	306.4
2012/10/28	3168.7	296.4
2012/10/29	3362.3	279.8
2012/10/30	2238.5	226.4
2012/10/31	1928.3	172.5
2012/11/01	1841.0	167.0
2012/11/02	2196.0	194.7
2012/11/04	2642.5	211.2
2012/11/05	2524.6	212.7
2012/11/06	2651.2	219.3
2012/11/07	2850.0	261.1
2012/11/08	2909.8	262.0
2012/11/09	2820.7	227.3
2012/11/10	2935.7	223.3
2012/11/11	3248.1	311.2
2012/11/12	3752.5	335.6
2012/11/13	3184.4	258.7
2012/11/14	3073.8	250.0
2012/11/15	3379.7	284.9
2012/11/16	3406.6	339.0
2012/11/17	2668.2	229.5
2012/11/18	3278.9	321.5

2012/11/19	3116.2	287.1
2012/11/20	2606.4	198.0
2012/11/22	3613.4	317.2
2012/11/23	3580.0	331.6
2012/11/25	2683.8	216.1
2012/11/26	2132.0	174.1
2012/11/27	3018.6	245.8
2012/11/28	2998.5	247.3
2012/11/29	2985.1	248.7
2012/11/30	2808.2	252.3
2012/12/01	2856.1	262.3
2012/12/02	3183.1	278.3
2012/12/03	2735.5	261.9
2012/12/04	2514.9	222.8
2012/12/05	3022.5	232.7
2012/12/11	3198.6	311.8
2012/12/12	3429.5	329.9
2012/12/13	3629.3	310.8
2012/12/14	3657.5	295.4
2012/12/15	2568.2	173.1
2012/12/16	2562.6	174.9
2012/12/17	2324.5	171.1
2012/12/18	2535.6	168.3
2012/12/19	3249.1	268.7
2012/12/20	3600.3	285.2
2012/12/21	3156.8	301.8
2012/12/22	3001.4	230.6
2012/12/23	2368.4	157.5
2012/12/29	2011.3	124.1
2012/12/30	1619.7	90.3

Appendix B – Power data collection validation

The images below show the calibration certificates for the portable loggers used. The data of the portable loggers versus the permanent loggers later installed is also validated in Figure 76. The data had an average error of 0.6% over the comparison period, indicating that the permanent loggers had been set up correctly. The calibration of the permanent loggers was, in addition, verified.

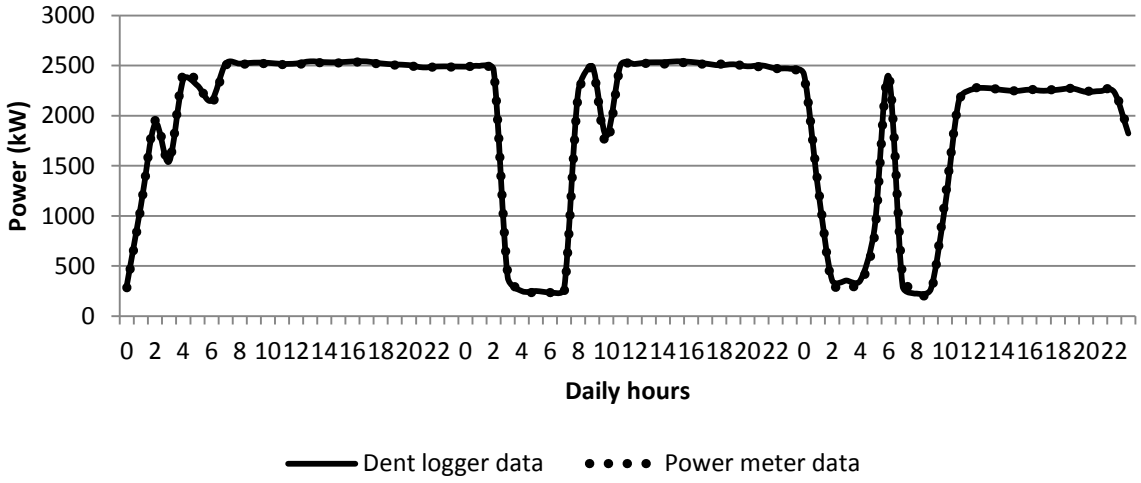

Figure 76: Portable and permanent power meter data comparison

DENT INSTRUMENTS

Phone: 541.388.4774
Fax: 541.385.9333
925 SW Emkay Drive
Bend, OR 97702 USA
www.DentInstruments.com

Logger Calibration Data Sheet

Logger Information

Date: 12/2/2010	**Time:** 15:09:43	**Serial #:** EAAC3
ID: IL400.064 Logger	**Type:** ELITEpro	**Description:** DENT ELITEpro
Modem: NONE	**Memory:** 512K	**Amp Scalar:** 0.00091769
Technician: KCH		**Volt Scalar:** 0.42467448

Logger Measurements

Channel Measurements	Description	Reference Measurement	Logger Values	Per Cent Error
Channel 1	Amp	150.45	150.44	0.01%
Channel 2	Amp	150.45	150.44	0%
Channel 3	Amp	150.45	150.46	0%
Channel 4	Amp	150.45	150.46	0%
Channel 1	Volt	500.24	500.19	0.01%
Channel 2	Volt	500.24	500.37	-0.03%
Channel 3	Volt	500.24	500	0.05%

Calibration Reference Instruments used:

Hewlett Packard 34411A Multimeter, Serial #s MY48004529

The calibration of this logger is traceable to the National Institute of Standards and Technology (NIST) using the above reference instruments.

Version 64 Firmware Note: If external power to the ELITEpro is lost (no wall transformer or line power) the logger will automatically switch to internal battery UNLESS the logging interval is 3, 15 or 30 seconds. For these intervals logging will stop until power is again applied.

Figure 77: Incomer one logger calibration sheet

Phone: 541.388.4774
Fax: 541.385.9333
925 SW Emkay Drive
Bend, OR 97702 USA
www.DentInstruments.com

Logger Calibration Data Sheet

Logger Information

Date: 12/2/2010	**Time:** 15:22:03	**Serial #:** EAAC4
ID: IL400.064 Logger	**Type:** ELITEpro	**Description:** DENT ELITEpro
Modem: NONE	**Memory:** 512K	**Amp Scalar:** 0.00091714
Technician: KCH		**Volt Scalar:** 0.42435628

Logger Measurements

Channel Measurements	Description	Reference Measurement	Logger Values	Per Cent Error
Channel 1	Amp	150.45	150.47	-0.01%
Channel 2	Amp	150.45	150.46	0%
Channel 3	Amp	150.45	150.46	0%
Channel 4	Amp	150.45	150.44	0.01%
Channel 1	Volt	500.21	500.16	0.01%
Channel 2	Volt	500.21	500.24	-0.01%
Channel 3	Volt	500.21	499.84	0.07%

Calibration Reference Instruments used:

Hewlett Packard 34411A Multimeter, Serial #s MY48004529

The calibration of this logger is traceable to the National Institute of Standards and Technology (NIST) using the above reference instruments.

Version 64 Firmware Note: If external power to the ELITEpro is lost (no wall transformer or line power) the logger will automatically switch to internal battery UNLESS the logging interval is 3, 15 or 30 seconds. For these intervals logging will stop until power is again applied.

Figure 78: Incomer two logger calibration sheet

DENT INSTRUMENTS

Phone: 541.388.4774
Fax: 541.385.9333
925 SW Emkay Drive
Bend, OR 97702 USA
www.DentInstruments.com

Logger Calibration Data Sheet

Logger Information

Date: 10/9/2009	**Time:** 8:23:16	**Serial #:** E9A13
ID: IL400.064 Logger	**Type:** ELITEpro	**Description:** DENT ELITEpro
Modem: NONE	**Memory:** 512K	**Amp Scalar:** 0.00091731
Technician: BDL		**Volt Scalar:** 0.42476189

Logger Measurements

Channel Measurements	Description	Reference Measurement	Logger Values	Per Cent Error
Channel 1	Amp	150.06	150.05	0%
Channel 2	Amp	150.06	150.03	0.02%
Channel 3	Amp	150.06	150.04	0.02%
Channel 4	Amp	150.06	150.04	0.02%
Channel 1	Volt	499.52	499.52	0%
Channel 2	Volt	499.52	499.57	-0.01%
Channel 3	Volt	499.52	499.15	0.07%

Calibration Reference Instruments used:

Hewlett Packard 34411A Multimeter, Serial #s MY48004529

The calibration of this logger is traceable to the National Institute of Standards and Technology (NIST) using the above reference instruments.

Version 64 Firmware Note: If external power to the ELITEpro is lost (no wall transformer or line power) the logger will automatically switch to internal battery UNLESS the logging interval is 3, 15 or 30 seconds. For these intervals logging will stop until power is again applied.

Figure 79: Incomer three logger calibration sheet

Appendix C – Additional chiller constraints

Table 30: York chiller operating constraints

Constraints	Operating range and trip values			
	High Trip	High Alarm	Low Alarm	Low Trip
Compressor discharge temperature (˚C)	50	47	35	30
Compressor suction temperature (˚C)	35	30	3	2
Compressor trust oil temperature (˚C)	70	62	0	0
Drive motor bearing (DE) (˚C)	75	70	0	0
Drive motor bearing (NDE) (˚C)	75	70	0	0
Gearbox bearing temperature (˚C)	85	80	0	0
Gearbox bearing temperature (˚C)	85	80	0	0
Gearbox bearing temperature (˚C)	85	80	0	0
Gearbox bearing temperature(˚C)	85	80	0	0
Gearbox oil temperature (˚C)	70	60	0	0
Evaporator liquid temperature (˚C)	12	10	1	0.5
Compressor oil sump temperature (˚C)	60	55	40	35
Motor-winding temperature 1 (˚C)	110	105	0	0
Motor-winding temperature 2 (˚C)	110	105	0	0
Motor-winding temperature 3 (˚C)	110	105	0	0
Evaporator pressure (kPa)	350	300	220	208
Condenser pressure (kPa)	850	840	500	450
Compressor auxiliary oil pressure (kPa)	550	500	250	200
Compressor main oil pressure (kPa)	550	540	250	200
Gearbox oil pressure (kPa)	280	250	130	120
Economiser pressure (kPa)	350	300	200	180
Drive motor vibration 1 (mm/s)	6	5	0	0
Drive motor vibration 2 (mm/s)	6	5	0	0
Gearbox vibration 1 (mm/s)	6	5	0	0
Gearbox vibration 2 (mm/s)	6	5	0	0
Compressor vibration 1 (mm/s)	6	5	0	0
Compressor vibration 2 (mm/s)	6	5	0	0
Compressor motor Amps (A)	93	90	40	30

Table 31: Howden chiller operating constraints

Constraints	Operating range and trip values	
	High trip	Low trip
Axial vibration (mm/s)	7	-
Radial vibration (mm/s)	7	-
Compressor shaft movement (mm)	1.7	-
Condenser water differential pressure (kPa)	250	-
Condenser water filter differential pressure (kPa)	100	-
Condenser ammonia temperature (˚C)	55	-
Condenser ammonia inlet temperature (˚C)	55	-
Condenser ammonia outlet temperature (˚C)	38	10
Condenser filter differential pressure (kPa)	100	10
Evaporator water differential pressure (kPa)	250	-
Evaporator water filter differential pressure (kPa)	50	-
Evaporator water ammonia inlet temperature (˚C)	-	-3
Evaporator water ammonia outlet temperature (˚C)	-	-3
Discharge pressure (kPa)	1380	-
Discharge temperature (˚C)	-	30
Liquid receiver level (%)	80	10
Manifold oil temperature (˚C)	55	20
Separator oil temperature (˚C)	50	25
Compressor oil differential pressure (kPa)	600	230
Surge drum level (%)	50	-5
Surge drum pressure (kPa)	-	305
Suction temperature (kPa)	-	-3
Motor DE bearing temperature (˚C)	95	-
Motor NDE bearing temperature (˚C)	95	-
Motor winding temperature 1 ,2 and 3 (˚C)	120	-
Motor power (kW)	1850	-

Appendix D – Additional COP plots

Figure 80 to Figure 97 only have data plotted where the respective chiller was operational for an entire hour. The scattering of the data has no link to the respective hour each data point was obtained from.

Baseline period plots

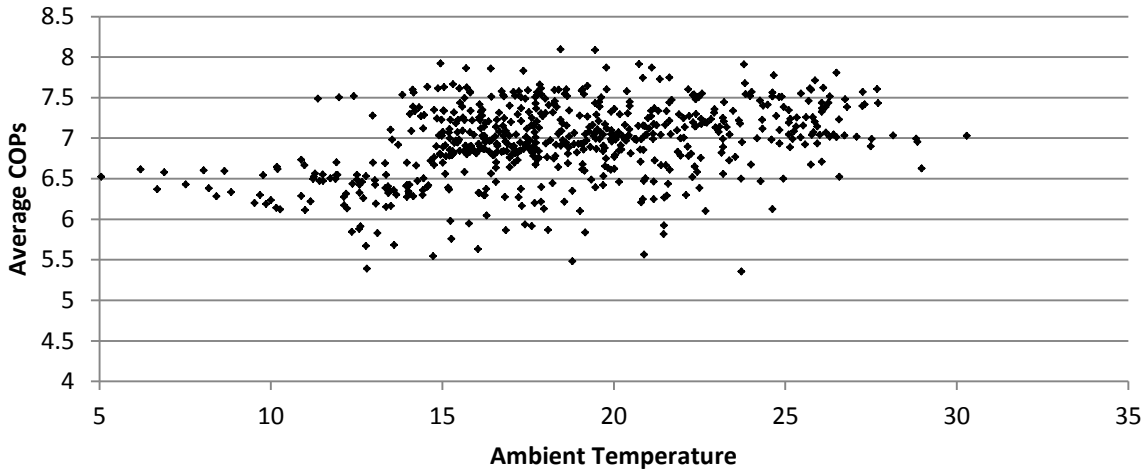

Figure 80: York 1 COPs plotted against ambient temperature for operational hours during the baseline period

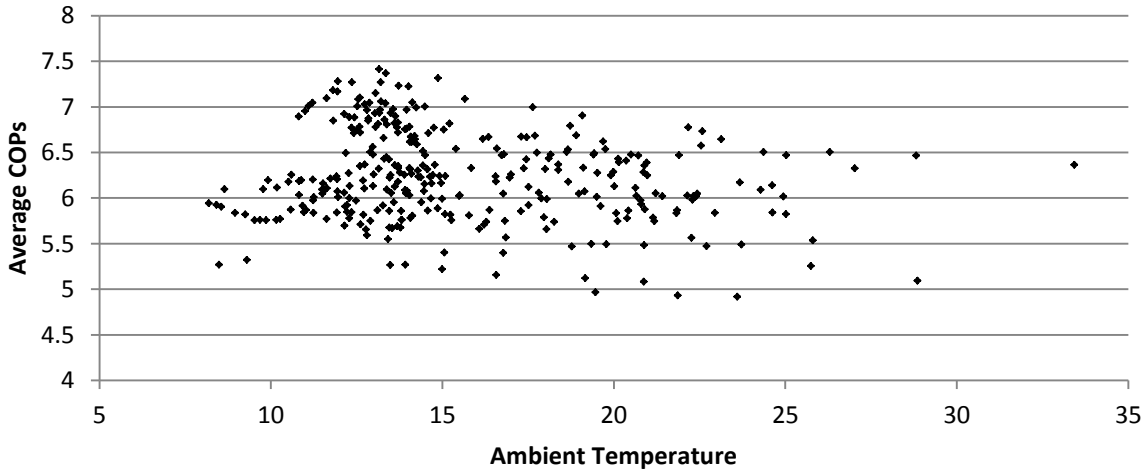

Figure 81: York 2 COPs plotted against ambient temperature for operational hours during the baseline period

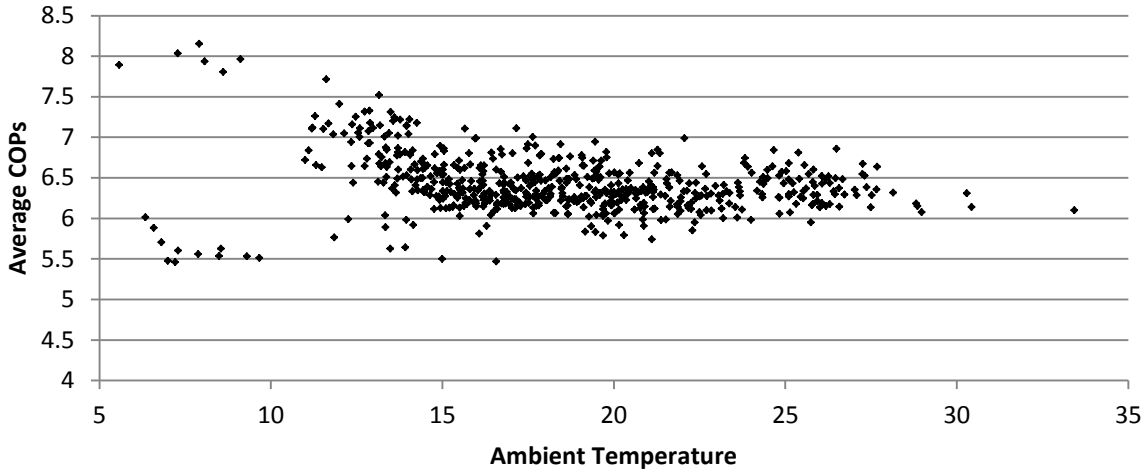

Figure 82: York 3 COPs plotted against ambient temperature for operational hours during the baseline period

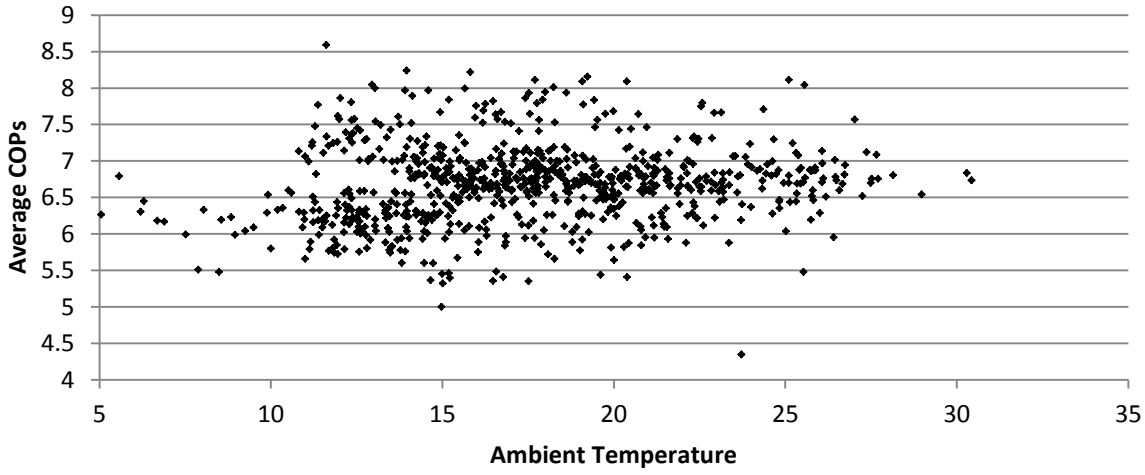

Figure 83: York 4 COPs plotted against ambient temperature for operational hours during the baseline period

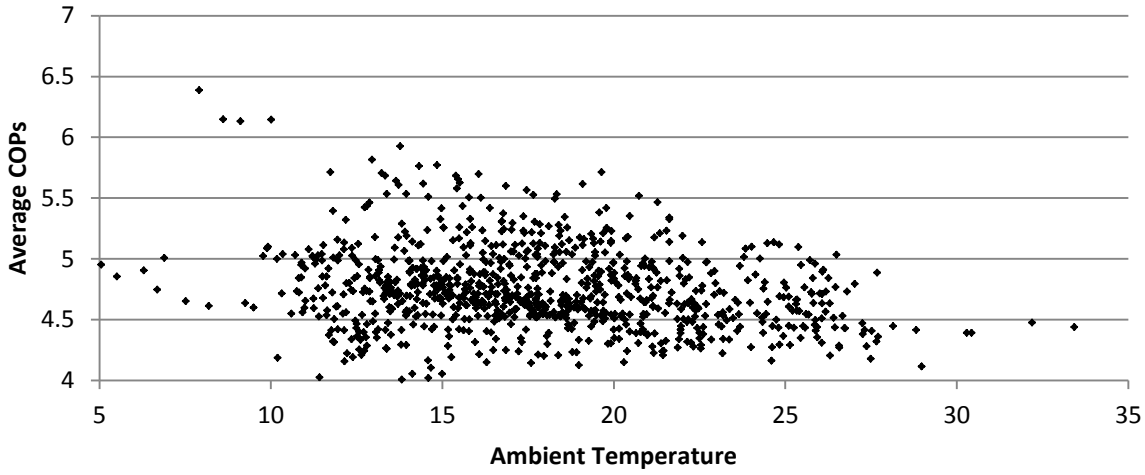

Figure 84: Howden COPs plotted against ambient temperature for operational hours during the baseline period

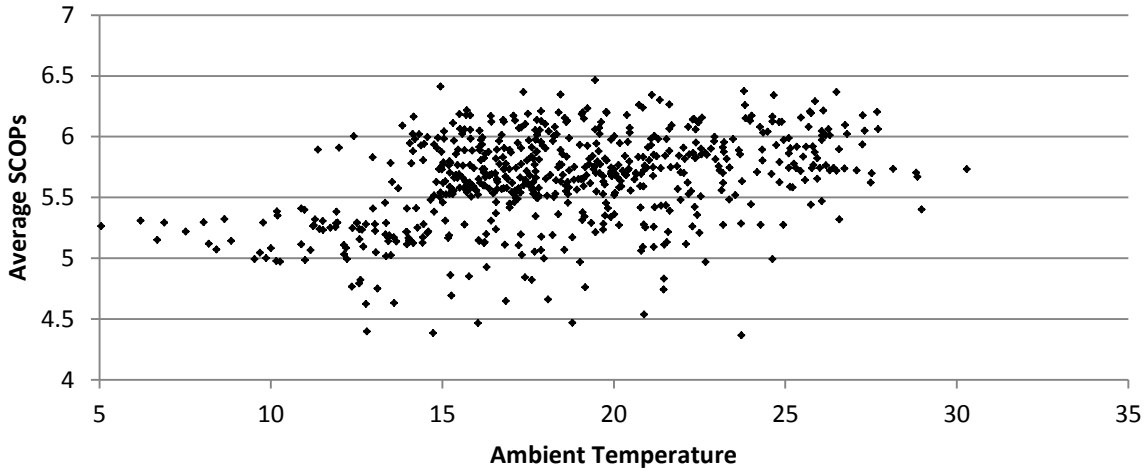

Figure 85: York 1 SCOPs plotted against ambient temperature for operational hours during the baseline period

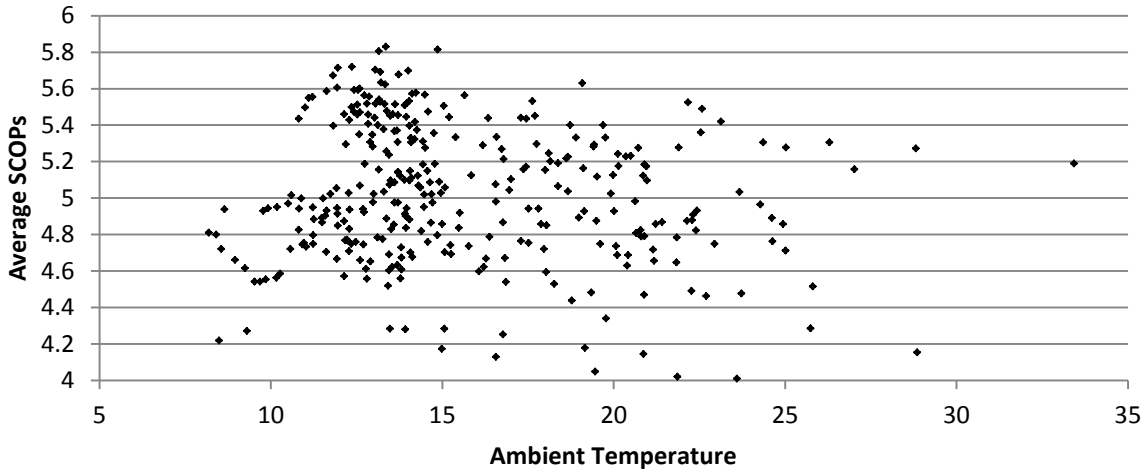

Figure 86: York 2 SCOPs plotted against ambient temperature for operational hours during the baseline period

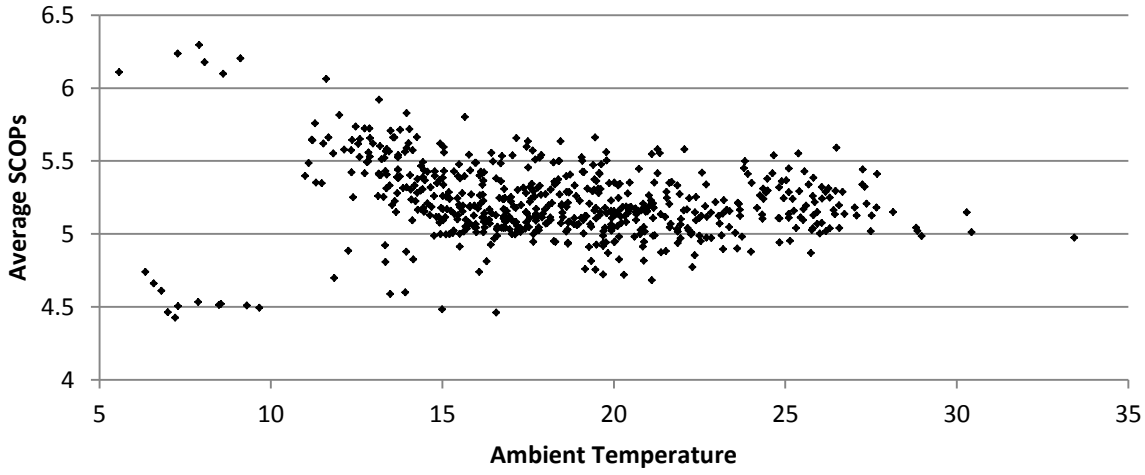

Figure 87: York 3 SCOPs plotted against ambient temperature for operational hours during the baseline period

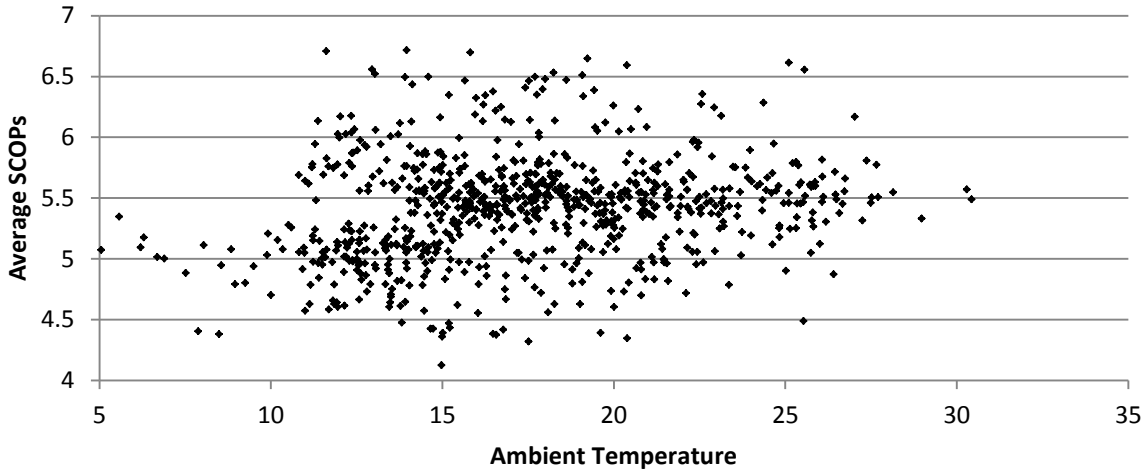

Figure 88: York 4 SCOPs plotted against ambient temperature for operational hours during the baseline period

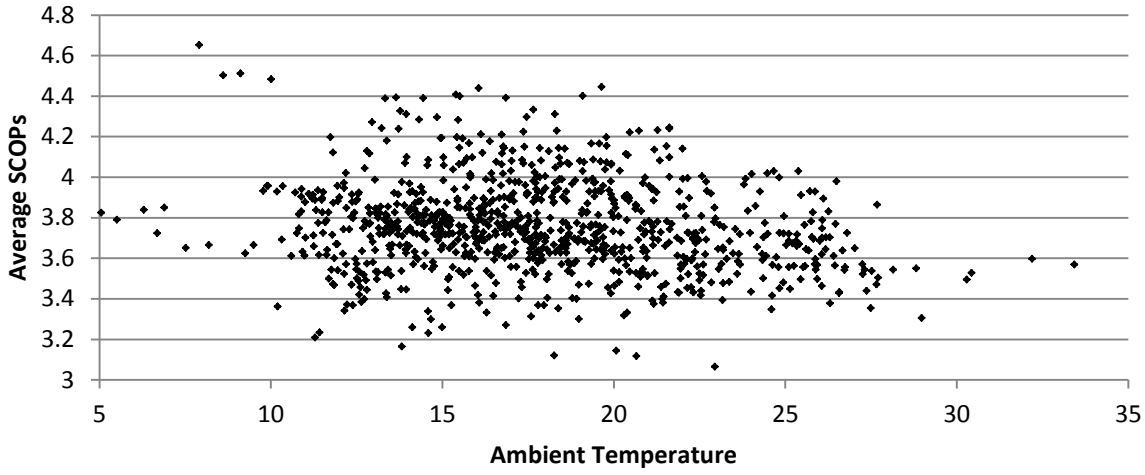

Figure 89: Howden SCOPs plotted against ambient temperature for operational hours during the baseline period

Assessment period plots

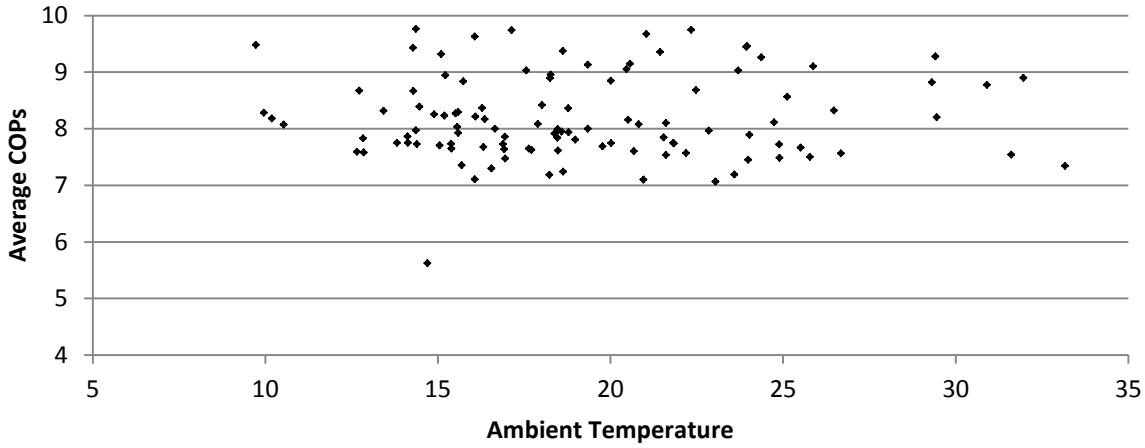

Figure 90: York 1 COPs plotted against ambient temperature for operational hours during the assessment period

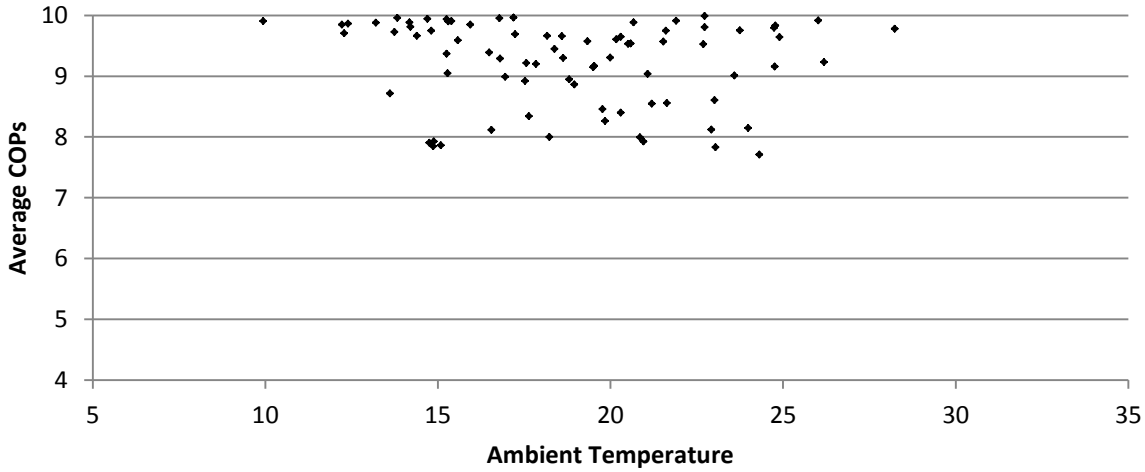

Figure 91: York 3 COPs plotted against ambient temperature for operational hours during the assessment period

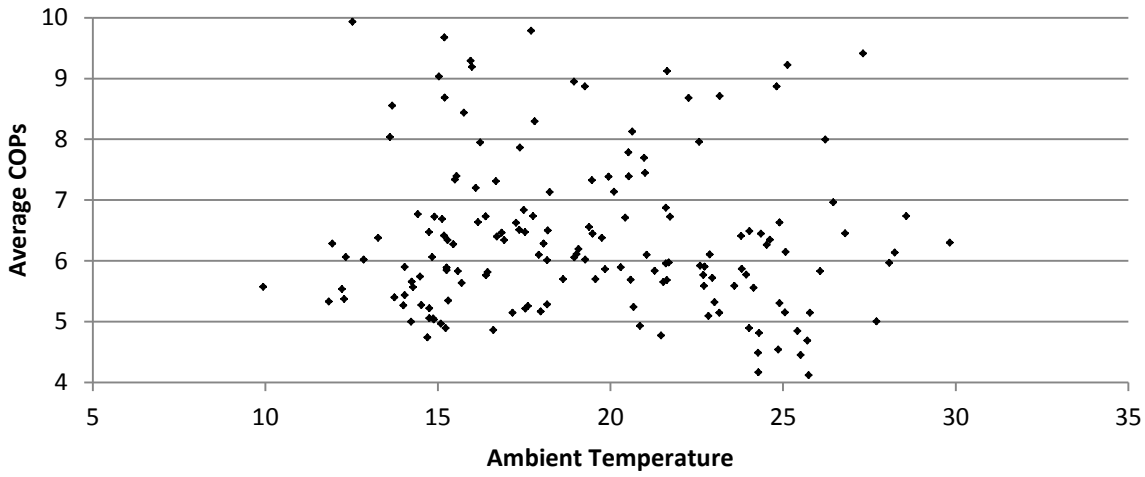

Figure 92: York 4 COPs plotted against ambient temperature for operational hours during the assessment period

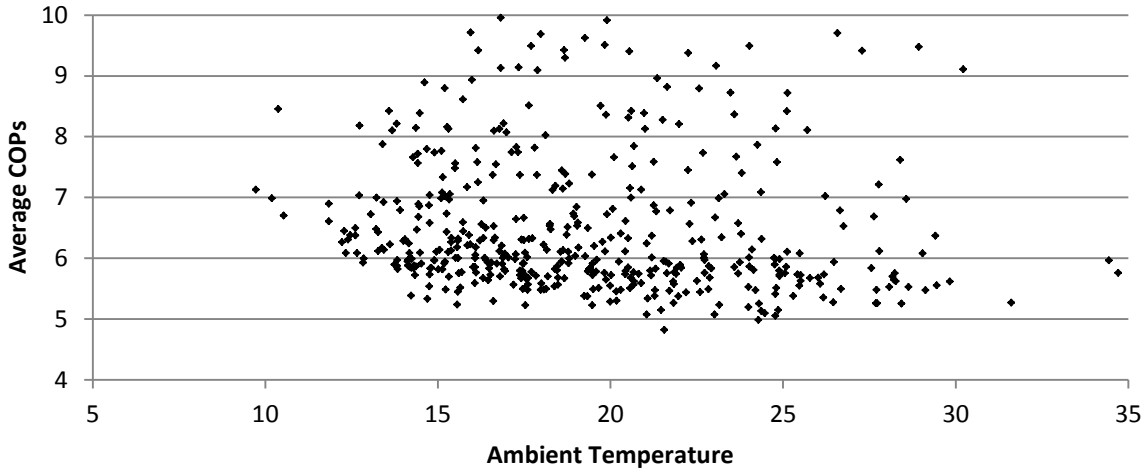

Figure 93: Howden COPs plotted against ambient temperature for operational hours during the assessment period

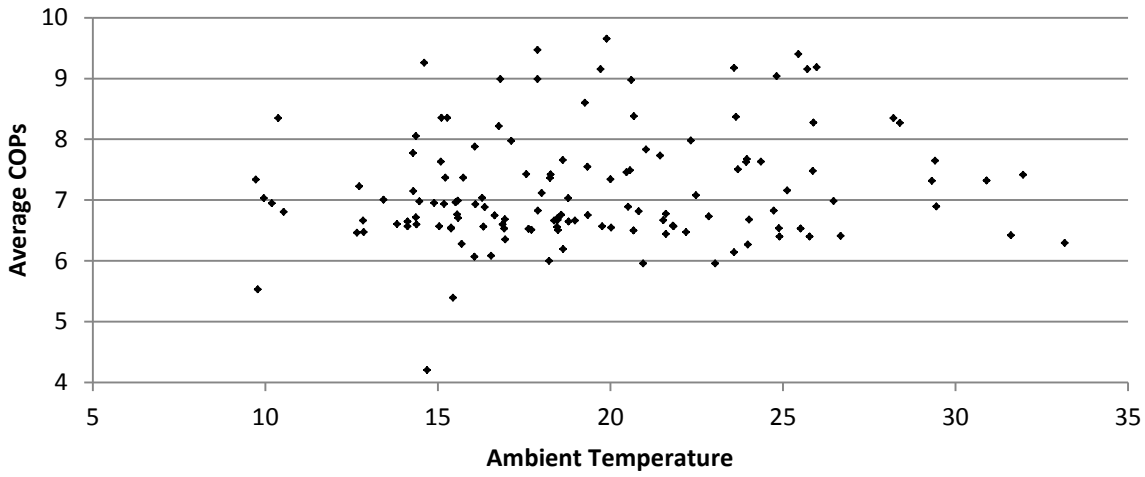

Figure 94: York 1 SCOPs plotted against ambient temperature for operational hours during the assessment period

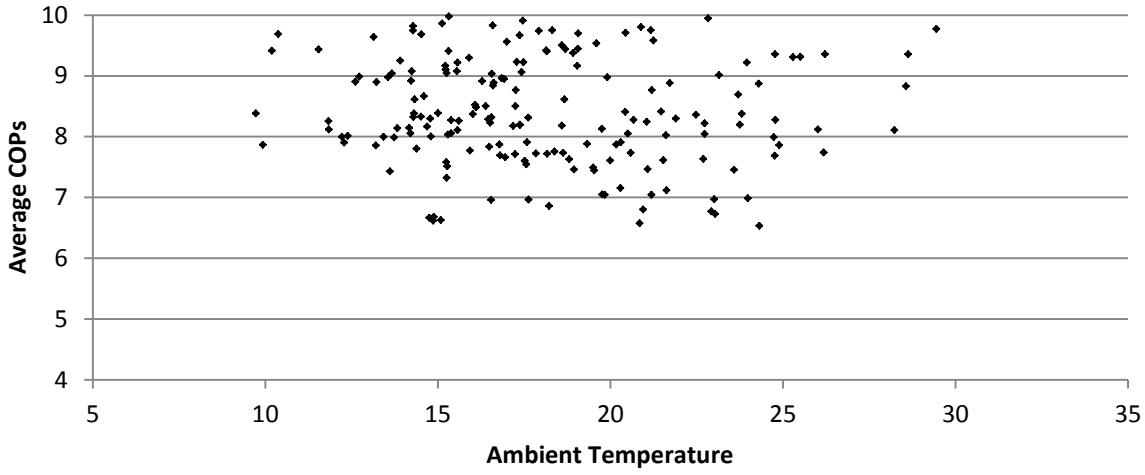

Figure 95: York 3 SCOPs plotted against ambient temperature for operational hours during the assessment period

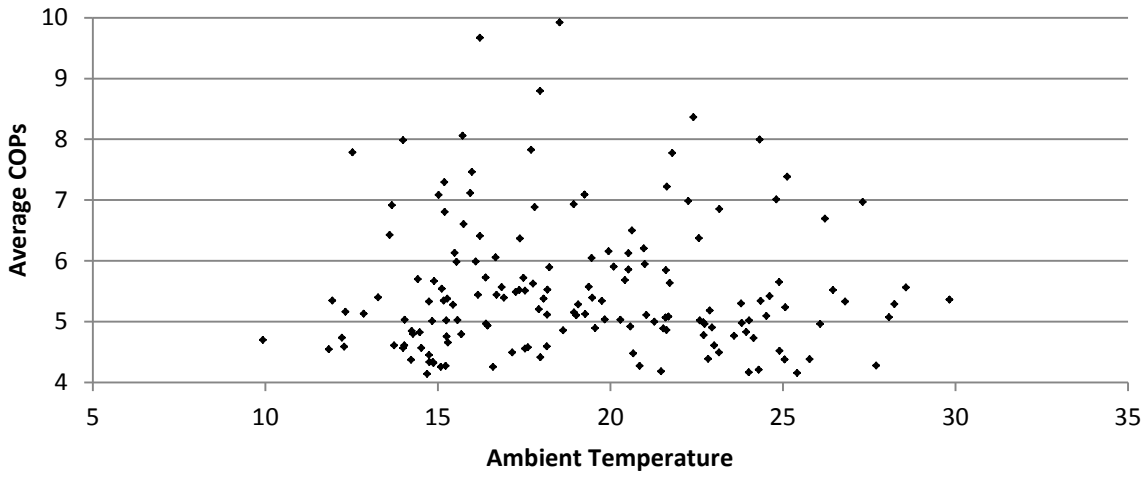

Figure 96: York 4 SCOPs plotted against ambient temperature for operational hours during the assessment period

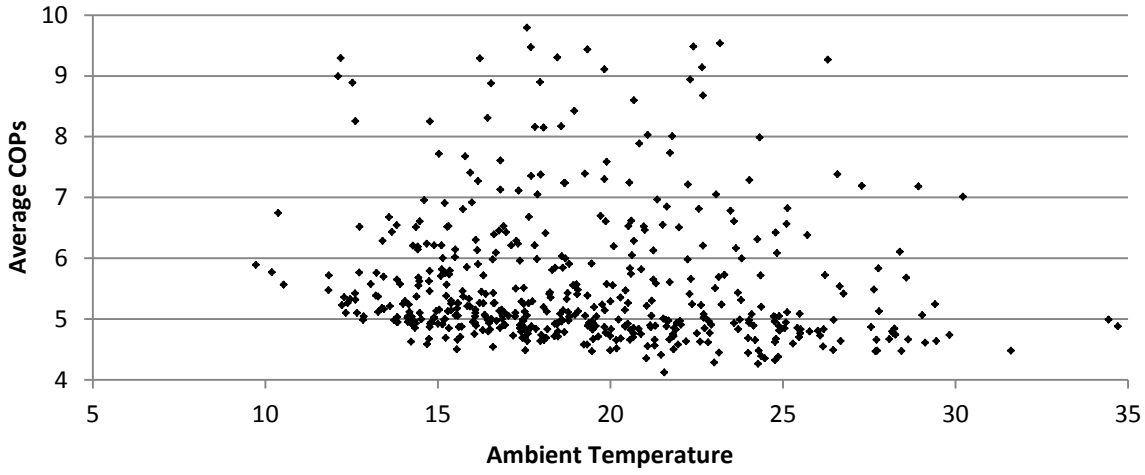

Figure 97: Howden SCOPs plotted against ambient temperature for operational hours during the assessment period

Appendix E – Additional Images

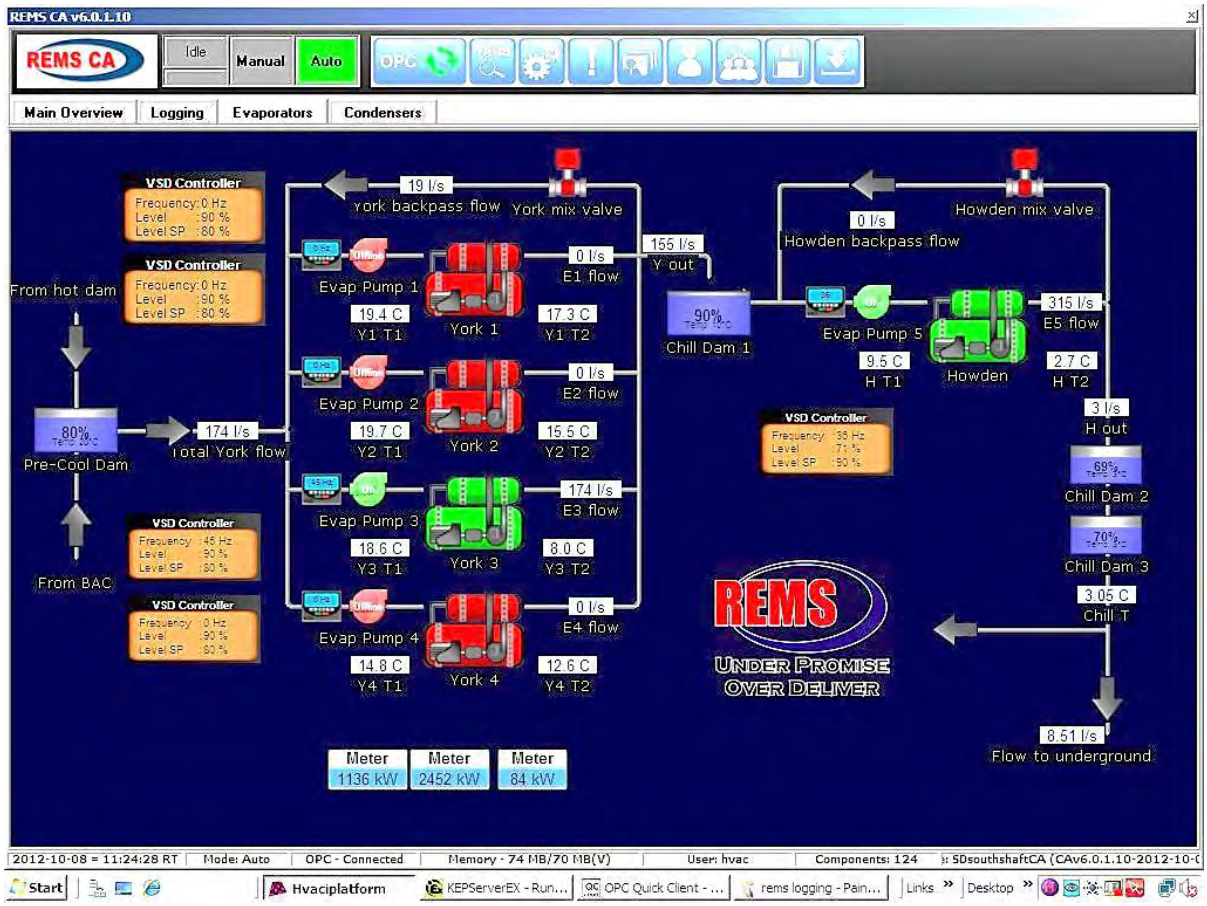

Figure 98: EMS print screen – evaporator water network and respective VSD controllers

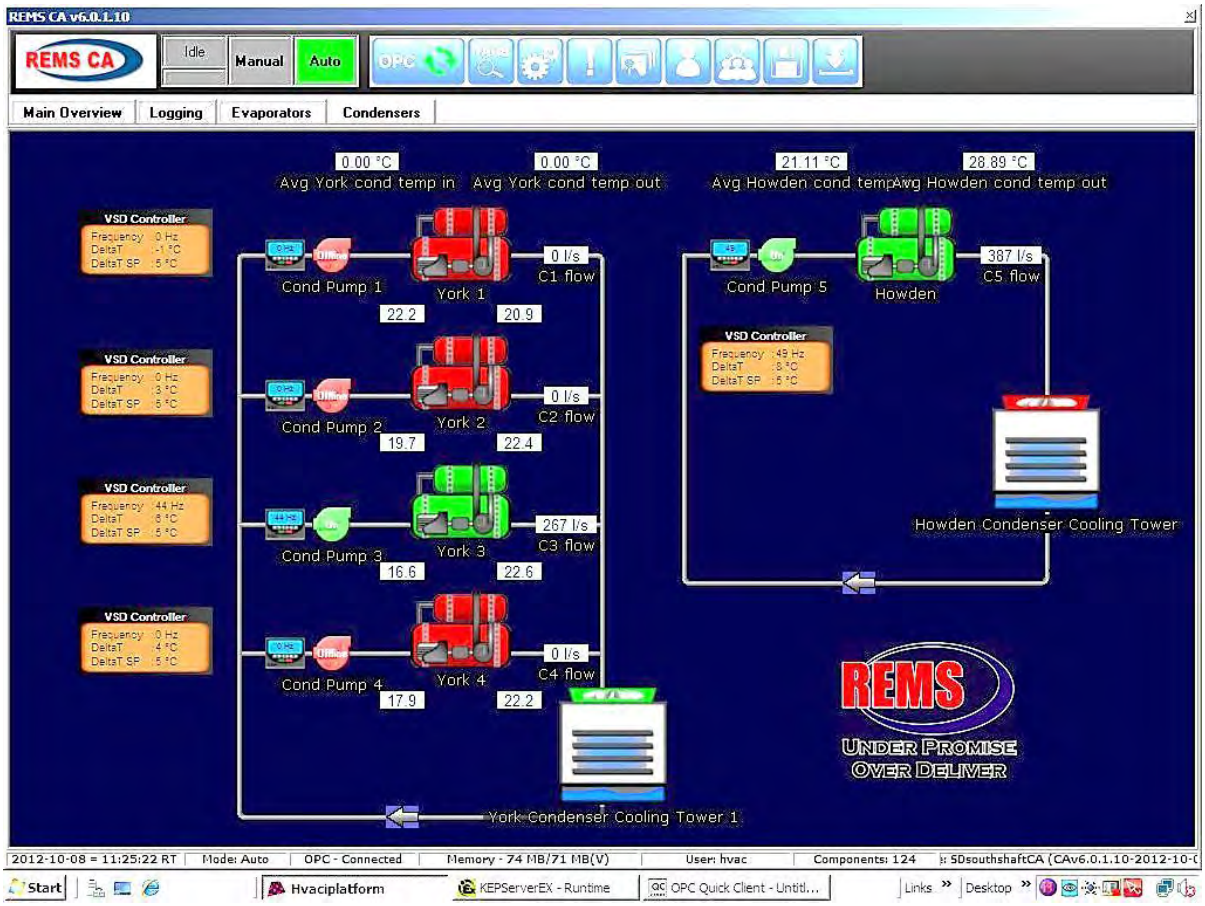

Figure 99: EMS print screen – condenser water network and respective VSD controllers

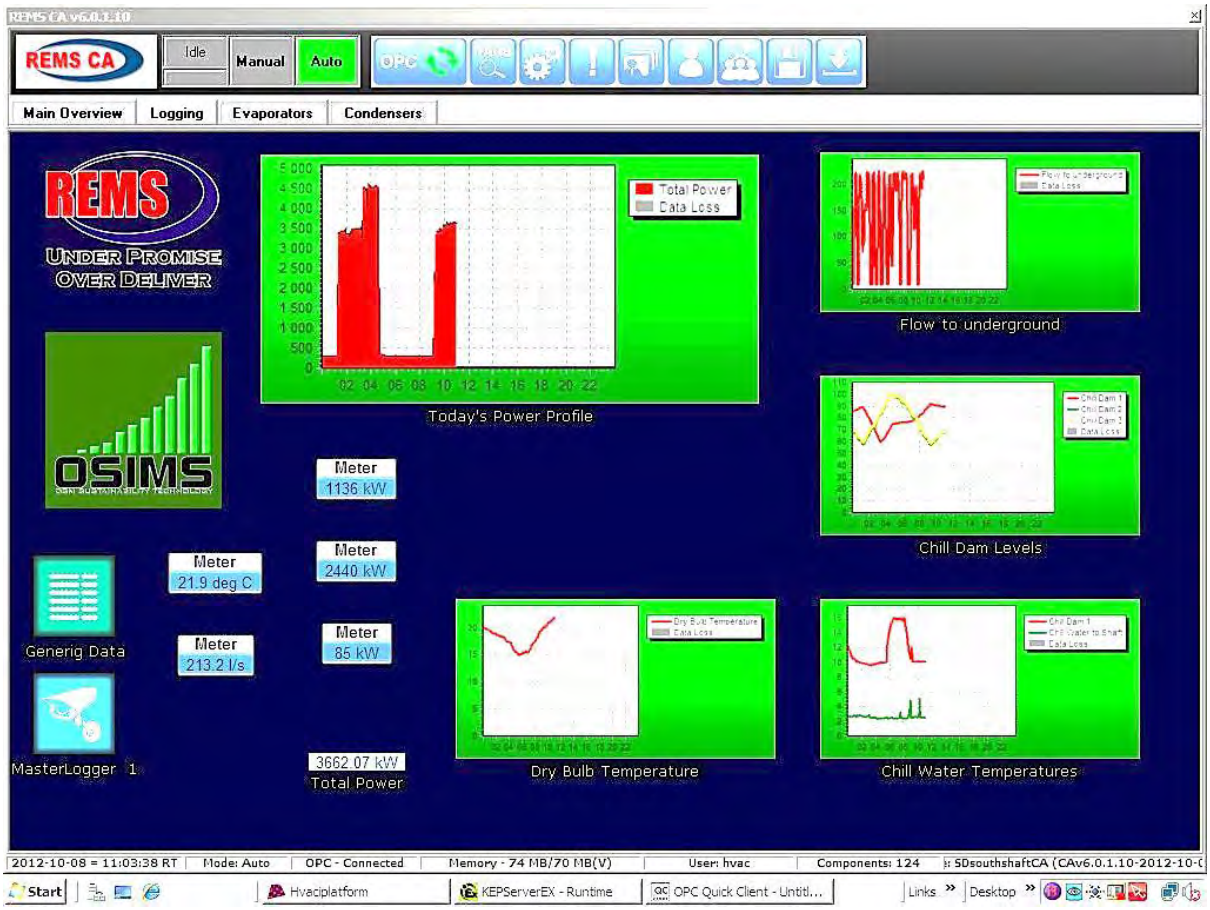

Figure 100: EMS print screen – data logging and trending

Figure 101: York 1 to 3 condenser pump VSDS

Figure 102: York 1 to 4 evaporator pump VSDS

Figure 103: York 4 condenser pump VSD (right)

Figure 104: Howden condenser (left) and evaporator (right) pump VSDs

Appendix F – Simulation model

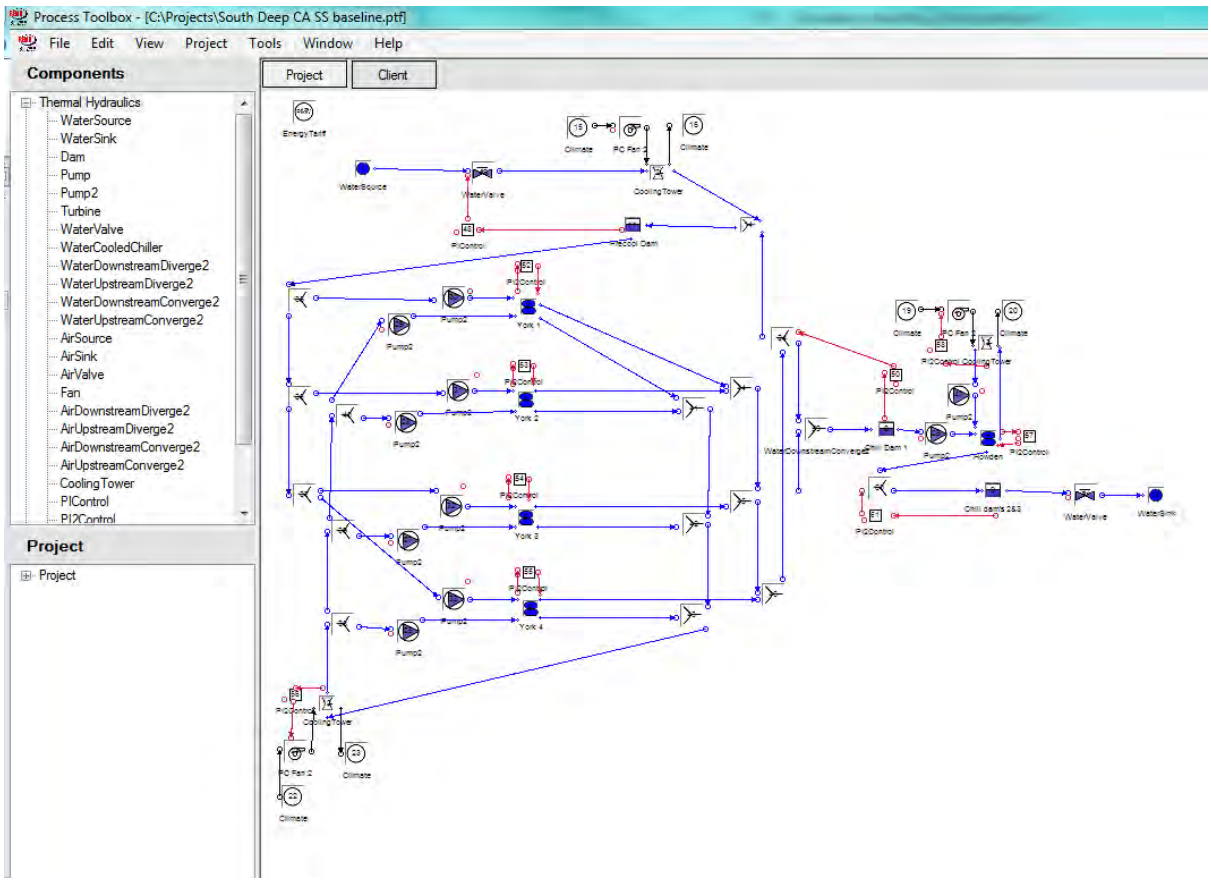

Figure 105: Baseline simulation model partial screen shot

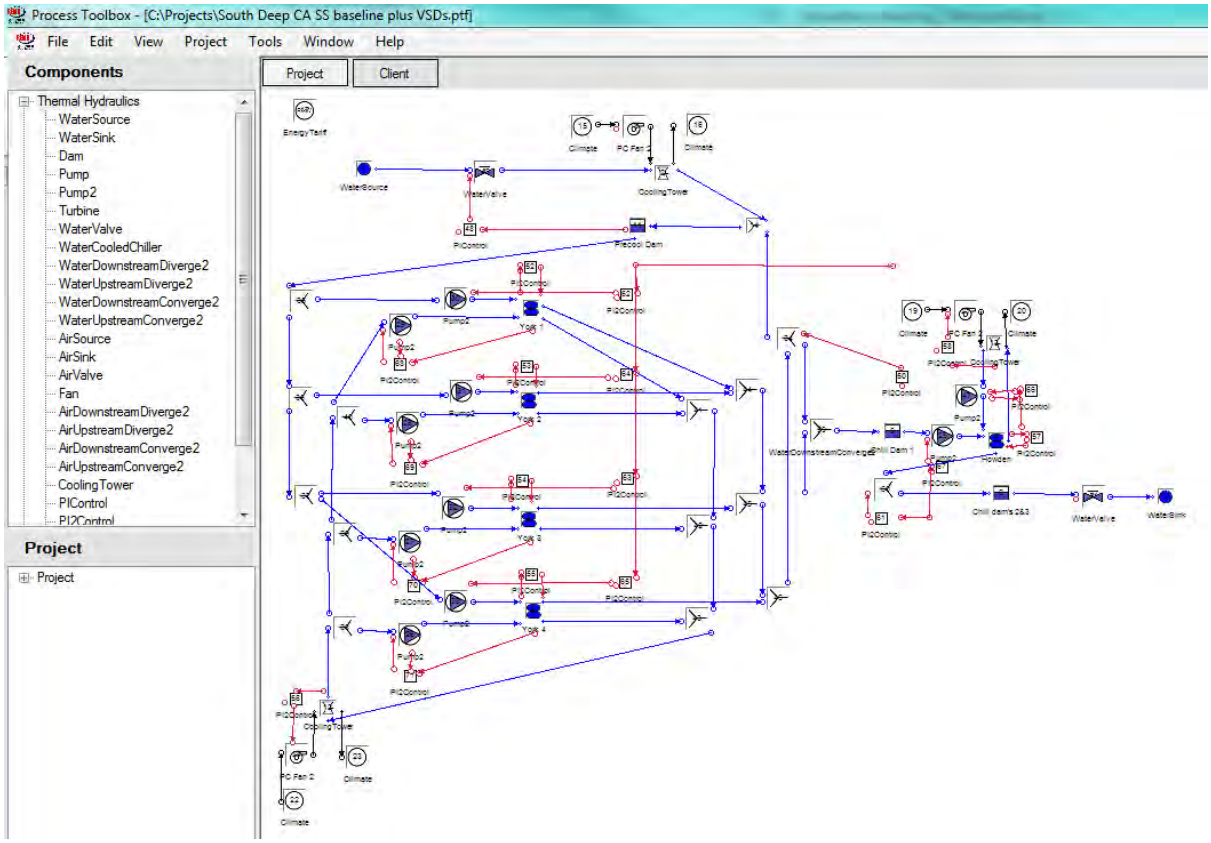

Figure 106: Baseline VSD simulation model partial screen shot

Status in Table 32 refers to operational status of a chiller. A 0.07 status indicates that the chiller was operational for 7% of the respective hour.

Table 32: Simulation verification input variables

Hour	York 1 Status	York 2 Status	York 3 Status	York 4 Status	Howden Status	Drybulb Temp	Flow to underground
1	0.07	0.17	0.23	0.2	0.27	14.14	268.69
2	0	1	0.07	0.93	1	13.73	262.34
3	0	1	1	0.9	1	13.38	156.83
4	0	0.83	1	0.77	1	13.23	270.78
5	0	0.8	0.6	1	1	12.95	269.25
6	0.37	0.83	0.33	0.9	0.63	12.25	271.4
7	0	0.07	0	0.03	0.55	12.15	267.67
8	0.97	0.43	0.67	0.9	1	13.78	268.03
9	1	0.03	0	1	1	15.81	239.04
10	1	1	0	1	0.6	17.76	271.53
11	0.07	1	0	1	0.66	19.11	257.22
12	0	1	0.9	1	1	19.98	258.4
13	0	1	1	0.9	1	23.67	273.83
14	0	1	1	0.1	1	25.03	273.31
15	0	1	1	1	1	27.03	275.75
16	0	0.67	0.73	0.9	0.57	24.56	276.66
17	0	0.07	0.03	0	0.53	21.45	270.58
18	0	1	1	0.97	0.97	20.13	268.61
19	0	0	0	0	0	18.94	269.44
20	0	0	0	0	0	17.96	264.31
21	0	0.97	0.9	0.83	1	17.33	264.53
22	0	1	1	1	1	17	261.56
23	0	0.67	1	1	1	16.83	266.2
24	0	0	1	1	1	16.48	225.89
1	0	0.83	1	1	1	16.2	266.66
2	0	1	1	1	1	16.18	268.32
3	0	1	0	1	1	14.13	268.68
4	0	1	0.21	1	1	13.03	268.19
5	0	1	1	0.43	1	12.8	268.02
6	0.53	1	0.17	0.57	1	11.81	267.52
7	0.97	0.97	0	0.97	1	11.73	269.33
8	0	0.9	0	0.38	1	12.88	267.3
9	0.97	1	0	1	1	14.59	266.53
10	1	0.63	0	1	1	16.26	257.58
11	0.43	0	0.43	0.3	0.2	17.93	237.18
12	0	0.14	0.34	0.1	0.52	19.37	270.5
13	0.83	0.4	0.93	0.67	1	22.27	272.48

14	0.67	0	1	0	0.57	24.67	272.19
15	0	0.63	1	0.7	1	22.06	268.9
16	0	1	1	1	1	20.5	266.71
17	0	1	1	1	1	20.96	269.92
18	0	1	1	1	1	20.15	267.99
19	0	0.07	0.1	0.07	0	17.36	268.45
20	0	0	0	0	0.03	15.81	265.09
21	0	0.86	0.93	0.97	1	15.93	267.38
22	0	1	1	1	1	14.78	264.96
23	0	1	1	1	1	14.06	267.57
24	0	1	1	0.97	1	13.46	263.54

Table 33: Simulation summer power and weekday cost profile

	Simulation power output (kW)		2011/2012 tariff structure costs (R)		2012/2013 tariff structure costs (R)	
Hour	Baseline	VSD	Baseline	VSD	Baseline	VSD
1	5 774	4 693	1 439	1 163	1 656	1 338
2	5 802	4 695	1 446	1 165	1 664	1 341
3	5 736	4 699	1 430	1 167	1 645	1 344
4	5 633	4 700	1 404	1 169	1 616	1 345
5	5 533	4 701	1 379	1 170	1 587	1 346
6	5 466	4 713	1 362	1 173	1 568	1 350
7	5 436	4 742	1 938	1 688	2 231	1 944
8	5 435	4 783	3 162	2 781	3 640	3 201
9	5 440	4 822	3 165	2 804	3 644	3 227
10	5 447	4 854	3 169	2 823	3 648	3 249
11	5 455	4 882	1 944	1 739	2 238	2 002
12	5 462	4 904	1 947	1 747	2 241	2 012
13	5 462	4 916	1 947	1 752	2 241	2 017
14	5 445	4 909	1 941	1 750	2 234	2 014
15	5 431	4 904	1 936	1 748	2 229	2 012
16	5 417	4 896	1 931	1 745	2 223	2 009
17	5 403	4 886	1 926	1 742	2 217	2 005
18	5 392	4 879	1 922	1 739	2 213	2 002
19	5 366	4 856	3 122	2 826	3 594	3 253
20	272	272	158	158	182	182
21	264	264	94	94	108	108
22	5 400	4 915	1 925	1 730	2 216	1 991
23	5 435	4 804	1 354	1 184	1 559	1 363
24	5 621	4 773	1 401	1 180	1 612	1 358

Table 34: Simulation autumn power and weekday cost profile

Hour	Simulation power output (kW)		2011/2012 tariff structure costs (R)		2012/2013 tariff structure costs (R)	
	Baseline	VSD	Baseline	VSD	Baseline	VSD
1	5 547	4 630	1 382	1 148	1 591	1 321
2	5 490	4 573	1 368	1 135	1 575	1 307
3	5 419	4 554	1 351	1 131	1 554	1 302
4	5 333	4 515	1 329	1 120	1 530	1 289
5	5 250	4 480	1 308	1 114	1 506	1 282
6	5 185	4 466	1 292	1 111	1 487	1 279
7	5 143	4 476	1 833	1 593	2 110	1 834
8	5 142	4 545	2 992	2 643	3 444	3 042
9	5 163	4 586	3 004	2 667	3 458	3 070
10	5 182	4 620	3 015	2 687	3 471	3 093
11	5 191	4 642	1 850	1 654	2 130	1 904
12	5 190	4 651	1 850	1 657	2 130	1 908
13	5 187	4 655	1 849	1 659	2 128	1 910
14	5 186	4 661	1 848	1 661	2 128	1 912
15	5 181	4 661	1 847	1 661	2 126	1 912
16	5 175	4 659	1 845	1 660	2 124	1 912
17	5 166	4 653	1 841	1 658	2 120	1 909
18	5 149	4 638	1 835	1 653	2 113	1 903
19	5 123	4 614	2 981	2 685	3 431	3 091
20	272	272	158	158	182	182
21	264	264	94	94	108	108
22	5 178	4 725	1 846	1 659	2 125	1 910
23	5 146	4 572	1 283	1 126	1 476	1 296
24	5 275	4 543	1 315	1 122	1 513	1 292

Table 35: Simulation winter power and weekday cost profile

Hour	Simulation power output (kW)		2011/2012 tariff structure costs (R)		2012/2013 tariff structure costs (R)	
	Baseline	VSD	Baseline	VSD	Baseline	VSD
1	4 312	3 251	1 247	926	1 436	1 067
2	4 194	3 173	1 213	908	1 397	1 046
3	4 043	3 127	1 170	898	1 347	1 034
4	3 899	3 094	1 128	890	1 299	1 025
5	3 776	3 068	1 093	884	1 258	1 018
6	3 681	3 049	1 065	879	1 226	1 012
7	3 610	3 035	1 955	1 640	2 251	1 888
8	3 572	3 035	7 446	6 316	8 571	7 270
9	3 574	3 060	7 450	6 370	8 576	7 332
10	3 608	3 105	7 521	6 466	8 657	7 443
11	3 650	3 153	1 977	1 707	2 276	1 965
12	3 675	3 184	1 991	1 723	2 292	1 984
13	3 687	3 201	1 997	1 733	2 299	1 995
14	3 693	3 212	2 000	1 739	2 303	2 002
15	3 694	3 218	2 001	1 742	2 303	2 006
16	3 683	3 211	1 995	1 739	2 296	2 002
17	3 665	3 199	1 985	1 732	2 285	1 994
18	3 619	3 159	1 960	1 711	2 256	1 970
19	3 585	3 132	7 473	6 527	8 603	7 513
20	270	270	563	563	648	648
21	264	264	143	143	164	164
22	3 617	3 244	1 959	1 695	2 256	1 952
23	3 574	3 114	1 034	873	1 191	1 005
24	3 735	3 073	1 081	868	1 244	1 000

Table 36: Simulation spring power and weekday cost profile

Hour	Simulation power output (kW)		2011/2012 tariff structure costs (R)		2012/2013 tariff structure costs (R)	
	Baseline	VSD	Baseline	VSD	Baseline	VSD
1	5 070	4 235	1 264	1 043	1 454	1 200
2	5 084	4 090	1 267	1 009	1 458	1 162
3	5 149	4 143	1 283	1 025	1 477	1 180
4	5 148	4 184	1 283	1 037	1 476	1 194
5	5 124	4 215	1 277	1 046	1 470	1 204
6	5 095	4 258	1 270	1 058	1 461	1 218
7	5 089	4 383	1 814	1 558	2 088	1 794
8	5 102	4 465	2 969	2 595	3 417	2 987
9	5 122	4 506	2 980	2 619	3 430	3 015
10	5 140	4 540	2 991	2 640	3 442	3 039
11	5 152	4 567	1 836	1 627	2 114	1 873
12	5 162	4 589	1 840	1 635	2 118	1 882
13	5 168	4 604	1 842	1 640	2 121	1 888
14	5 171	4 615	1 843	1 645	2 122	1 893
15	5 170	4 629	1 843	1 649	2 122	1 899
16	5 169	4 636	1 842	1 652	2 121	1 902
17	5 163	4 635	1 840	1 652	2 119	1 902
18	5 147	4 625	1 835	1 648	2 112	1 897
19	5 124	4 606	2 981	2 680	3 432	3 085
20	272	272	158	158	182	182
21	264	264	94	94	108	108
22	5 179	4 719	1 846	1 657	2 125	1 908
23	5 145	4 564	1 282	1 124	1 476	1 294
24	5 276	4 539	1 315	1 121	1 513	1 290

Appendix G – Affinity Laws calculation example

The calculations below indicate the savings as per the York evaporators in Table 13.

$$\frac{P_1}{P_2} = \left(\frac{Q_1}{Q_2}\right)^3$$

$$P_2 = P_1\left(\frac{Q_1}{Q_2}\right)^{\frac{1}{3}}$$

$$P_2 = 55\left(\frac{180}{125}\right)^{\frac{1}{3}}$$

$$P_2 = 18.42\ kW$$

The potential savings of each pump is thus 36.58 kW (55-18.42).

The total potential savings are 146.32 kW, as four pumps are available.